Scattering, Absorption, and Emission of Light by Small Particles

This volume provides a thorough and up-to-date treatment of electromagnetic scattering by small particles. First, the general formalism of scattering, absorption, and emission of light and other electromagnetic radiation by arbitrarily shaped and arbitrarily oriented particles is introduced, and the relation of radiative transfer theory to single-scattering solutions of Maxwell's equations is discussed. Then exact theoretical methods and computer codes for calculating scattering, absorption, and emission properties of arbitrarily shaped particles are described in detail. Further chapters demonstrate how the scattering and absorption characteristics of small particles depend on particle size, refractive index, shape, and orientation. The work illustrates how the high efficiency and accuracy of existing theoretical and experimental techniques and the availability of fast scientific workstations result in advanced physically based applications of electromagnetic scattering to noninvasive particle characterization and remote sensing. This book will be valuable for science professionals, engineers, and graduate students in a wide range of disciplines including optics, electromagnetics, remote sensing, climate research, and biomedicine.

MICHAEL I. MISHCHENKO is a Senior Scientist at the NASA Goddard Institute for Space Studies in New York City. After gaining a Ph.D. in physics in 1987, he has been principal investigator on several NASA and DoD projects and has served as topical editor and editorial board member of leading scientific journals such as *Applied Optics, Journal of Quantitative Spectroscopy and Radiative Transfer, Journal of the Atmospheric Sciences, Waves in Random Media, Journal of Electromagnetic Waves and Applications, and Kinematics and Physics of Celestial Bodies.* Dr. MISHCHENKO is a recipient of the Henry G. Houghton Award of the American Meteorological Society, a Fellow of the American Geophysical Union, a Fellow of the Optical Society of America, and a Fellow of The Institute of Physics. His research interests include electromagnetic scattering, radiative transfer in planetary atmospheres and particulate surfaces, and remote sensing.

LARRY D. TRAVIS is presently Associate Chief of the NASA Goddard Institute for Space Studies. He gained a Ph.D. in astronomy at Pennsylvania State University in 1971. Dr. TRAVIS has acted as principal investigator on several NASA projects and was awarded a NASA Exceptional Scientific Achievement Medal. His research interests include the theoretical interpretation of remote sensing measurements of polarization, planetary atmospheres, atmospheric dynamics, and radiative transfer.

ANDREW A. LACIS is a Senior Scientist at the NASA Goddard Institute for Space Studies, and teaches radiative transfer at Columbia University. He gained a Ph.D. in physics at the University of Iowa in 1970 and has acted as principal investigator on numerous NASA and DoE projects. His research interests include radiative transfer in planetary atmospheres, the absorption of solar radiation by the Earth's atmosphere, and climate modeling.

M. I. MISHCHENKO and L. D. TRAVIS co-edited a monograph on *Light Scattering by Nonspherical Particles: Theory, Measurements, and Applications* published in 2000 by Academic Press.

Scattering, Absorption, and Emission of Light by Small Particles

Revised electronic edition

Michael I. Mishchenko
Larry D. Travis
Andrew A. Lacis

NASA Goddard Institute for Space Studies, New York

CAMBRIDGE
UNIVERSITY PRESS

The first hardcopy edition of this book was published in 2002 by

CAMBRIDGE UNIVERSITY PRESS
The Edinburgh Building
Cambridge CB2 2RU
UK
http://www.cambridge.org

A catalogue record for this book is available from the British Library

ISBN 0 521 78252 X hardback

The first electronic edition of this book was published in 2004 by

NASA Goddard Institute for Space Studies
2880 Broadway
New York, NY 10025
USA
http://www.giss.nasa.gov

The electronic edition is available at the following Internet site:

http://www.giss.nasa.gov/~crmim/books.html

Contents

Preface to the electronic edition

This book was originally published by Cambridge University Press in June of 2002. The entire print run was sold out in less than 16 months, and the book has been officially out of print since October of 2003. By agreement with Cambridge University Press, this electronic edition is intended to make the book continually available via the Internet at the World Wide Web site

http://www.giss.nasa.gov/~crmim/books.html

No significant revision of the text has been attempted; the pagination and the numbering of equations follow those of the original hardcopy edition. However, almost all illustrations have been improved, several typos have been corrected, some minor improvements of the text have been made, and a few recent references have been added.

We express sincere gratitude to Andrew Mishchenko for excellent typesetting and copy-editing work and to Nadia Zakharova and Lilly Del Valle for help with graphics. The preparation of this electronic edition was sponsored by the NASA Radiation Sciences Program managed by Donald Anderson.

We would greatly appreciate being informed of any typos and/or factual inaccuracies that you may find either in the original hardcopy edition of the book or in this electronic release. Please communicate them to Michael Mishchenko at

crmim@giss.nasa.gov

Michael I. Mishchenko
Larry D. Travis
Andrew A. Lacis

New York
May 2004

Preface to the original hardcopy edition

The phenomena of scattering, absorption, and emission of light and other electromagnetic radiation by small particles are ubiquitous and, therefore, central to many science and engineering disciplines. Sunlight incident on the earth's atmosphere is scattered by gas molecules and suspended particles, giving rise to blue skies, white clouds, and various optical displays such as rainbows, coronae, glories, and halos. By scattering and absorbing the incident solar radiation and the radiation emitted by the underlying surface, cloud and aerosol particles affect the earth's radiation budget. The strong dependence of the scattering interaction on particle size, shape, and refractive index makes measurements of electromagnetic scattering a powerful noninvasive means of particle characterization in terrestrial and planetary remote sensing, biomedicine, engineering, and astrophysics. Meaningful interpretation of laboratory and field measurements and remote sensing observations and the widespread need for calculations of reflection, transmission, and emission properties of various particulate media require an understanding of the underlying physics and accurate quantitative knowledge of the electromagnetic interaction as a function of particle physical parameters.

This volume is intended to provide a thorough updated treatment of electromagnetic scattering, absorption, and emission by small particles. Specifically, the book

- introduces a general formalism for the scattering, absorption, and emission of light and other electromagnetic radiation by arbitrarily shaped and arbitrarily oriented particles;
- discusses the relation of radiative transfer theory to single-scattering solutions of Maxwell's equations;
- describes exact theoretical methods and computer codes for calculating the scat-

tering, absorption, and emission properties of arbitrarily shaped small particles;

- demonstrates how the scattering and absorption characteristics of small particles depend on particle size, refractive index, shape, and orientation; and
- illustrates how the high efficiency and accuracy of existing theoretical and experimental techniques and the availability of fast scientific workstations can result in advanced physically based applications.

The book is intended for science professionals, engineers, and graduate students working or specializing in a wide range of disciplines: optics, electromagnetics, optical and electrical engineering, biomedical optics, atmospheric radiation and remote sensing, climate research, radar meteorology, planetary physics, oceanography, and astrophysics. We assume that the reader is familiar with the fundamentals of classical electromagnetics, optics, and vector calculus. Otherwise the book is sufficiently self-contained and provides explicit derivations of all important results. Although not formally a textbook, this volume can be a useful supplement to relevant graduate courses.

The literature on electromagnetic scattering is notorious for discrepancies and inconsistencies in the definition and usage of terms. Among the commonly encountered differences are the use of right-handed as opposed to left-handed coordinate systems, the use of the time-harmonic factor $\exp(-i\omega t)$ versus $\exp(i\omega t)$, and the way an angle of rotation is defined. Because we extensively employ mathematical techniques of the quantum theory of angular momentum and because we wanted to make the book self-consistent, we use throughout only right-handed (spherical) coordinate systems and always consider an angle of rotation positive if the rotation is performed in the *clockwise* direction when one is looking in the positive direction of the rotation axis (or in the direction of light propagation). Also, we adopt the time-harmonic factor $\exp(-i\omega t)$, which seems to be the preferred choice in the majority of publications and implies a non-negative imaginary part of the relative refractive index.

Because the subject of electromagnetic scattering crosses the boundaries between many disciplines, it was very difficult to develop a clear and unambiguous notation system. In many cases we found that the conventional symbol for a quantity in one discipline was the same as the conventional symbol for a different quantity in another discipline. Although we have made an effort to reconcile tradition and simplicity with the desire of having a unique symbol for every variable, some symbols ultimately adopted for the book still represent more than one variable. We hope, however, that the meaning of all symbols is clear from the context. We denote vectors using the Times bold font and matrices using the Arial bold or bold italic font. Unit vectors are denoted by a caret, whereas tensors and dyadics are denoted by the dyadic symbol $\leftrightarrow$. The Times italic font is usually reserved for scalar variables. However, the square root of minus one, the base of natural logarithms, and the differential sign are denoted by Times roman (upright) characters i, e, and d, respectively. A table

containing the symbols used, their meaning and dimension, and the section where they first appear is provided at the end of the book, to assist the reader.

We have not attempted to compile a comprehensive list of relevant publications and often cite a book or a review article where further references can be found. In this regard, two books deserve to be mentioned specifically. The monograph by Kerker (1969) provides a list of nearly a thousand papers on light scattering published prior to 1970, while the recent book edited by Mishchenko *et al*. (2000a) lists nearly 1400 publications on all aspects of electromagnetic scattering by nonspherical and heterogeneous particles.

We provide references to many relevant computer programs developed by various research groups and individuals, including ourselves, and made publicly available through the Internet. Easy accessibility of these programs can be beneficial both to individuals who are mostly interested in applications and to those looking for sources of benchmark results for testing their own codes. Although the majority of these programs have been extensively tested and are expected to generate reliable results in most cases provided that they are used as instructed, it is not inconceivable that some of them contain errors or idiosyncrasies. Furthermore, input parameters can be used that are outside the range of values for which results can be computed accurately. For these reasons the authors of this book and the publisher disclaim all liability for any damage that may result from the use of the programs. In addition, although the publisher and the authors have used their best endeavors to ensure that the URLs for the external websites referred to in this book are correct and active at the time of going to press, the publisher and the authors have no responsibility for the websites and can make no guarantee that a site will remain live or that the content is or will remain appropriate.

Michael I. Mishchenko
Larry D. Travis
Andrew A. Lacis

New York
November 2001

Acknowledgments

Our efforts to understand electromagnetic scattering and its role in remote sensing and atmospheric radiation better have been generously funded over the years by research grants from the United States Government. We thankfully acknowledge the continuing support from the NASA Earth Observing System Program and the Department of Energy Atmospheric Radiation Measurement Program. The preparation of this book was sponsored by a grant from the NASA Radiation Sciences Program managed by Donald Anderson.

We have greatly benefited from extensive discussions with Oleg Bugaenko, Brian Cairns, Barbara Carlson, Helmut Domke, Kirk Fuller, James Hansen, Joop Hovenier, Vsevolod Ivanov, Kuo-Nan Liou, Kari Lumme, Andreas Macke, Daniel Mackowski, Alexander Morozhenko, William Rossow, Kenneth Sassen, Cornelis van der Mee, Bart van Tiggelen, Gorden Videen, Tõnu Viik, Hester Volten, Ping Yang, Edgard Yanovitskij, and many other colleagues.

We thank Cornelis van der Mee and Joop Hovenier for numerous comments which resulted in a much improved manuscript. Our computer codes have benefited from comments and suggestions made by Michael Wolff, Raphael Ruppin, and many other individuals using the codes in their research. We thank Lilly Del Valle for contributing excellent drawings and Zoe Wai and Josefina Mora for helping to find papers and books that were not readily accessible.

We acknowledge with many thanks the fine cooperation that we received from the staff of Cambridge University Press. We are grateful to Matt Lloyd, Jacqueline Garget, and Jane Aldhouse for their patience, encouragement, and help and to Susan Parkinson for careful copy-editing work.

Our gratitude is deepest, however, to Nadia Zakharova who provided invaluable

assistance at all stages of preparing this book and contributed many numerical results and almost all the computer graphics.

Part I

Basic Theory of Electromagnetic Scattering, Absorption, and Emission

A parallel monochromatic beam of light propagates in a vacuum without any change in its intensity or polarization state. However, interposing a small particle into the beam, as illustrated in panel (a) of the diagram on the next page, causes several distinct effects. First, the particle may convert some of the energy contained in the beam into other forms of energy such as heat. This phenomenon is called *absorption*. Second, it extracts some of the incident energy and scatters it in all directions at the frequency of the incident beam. This phenomenon is called *elastic scattering* and, in general, gives rise to light with a polarization state different from that of the incident beam. As a result of absorption and scattering, the energy of the incident beam is reduced by an amount equal to the sum of the absorbed and scattered energy. This reduction is called *extinction*. The extinction rates for different polarization components of the incident beam can be different. This phenomenon is called *dichroism* and may cause a change in the polarization state of the beam after it passes the particle. In addition, if the absolute temperature of the particle is not equal to zero, then the particle also emits radiation in all directions and at all frequencies, the distribution by frequency being dependent on the temperature. This phenomenon is called *thermal emission*.

In electromagnetic terms, the parallel monochromatic beam of light is an oscillating plane electromagnetic wave, whereas the particle is an aggregation of a large number of discrete elementary electric charges. The oscillating electromagnetic field of the incident wave excites the charges to oscillate with the same frequency and thereby radiate secondary electromagnetic waves. The superposition of the secondary waves gives the total elastically scattered field. If the particle is absorbing, it causes dissipation of energy from the electromagnetic wave into the medium. The combined effect of scattering and absorption is to reduce the amount of energy contained in the incident wave. If the absolute temperature of the particle differs from zero, electron transitions from a higher to a lower energy level cause thermal emission of electromagnetic energy at specific frequencies. For complicated systems of molecules with a large number of degrees of freedom, many different transitions produce spectral emission lines so closely spaced that the resulting radiation spectrum becomes effectively continuous and includes emitted energy at all frequencies.

Electromagnetic scattering is a complex phenomenon because the secondary waves generated by each oscillating charge also stimulate oscillations of all other charges forming the particle. Furthermore, computation of the total scattered field by superposing the secondary waves must take account of their phase differences, which change every time the incidence and/or scattering direction is changed. Therefore, the total scattered radiation depends on the way the charges are arranged to form the particle with respect to the incident and scattered directions.

Since the number of elementary charges forming a micrometer-sized particle is extremely large, solving the scattering problem directly by computing and superposing all secondary waves is impracticable even with the aid of modern computers. Fortunately, however, the same problem can be solved using the concepts of macroscopic electromagnetics, which treat the large collection of charges as a macroscopic body with a specific distribution of the refractive index. In this case the scattered field

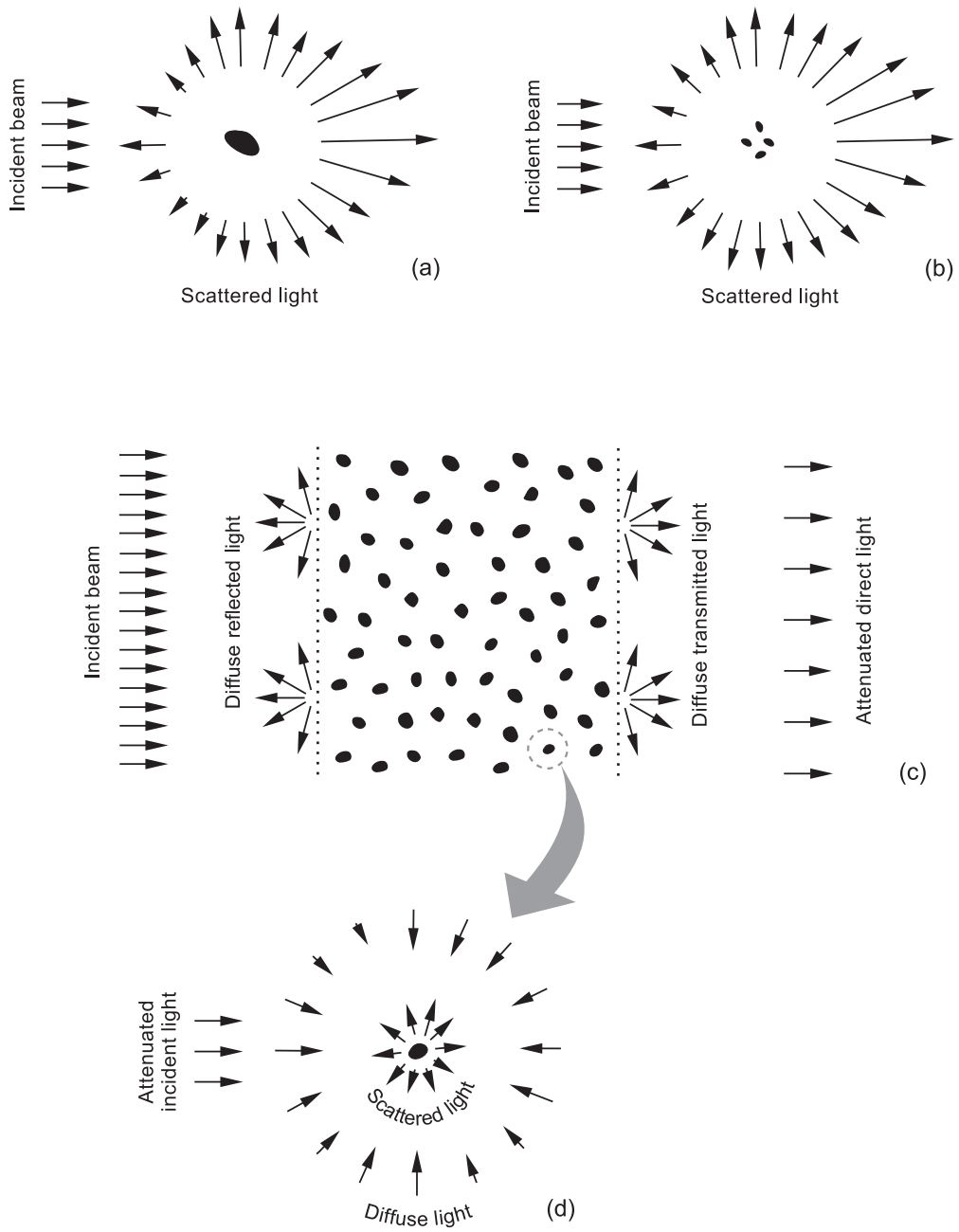

In (a), (b), and (c) a parallel beam of light is incident from the left. (a) Far-field electromagnetic scattering by an individual particle in the form of a single body or a fixed cluster. (b) Far-field scattering by a small volume element composed of randomly positioned, widely separated particles. (c) Multiple scattering by a layer of randomly and sparsely distributed particles. On the left of the layer, diffuse reflected light; on the right of the layer, diffuse transmitted light. On the far right, the attenuated incident beam. (d) Each individual particle in the layer receives and scatters both light from the incident beam, somewhat attenuated, and light diffusely scattered from the other particles.

can be computed by solving the Maxwell equations for the macroscopic electromagnetic field subject to appropriate boundary conditions. This approach appears to be quite manageable and forms the basis of the modern theory of electromagnetic scattering by small particles.

We do not aim to cover all aspects of electromagnetic scattering and absorption by a small particle and limit our treatment by imposing several well-defined restrictions, as follows.

- We consider only the scattering of time-harmonic, monochromatic or quasi-monochromatic light in that we assume that the amplitude of the incident electric field is either constant or fluctuates with time much more slowly than the time factor $\exp(-i\omega t)$, where ω is the angular frequency and t is time.
- It is assumed that electromagnetic scattering occurs without frequency redistribution, i.e., the scattered light has the same frequency as the incident light. This restriction excludes inelastic scattering phenomena such as Raman and Brillouin scattering and fluorescence.
- We consider only finite scattering particles and exclude such peculiar two-dimensional scatterers as infinite cylinders.
- It is assumed that the unbounded host medium surrounding the scatterer is homogeneous, linear, isotropic, and nonabsorbing.
- We study only scattering in the far-field zone, where the propagation of the scattered wave is away from the particle, the electric field vector vibrates in the plane perpendicular to the propagation direction, and the scattered field amplitude decays inversely with distance from the particle.

By directly solving the Maxwell equations, one can find the field scattered by an object in the form of a single body or a fixed cluster consisting of a limited number of components. However, one often encounters situations in which light is scattered by a very large group of particles forming a constantly varying spatial configuration. A typical example is a cloud of water droplets or ice crystals in which the particles are constantly moving, spinning, and even changing their shapes and sizes due to oscillations of the droplet surface, evaporation, condensation, sublimation, and melting. Although such a particle collection can be treated at each given moment as a fixed cluster, a typical measurement of light scattering takes a finite amount of time, over which the spatial configuration of the component particles and their sizes, orientations, and/or shapes continuously and randomly change. Therefore, the registered signal is in effect a statistical average over a large number of different cluster realizations.

A logical way of modeling the measurement of light scattering by a random collection of particles would be to solve the Maxwell equations for a statistically representative range of fixed clusters and then take the average. However, this approach becomes prohibitively time consuming if the number of cluster components is large and is impractical for objects such as clouds in planetary atmospheres, oceanic hydrosols, or stellar dust envelopes. Moreover, in the traditional far-field scattering formalism a cluster is treated as a single scatterer and it is assumed that the distance from the

cluster to the observation point is much larger than any linear dimension of the cluster. This assumption may well be violated in laboratory and remote sensing measurements, thereby making necessary explicit computations of the scattered light in the near-field zone of the cluster as a whole.

Fortunately, particles forming a random group can often be considered as independent scatterers. This means that the electromagnetic response of each particle in the group can be calculated using the extinction and phase matrices that describe the scattering of a plane electromagnetic wave by the same particle but placed in an infinite homogeneous space in complete isolation from all other particles (panel (a) of the diagram). In general, this becomes possible when (i) each particle resides in the far-field zones of all the other particles forming the group, and (ii) scattering by individual particles is incoherent, i.e., there are no systematic phase relations between partial waves scattered by individual particles during the time interval necessary to take the measurement. As a consequence of condition (ii), the intensities (or, more generally, the Stokes parameters) of the partial waves can be added without regard to phase. An important exception is scattering in the exact forward direction, which is always coherent and causes attenuation of the incident wave.

The assumption of independent scattering greatly simplifies the problem of computing light scattering by groups of randomly positioned, widely separated particles. Consider first the situation when a plane wave illuminates a small volume element containing a tenuous particle collection, as depicted schematically in panel (b) of the diagram. Each particle is excited by the external field and the secondary fields scattered by all other particles. However, if the number of particles is sufficiently small and their separation is sufficiently large then the contribution of the secondary waves to the field exciting each particle is much smaller than the external field. Therefore, the total scattered field can be well approximated by the sum of the fields generated by the individual particles in response to the external field in isolation from the other particles. This approach is called the single-scattering approximation. By assuming also that particle positions are sufficiently random, one can show that the optical cross sections and the extinction and phase matrices of the volume element are obtained by simply summing the respective characteristics of all constituent particles.

When the scattering medium contains very many particles, the single-scattering approximation is no longer valid. Now one must explicitly take into account that each particle is illuminated by light scattered by other particles as well as by the (attenuated) incident light, as illustrated in panels (c) and (d) of the diagram. This means that each particle scatters light that has already been scattered by other particles, so that the light inside the scattering medium and the light leaving the medium have a significant *multiply scattered* (or *diffuse*) component. A traditional approach in this case is to find the intensity and other Stokes parameters of the diffuse light by solving the so-called radiative transfer equation. This technique still assumes that particles forming the scattering medium are randomly positioned and widely separated and that the extinction and phase matrices of each small volume element can be obtained by incoherently adding the respective characteristics of the constituent particles.

Thus, the treatment of light scattering by a large group of randomly positioned,

widely separated particles can be partitioned into three consecutive steps:

- computation of the far-field scattering and absorption properties of an individual particle by solving the Maxwell equations;
- computation of the scattering and absorption properties of a small volume element containing a tenuous particle collection by using the single-scattering approximation; and
- computation of multiple scattering by the entire particle group by solving the radiative transfer equation supplemented by appropriate boundary conditions.

Although the last two steps are inherently approximate, they are far more practicable than attempting to solve the Maxwell equations for large particle collections and usually provide results accurate enough for many applications. A notable exception is the exact backscattering direction, where so-called self-avoiding reciprocal multiple-scattering paths in the particle collection always interfere constructively and cause a coherent intensity peak. This phenomenon is called coherent backscattering (or weak photon localization) and is not explicitly described by the standard radiative transfer theory.

When a group of randomly moving and spinning particles is illuminated by a monochromatic, spatially coherent plane wave (e.g., laser light), the random constructive and destructive interference of the light scattered by individual particles generates in the far-field zone a speckle pattern that fluctuates in time and space. In this book we eliminate the effect of fluctuations by assuming that the Stokes parameters of the scattered light are averaged over a period of time much longer than the typical period of the fluctuations. In other words, we deal with the average, *static* component of the scattering pattern. Therefore, the subject of the book could be called static light scattering. Although explicit measurements of the spatial and temporal fluctuations of the speckle pattern are more complicated than measurements of the averages, they can contain useful information about the particles complementary to that carried by the mean Stokes parameters. Statistical analyses of light scattered by systems of suspended particles are the subject of the discipline called photon correlation spectroscopy (or dynamic light scattering) and form the basis of many well established experimental techniques. For example, instruments for the measurement of particle size and dispersity and laser Doppler velocimeters and transit anemometers have been commercially available for many years. More recent research has demonstrated the application of polarization fluctuation measurements to particle shape characterization (Pitter *et al*. 1999; Jakeman 2000). Photon correlation spectroscopy is not discussed in this volume; the interested reader can find the necessary information in the books by Cummins and Pike (1974, 1977), Pecora (1985), Brown (1993), Pike and Abbiss (1997), and Berne and Pecora (2000) as well as in the recent feature issues of *Applied Optics* edited by Meyer *et al.* (1997, 2001).

Chapter 1

Polarization characteristics of electromagnetic radiation

The analytical and numerical basis for describing scattering properties of media composed of small discrete particles is formed by the classical electromagnetic theory. Although there are several excellent textbooks outlining the fundamentals of this theory, it is convenient for our purposes to begin with a summary of those concepts and equations that are central to the subject of this book and will be used extensively in the following chapters.

We start by formulating Maxwell's equations and constitutive relations for time-harmonic macroscopic electromagnetic fields and derive the simplest plane-wave solution, which underlies the basic optical idea of a monochromatic parallel beam of light. This solution naturally leads to the introduction of such fundamental quantities as the refractive index and the Stokes parameters. Finally, we define the concept of a quasi-monochromatic beam of light and discuss its implications.

1.1 Maxwell's equations, time-harmonic fields, and the Poynting vector

The mathematical description of all classical optics phenomena is based on the set of Maxwell's equations for the macroscopic electromagnetic field at interior points in matter, which in SI units are as follows (Jackson 1998):

$$\nabla \cdot \mathbf{D} = \rho, \tag{1.1}$$

$$\nabla \times \mathbf{E} = -\frac{\partial \mathbf{B}}{\partial t}, \tag{1.2}$$

$$\nabla \cdot \mathbf{B} = 0, \tag{1.3}$$

$$\nabla \times \mathbf{H} = \mathbf{J} + \frac{\partial \mathbf{D}}{\partial t}, \tag{1.4}$$

where t is time, **E** the electric and **H** the magnetic field, **B** the magnetic induction, **D** the electric displacement, and ρ and **J** the macroscopic (free) charge density and current density, respectively. All quantities entering Eqs. (1.1)–(1.4) are functions of time and spatial coordinates. Implicit in the Maxwell equations is the continuity equation

$$\frac{\partial \rho}{\partial t} + \nabla \cdot \mathbf{J} = 0, \tag{1.5}$$

which can be derived by combining the time derivative of Eq. (1.1) with the divergence of Eq. (1.4). The vector fields entering Eqs. (1.1)–(1.4) are related by

$$\mathbf{D} = \varepsilon_0 \mathbf{E} + \mathbf{P}, \tag{1.6}$$

$$\mathbf{H} = \frac{1}{\mu_0}\mathbf{B} - \mathbf{M}, \tag{1.7}$$

where **P** is the electric polarization (average electric dipole moment per unit volume), **M** is the magnetization (average magnetic dipole moment per unit volume), and ε_0 and μ_0 are the electric permittivity and the magnetic permeability of free space. Equations (1.1)–(1.7) are insufficient for a unique determination of the electric and magnetic fields from a given distribution of charges and currents and must be supplemented with so-called constitutive relations:

$$\mathbf{J} = \sigma \mathbf{E}, \tag{1.8}$$

$$\mathbf{B} = \mu \mathbf{H}, \tag{1.9}$$

$$\mathbf{P} = \varepsilon_0 \chi \mathbf{E}, \tag{1.10}$$

where σ is the conductivity, μ the permeability, and χ the electric susceptibility. For linear and isotropic media, σ, μ, and χ are scalars independent of the fields. The microphysical derivation and the range of validity of the macroscopic Maxwell equations are discussed in detail by Jackson (1998).

The Maxwell equations are strictly valid only for points in whose neighborhood the physical properties of the medium, as characterized by σ, μ, and χ, vary continuously. Across an interface separating one medium from another the field vectors **E**, **D**, **B**, and **H** may be discontinuous. The boundary conditions at such an interface can be derived from the integral equivalents of the Maxwell equations (Jackson 1998) and are as follows:

1. There is a discontinuity in the normal component of **D**:

$$(\mathbf{D}_2 - \mathbf{D}_1) \cdot \hat{\mathbf{n}} = \rho_S, \tag{1.11}$$

where $\hat{\mathbf{n}}$ is the unit vector directed along the local normal to the interface separating media 1 and 2 and pointing toward medium 2 and ρ_S is the surface charge density (the charge per unit area).

2. There is a discontinuity in the tangential component of **H**:

$$\hat{\mathbf{n}}\times(\mathbf{H}_2-\mathbf{H}_1)=\mathbf{J}_S, \tag{1.12}$$

where $\mathbf{J}_S$ is the surface current density. However, media with finite conductivity cannot support surface currents, so that

$$\hat{\mathbf{n}}\times(\mathbf{H}_2-\mathbf{H}_1)=0 \quad (\text{finite conductivity}). \tag{1.13}$$

3. The normal component of **B** and the tangential component of **E** are continuous:

$$(\mathbf{B}_2-\mathbf{B}_1)\cdot\hat{\mathbf{n}}=0, \tag{1.14}$$

$$\hat{\mathbf{n}}\times(\mathbf{E}_2-\mathbf{E}_1)=0. \tag{1.15}$$

The boundary conditions (1.11)–(1.15) are useful in solving the Maxwell equations in different adjacent regions with continuous physical properties and then linking the partial solutions to determine the fields throughout all space.

We assume that all fields and sources are time-harmonic and adopt the standard practice of representing real time-dependent fields as real parts of the respective complex fields, viz.,

$$\mathbf{E}(\mathbf{r},t)=\mathrm{Re}\,\mathbf{E}_{\mathrm{c}}(\mathbf{r},t)=\mathrm{Re}[\mathbf{E}(\mathbf{r})\mathrm{e}^{-\mathrm{i}\omega t}]\equiv\tfrac{1}{2}[\mathbf{E}(\mathbf{r})\mathrm{e}^{-\mathrm{i}\omega t}+\mathbf{E}^*(\mathbf{r})\mathrm{e}^{\mathrm{i}\omega t}], \tag{1.16}$$

where **r** is the position (radius) vector, ω the angular frequency, $\mathrm{i}=\sqrt{-1}$, and the asterisk denotes a complex-conjugate value. Then we can derive from Eqs. (1.1)–(1.10)

$$\nabla\cdot\mathbf{D}(\mathbf{r})=\rho(\mathbf{r}) \quad \text{or} \quad \nabla\cdot[\varepsilon\mathbf{E}(\mathbf{r})]=0, \tag{1.17}$$

$$\nabla\times\mathbf{E}(\mathbf{r})=\mathrm{i}\omega\mu\mathbf{H}(\mathbf{r}), \tag{1.18}$$

$$\nabla\cdot[\mu\mathbf{H}(\mathbf{r})]=0, \tag{1.19}$$

$$\nabla\times\mathbf{H}(\mathbf{r})=\mathbf{J}(\mathbf{r})-\mathrm{i}\omega\mathbf{D}(\mathbf{r})=-\mathrm{i}\omega\varepsilon\mathbf{E}(\mathbf{r}), \tag{1.20}$$

where

$$\varepsilon=\varepsilon_0(1+\chi)+\mathrm{i}\frac{\sigma}{\omega} \tag{1.21}$$

is the (complex) permittivity. Under the complex time-harmonic representation, the constitutive coefficients σ, μ, and χ can be frequency dependent and are not restricted to be real (Jackson 1998). For example, a complex permeability implies a difference in phase between the real time-harmonic magnetic field **H** and the corresponding real time-harmonic magnetic induction **B**. We will show later that complex ε and/or μ results in a non-zero imaginary part of the refractive index, Eq. (1.44),

thereby causing the absorption of electromagnetic energy, Eq. (1.45), by converting it into other forms of energy such as heat.

Note that the scalar or the vector product of two real vector fields is not equal to the real part of the respective product of the corresponding complex vector fields. Instead we have

$$\begin{aligned} c(\mathbf{r},t) &= \mathbf{a}(\mathbf{r},t)\cdot\mathbf{b}(\mathbf{r},t) \\ &= \tfrac{1}{4}[\mathbf{a}(\mathbf{r})\mathrm{e}^{-\mathrm{i}\omega t}+\mathbf{a}^*(\mathbf{r})\mathrm{e}^{\mathrm{i}\omega t}]\cdot[\mathbf{b}(\mathbf{r})\mathrm{e}^{-\mathrm{i}\omega t}+\mathbf{b}^*(\mathbf{r})\mathrm{e}^{\mathrm{i}\omega t}] \\ &= \tfrac{1}{2}\mathrm{Re}[\mathbf{a}(\mathbf{r})\cdot\mathbf{b}^*(\mathbf{r})+\mathbf{a}(\mathbf{r})\cdot\mathbf{b}(\mathbf{r})\mathrm{e}^{-2\mathrm{i}\omega t}] \end{aligned} \tag{1.22}$$

and similarly for a vector product. A common situation in practice is that the angular frequency ω is so high that a measuring instrument is not capable of following the rapid oscillations of the instantaneous product values but rather responds to a time average

$$\langle c(\mathbf{r})\rangle = \frac{1}{\Delta t}\int_t^{t+\Delta t}\mathrm{d}t' c(\mathbf{r},t'), \tag{1.23}$$

where Δt is a time interval long compared with $1/\omega$. Therefore, it follows from Eq. (1.22) that for time averages of products, one must take the real part of the product of one complex field with the complex conjugate of the other, e.g.,

$$\langle c(\mathbf{r})\rangle = \tfrac{1}{2}\mathrm{Re}[\mathbf{a}(\mathbf{r})\cdot\mathbf{b}^*(\mathbf{r})]. \tag{1.24}$$

The flow of the electromagnetic energy is described by the so-called Poynting vector **S**. The expression for **S** can be derived by considering the conservation of energy and taking into account that the magnetic field can do no work and that for a local charge q the rate of doing work by the electric field is $q(\mathbf{r})\mathbf{v}(\mathbf{r})\cdot\mathbf{E}(\mathbf{r},t)$, where **v** is the velocity of the charge. Accordingly, consider the integral

$$\frac{1}{2}\int_V \mathrm{d}V\,\mathbf{J}^*(\mathbf{r})\cdot\mathbf{E}(\mathbf{r}) \tag{1.25}$$

over a finite volume V, whose real part gives the time-averaged rate of work done by the electromagnetic field and which must be balanced by the corresponding rate of decrease of the electromagnetic energy within V. Using Eqs. (1.18) and (1.20) and the vector identity

$$\nabla\cdot(\mathbf{a}\times\mathbf{b}) = \mathbf{b}\cdot(\nabla\times\mathbf{a})-\mathbf{a}\cdot(\nabla\times\mathbf{b}), \tag{1.26}$$

we derive

$$\begin{aligned} \frac{1}{2}\int_V \mathrm{d}V\,\mathbf{J}^*(\mathbf{r})\cdot\mathbf{E}(\mathbf{r}) &= \frac{1}{2}\int_V \mathrm{d}V\,\mathbf{E}(\mathbf{r})\cdot[\nabla\times\mathbf{H}^*(\mathbf{r})-\mathrm{i}\omega\mathbf{D}^*(\mathbf{r})] \\ &= \frac{1}{2}\int_V \mathrm{d}V\{-\nabla\cdot[\mathbf{E}(\mathbf{r})\times\mathbf{H}^*(\mathbf{r})]-\mathrm{i}\omega[\mathbf{E}(\mathbf{r})\cdot\mathbf{D}^*(\mathbf{r})-\mathbf{B}(\mathbf{r})\cdot\mathbf{H}^*(\mathbf{r})]\}. \end{aligned} \tag{1.27}$$

If we now define the complex Poynting vector

$$\mathbf{S}(\mathbf{r}) = \tfrac{1}{2}[\mathbf{E}(\mathbf{r}) \times \mathbf{H}^*(\mathbf{r})] \tag{1.28}$$

and the harmonic electric and magnetic energy densities

$$w_{\rm e}(\mathbf{r}) = \tfrac{1}{4}[\mathbf{E}(\mathbf{r}) \cdot \mathbf{D}^*(\mathbf{r})], \qquad w_{\rm m}(\mathbf{r}) = \tfrac{1}{4}[\mathbf{B}(\mathbf{r}) \cdot \mathbf{H}^*(\mathbf{r})], \tag{1.29}$$

and use the Gauss theorem, we have instead of Eq. (1.27)

$$\frac{1}{2} \int_V {\rm d}V \, \mathbf{J}^*(\mathbf{r}) \cdot \mathbf{E}(\mathbf{r}) + \int_S {\rm d}S \, \mathbf{S}(\mathbf{r}) \cdot \hat{\mathbf{n}} + 2{\rm i}\omega \int_V {\rm d}V [w_{\rm e}(\mathbf{r}) - w_{\rm m}(\mathbf{r})] = 0, \tag{1.30}$$

where the closed surface S encloses the volume V and $\hat{\mathbf{n}}$ is a unit vector in the direction of the local outward normal to the surface. The real part of Eq. (1.30) manifests the conservation of energy for the time-averaged quantities by requiring that the rate of the total work done by the fields on the sources within the volume, the electromagnetic energy flowing out through the volume boundary per unit time, and the time rate of change of the electromagnetic energy within the volume add up to zero. The time-averaged Poynting vector $\langle \mathbf{S}(\mathbf{r}) \rangle$ is equal to the real part of the complex Poynting vector,

$$\langle \mathbf{S}(\mathbf{r}) \rangle = {\rm Re}[\mathbf{S}(\mathbf{r})],$$

and has the dimension of [energy/(area$\times$ time)]. The net rate W at which the electromagnetic energy crosses the surface S is

$$W = -\int_S {\rm d}S \, \langle \mathbf{S}(\mathbf{r}) \rangle \cdot \hat{\mathbf{n}}. \tag{1.31}$$

The rate is positive if there is a net transfer of electromagnetic energy into the volume V and is negative otherwise.

1.2 Plane-wave solution

A fundamental feature of the Maxwell equations is that they allow for a simple traveling-wave solution, which represents the transport of electromagnetic energy from one point to another and embodies the concept of a perfectly monochromatic parallel beam of light. This solution is a plane electromagnetic wave propagating in a *homogeneous* medium without sources and is given by

$$\mathbf{E}_{\rm c}(\mathbf{r}, t) = \mathbf{E}_0 \exp({\rm i}\mathbf{k} \cdot \mathbf{r} - {\rm i}\omega t), \qquad \mathbf{H}_{\rm c}(\mathbf{r}, t) = \mathbf{H}_0 \exp({\rm i}\mathbf{k} \cdot \mathbf{r} - {\rm i}\omega t), \tag{1.32}$$

where $\mathbf{E}_0$ and $\mathbf{H}_0$ are constant complex vectors. The wave vector $\mathbf{k}$ is also constant and may, in general, be complex:

$$\mathbf{k} = \mathbf{k}_{\rm R} + {\rm i}\mathbf{k}_{\rm I}, \tag{1.33}$$

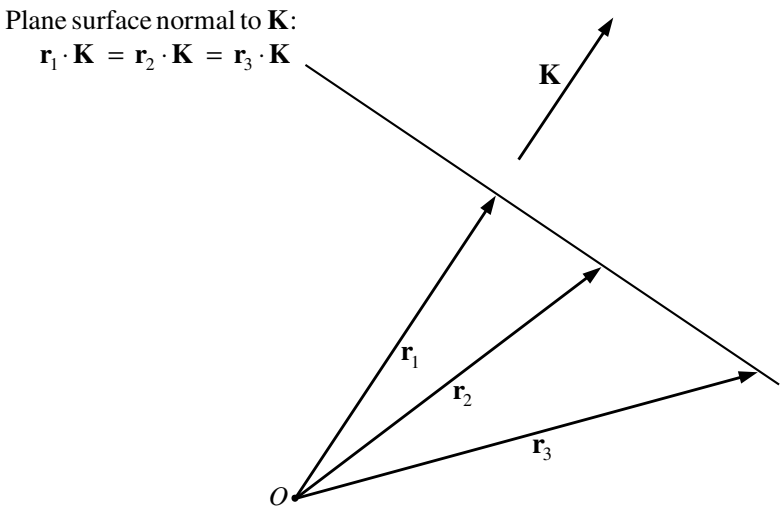

Figure 1.1. Plane surface normal to a real vector **K**.

where $\mathbf{k}_R$ and $\mathbf{k}_I$ are real vectors. We thus have

$$\mathbf{E}_c(\mathbf{r}, t) = \mathbf{E}_0 \exp(-\mathbf{k}_I \cdot \mathbf{r}) \exp(\mathrm{i}\mathbf{k}_R \cdot \mathbf{r} - \mathrm{i}\omega t), \tag{1.34}$$

$$\mathbf{H}_c(\mathbf{r}, t) = \mathbf{H}_0 \exp(-\mathbf{k}_I \cdot \mathbf{r}) \exp(\mathrm{i}\mathbf{k}_R \cdot \mathbf{r} - \mathrm{i}\omega t). \tag{1.35}$$

$\mathbf{E}_0 \exp(-\mathbf{k}_I \cdot \mathbf{r})$ and $\mathbf{H}_0 \exp(-\mathbf{k}_I \cdot \mathbf{r})$ are the amplitudes of the electric and magnetic waves, respectively, while $\mathbf{k}_R \cdot \mathbf{r} - \omega t$ is their phase. Obviously, $\mathbf{k}_R$ is normal to the surfaces of constant phase, whereas $\mathbf{k}_I$ is normal to the surfaces of constant amplitude. (A plane surface normal to a real vector **K** is defined as $\mathbf{r} \cdot \mathbf{K} = \text{constant}$, where **r** is the radius vector drawn from the origin of the reference frame to any point in the plane; see Fig. 1.1.) Surfaces of constant phase propagate in the direction of $\mathbf{k}_R$ with the phase velocity $v = \omega/|\mathbf{k}_R|$. The electromagnetic wave is called homogeneous when $\mathbf{k}_R$ and $\mathbf{k}_I$ are parallel (including the case $\mathbf{k}_I = 0$); otherwise it is called inhomogeneous. When $\mathbf{k}_R \| \mathbf{k}_I$, the complex wave vector can be written as $\mathbf{k} = (k_R + \mathrm{i}k_I)\hat{\mathbf{n}}$, where $\hat{\mathbf{n}}$ is a real unit vector in the direction of propagation and both k_R and k_I are real and non-negative.

The Maxwell equations for the plane wave take the form

$$\mathbf{k} \cdot \mathbf{E}_0 = 0, \tag{1.36}$$

$$\mathbf{k} \cdot \mathbf{H}_0 = 0, \tag{1.37}$$

$$\mathbf{k} \times \mathbf{E}_0 = \omega\mu\mathbf{H}_0, \tag{1.38}$$

$$\mathbf{k} \times \mathbf{H}_0 = -\omega\varepsilon\mathbf{E}_0. \tag{1.39}$$

The first two equations indicate that the plane electromagnetic wave is transverse: both $\mathbf{E}_0$ and $\mathbf{H}_0$ are perpendicular to **k**. Furthermore, it is evident from Eq. (1.38) or (1.39) that $\mathbf{E}_0$ and $\mathbf{H}_0$ are mutually perpendicular: $\mathbf{E}_0 \cdot \mathbf{H}_0 = 0$. Since $\mathbf{E}_0$, $\mathbf{H}_0$, and $\mathbf{k}$ are, in general, complex vectors, the physical interpretation of these facts can be far from obvious. It becomes most transparent when ε, μ, and $\mathbf{k}$ are real. The

reader can verify that in this case the real field vectors **E** and **H** are mutually perpendicular and lie in a plane normal to the direction of wave propagation.

Equations (1.32) and (1.38) yield $\mathbf{H}_{\rm c}(\mathbf{r},t)=(\omega\mu)^{-1}\,\mathbf{k}\times\mathbf{E}_{\rm c}(\mathbf{r},t)$. Therefore, a plane electromagnetic wave can always be considered in terms of only the electric (or only the magnetic) field.

By taking the vector product of both sides of Eq. (1.38) with **k** and using Eq. (1.39) and the vector identity

$$\mathbf{a}\times(\mathbf{b}\times\mathbf{c})=\mathbf{b}(\mathbf{a}\cdot\mathbf{c})-\mathbf{c}(\mathbf{a}\cdot\mathbf{b}), \tag{1.40}$$

together with Eq. (1.36), we derive

$$\mathbf{k}\cdot\mathbf{k}=\omega^2\varepsilon\mu. \tag{1.41}$$

In the practically important case of a homogeneous plane wave, we obtain from Eq. (1.41)

$$k=k_{\rm R}+{\rm i}k_{\rm I}=\omega\sqrt{\varepsilon\mu}=\frac{\omega m}{c}, \tag{1.42}$$

where k is the wave number,

$$c=\frac{1}{\sqrt{\varepsilon_0\mu_0}} \tag{1.43}$$

is the speed of light in a vacuum, and

$$m=m_{\rm R}+{\rm i}m_{\rm I}=\sqrt{\frac{\varepsilon\mu}{\varepsilon_0\mu_0}}=c\sqrt{\varepsilon\mu} \tag{1.44}$$

is the complex refractive index with non-negative real part $m_{\rm R}$ and non-negative imaginary part $m_{\rm I}$. Thus, the plane homogeneous wave has the form

$$\mathbf{E}_{\rm c}(\mathbf{r},t)=\mathbf{E}_0\exp\left(-\frac{\omega}{c}m_{\rm I}\hat{\mathbf{n}}\cdot\mathbf{r}\right)\exp\left({\rm i}\frac{\omega}{c}m_{\rm R}\hat{\mathbf{n}}\cdot\mathbf{r}-{\rm i}\omega t\right). \tag{1.45}$$

If the imaginary part of the refractive index is non-zero, then it determines the decay of the amplitude of the wave as it propagates through the medium, which is thus absorbing. The real part of the refractive index determines the phase velocity of the wave: $v=c/m_{\rm R}$. For a vacuum, $m=m_{\rm R}=1$ and $v=c$.

As follows from Eqs. (1.28), (1.32), (1.38), and (1.40), the time-averaged Poynting vector of a plane wave is

$$\begin{aligned}\langle\mathbf{S}(\mathbf{r})\rangle&=\tfrac{1}{2}{\rm Re}[\mathbf{E}(\mathbf{r})\times\mathbf{H}^*(\mathbf{r})]\\&={\rm Re}\left\{\frac{\mathbf{k}^*[\mathbf{E}(\mathbf{r})\cdot\mathbf{E}^*(\mathbf{r})]-\mathbf{E}^*(\mathbf{r})[\mathbf{k}^*\cdot\mathbf{E}(\mathbf{r})]}{2\omega\mu^*}\right\}.\end{aligned} \tag{1.46}$$

If the wave is homogeneous, then $\mathbf{k}\cdot\mathbf{E}=0$ and so $\mathbf{k}^*\cdot\mathbf{E}=0$, and

$$\langle \mathbf{S}(\mathbf{r}) \rangle = \tfrac{1}{2} \mathrm{Re}\left\{ \sqrt{\frac{\varepsilon}{\mu}} \right\} |\mathbf{E}_0|^2 \exp\left(-2 \frac{\omega}{c} m_\mathrm{I} \hat{\mathbf{n}} \cdot \mathbf{r} \right) \hat{\mathbf{n}}. \tag{1.47}$$

Thus, $\langle \mathbf{S}(\mathbf{r}) \rangle$ is in the direction of propagation and its absolute value $I(\mathbf{r}) = |\langle \mathbf{S}(\mathbf{r}) \rangle|$, usually called the intensity (or irradiance), is exponentially attenuated provided that the medium is absorbing:

$$I(\mathbf{r}) = I_0 \mathrm{e}^{-\alpha \hat{\mathbf{n}} \cdot \mathbf{r}}, \tag{1.48}$$

where I_0 is the intensity at $\mathbf{r} = 0$. The absorption coefficient α is

$$\alpha = 2 \frac{\omega}{c} m_\mathrm{I} = \frac{4\pi m_\mathrm{I}}{\lambda}, \tag{1.49}$$

where

$$\lambda = \frac{2\pi c}{\omega} \tag{1.50}$$

is the free-space wavelength. The intensity has the dimension of monochromatic energy flux: [energy/(area × time)].

The reader can verify that the choice of the time dependence $\exp(\mathrm{i}\omega t)$ rather than $\exp(-\mathrm{i}\omega t)$ in the complex representation of time-harmonic fields in Eq. (1.16) would have led to $m = m_\mathrm{R} - \mathrm{i} m_\mathrm{I}$ with a non-negative m_I. The $\exp(-\mathrm{i}\omega t)$ time-factor convention adopted here has been used in many other books on optics and light scattering (e.g., Born and Wolf 1999; Bohren and Huffman 1983; Barber and Hill 1990) and is a nearly standard choice in electromagnetics (e.g., Stratton 1941; Tsang *et al*. 1985; Kong 1990; Jackson 1998) and solid-state physics. However, van de Hulst (1957) and Kerker (1969) used the time factor $\exp(\mathrm{i}\omega t)$, which implies a non-positive imaginary part of the complex refractive index. It does not matter in the final analysis which convention is chosen because all measurable quantities of practical interest are always real. However, it is important to remember that once a choice of the time factor has been made, its consistent use throughout all derivations is essential.

1.3 Coherency matrix and Stokes parameters

Most photometric and polarimetric optical instruments cannot measure the electric and magnetic fields associated with a beam of light; rather, they measure quantities that are time averages of real-valued linear combinations of products of field vector components and have the dimension of intensity. Important examples of such observable quantities are so-called Stokes parameters. In order to define them, we will use the spherical coordinate system associated with a local right-handed Cartesian coordinate system having its origin at the observation point, as shown in Fig. 1.2. The direction of propagation of a plane electromagnetic wave in a homogeneous nonab-

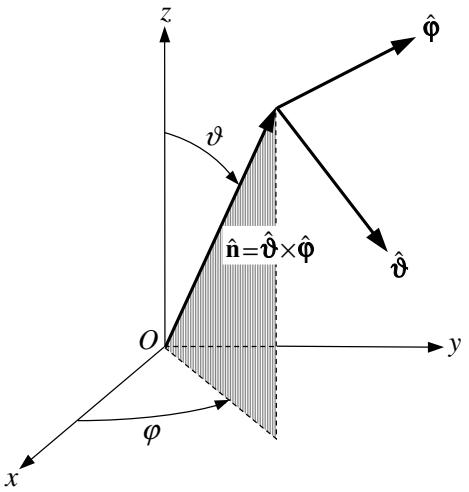

Figure 1.2. Coordinate system used to describe the direction of propagation and the polarization state of a plane electromagnetic wave.

sorbing medium is specified by a unit vector $\hat{\mathbf{n}}$ or, equivalently, by a couplet (ϑ, φ), where $\vartheta \in [0, \pi]$ is the polar (zenith) angle measured from the positive z-axis and $\varphi \in [0, 2\pi)$ is the azimuth angle measured from the positive x-axis in the clockwise direction when looking in the direction of the positive z-axis. Since the medium is assumed to be nonabsorbing, the component of the electric field vector along the direction of propagation $\hat{\mathbf{n}}$ is equal to zero, so that the electric field at the observation point is given by $\mathbf{E} = \mathbf{E}_\vartheta + \mathbf{E}_\varphi$, where $\mathbf{E}_\vartheta$ and $\mathbf{E}_\varphi$ are the ϑ- and φ-components of the electric field vector. The component $\mathbf{E}_\vartheta = E_\vartheta \hat{\boldsymbol{\vartheta}}$ lies in the meridional plane (i.e., plane through $\hat{\mathbf{n}}$ and the z-axis), whereas the component $\mathbf{E}_\varphi = E_\varphi \hat{\boldsymbol{\varphi}}$ is perpendicular to this plane; $\hat{\boldsymbol{\vartheta}}$ and $\hat{\boldsymbol{\varphi}}$ are the corresponding unit vectors such that $\hat{\mathbf{n}} = \hat{\boldsymbol{\vartheta}} \times \hat{\boldsymbol{\varphi}}$. Note that in the microwave remote sensing literature, $\mathbf{E}_\vartheta$ and $\mathbf{E}_\varphi$ are often denoted as $\mathbf{E}_\mathrm{v}$ and $\mathbf{E}_\mathrm{h}$ and called the vertical and horizontal electric field vector components, respectively (e.g., Tsang *et al.* 1985; Ulaby and Elachi 1990).

The specification of a unit vector $\hat{\mathbf{n}}$ uniquely determines the meridional plane of the propagation direction except when $\hat{\mathbf{n}}$ is oriented along the positive or negative direction of the z-axis. Although it may seem redundant to specify φ in addition to ϑ when $\vartheta = 0$ or π, the unit ϑ and φ vectors and, thus, the electric field vector components $\mathbf{E}_\vartheta$ and $\mathbf{E}_\varphi$ still depend on the orientation of the meridional plane. Therefore, we will always assume that the specification of $\hat{\mathbf{n}}$ implicitly includes the specification of the appropriate meridional plane in cases when $\hat{\mathbf{n}}$ is parallel to the z-axis. To minimize confusion, we often will specify explicitly the direction of propagation using the angles ϑ and φ; the latter uniquely defines the meridional plane when $\vartheta = 0$ or π.

Consider a plane electromagnetic wave propagating in a medium with constant real ε, μ, and k and given by

$$\mathbf{E}_{\mathrm{c}}(\mathbf{r}, t) = \mathbf{E}_0 \exp(\mathrm{i}k\hat{\mathbf{n}} \cdot \mathbf{r} - \mathrm{i}\omega t). \tag{1.51}$$

The simplest complete set of linearly independent quadratic combinations of the electric field vector components with non-zero time averages consists of the following four quantities:

$$E_{\mathrm{c}\vartheta}E^*_{\mathrm{c}\vartheta} = E_{0\vartheta}E^*_{0\vartheta}, \quad E_{\mathrm{c}\vartheta}E^*_{\mathrm{c}\varphi} = E_{0\vartheta}E^*_{0\varphi}, \quad E_{\mathrm{c}\varphi}E^*_{\mathrm{c}\vartheta} = E_{0\varphi}E^*_{0\vartheta}, \quad E_{\mathrm{c}\varphi}E^*_{\mathrm{c}\varphi} = E_{0\varphi}E^*_{0\varphi}.$$

The products of these quantities and $\frac{1}{2}\sqrt{\varepsilon/\mu}$ have the dimension of monochromatic energy flux and form the 2×2 so-called coherency (or density) matrix $\boldsymbol{\rho}$:

$$\boldsymbol{\rho} = \begin{bmatrix} \rho_{11} & \rho_{12} \\ \rho_{21} & \rho_{22} \end{bmatrix} = \frac{1}{2}\sqrt{\frac{\varepsilon}{\mu}} \begin{bmatrix} E_{0\vartheta}E^*_{0\vartheta} & E_{0\vartheta}E^*_{0\varphi} \\ E_{0\varphi}E^*_{0\vartheta} & E_{0\varphi}E^*_{0\varphi} \end{bmatrix}. \tag{1.52}$$

The completeness of the set of the four coherency matrix elements means that any plane-wave characteristic directly observable with a traditional optical instrument is a real-valued linear combination of these quantities.

Since ρ_{12} and ρ_{21} are, in general, complex, it is convenient to introduce an alternative complete set of four real, linearly independent quantities called Stokes parameters. Let us first group the elements of the 2×2 coherency matrix into a 4×1 coherency vector (O'Neill 1992):

$$\mathbf{J} = \begin{bmatrix} \rho_{11} \\ \rho_{12} \\ \rho_{21} \\ \rho_{22} \end{bmatrix} = \frac{1}{2}\sqrt{\frac{\varepsilon}{\mu}} \begin{bmatrix} E_{0\vartheta}E^*_{0\vartheta} \\ E_{0\vartheta}E^*_{0\varphi} \\ E_{0\varphi}E^*_{0\vartheta} \\ E_{0\varphi}E^*_{0\varphi} \end{bmatrix}. \tag{1.53}$$

The Stokes parameters I, Q, U, and V are then defined as the elements of a 4×1 column vector $\mathbf{I}$, otherwise known as the Stokes vector, as follows:

$$\mathbf{I} = \begin{bmatrix} I \\ Q \\ U \\ V \end{bmatrix} = \mathbf{D}\mathbf{J} = \frac{1}{2}\sqrt{\frac{\varepsilon}{\mu}} \begin{bmatrix} E_{0\vartheta}E^*_{0\vartheta} + E_{0\varphi}E^*_{0\varphi} \\ E_{0\vartheta}E^*_{0\vartheta} - E_{0\varphi}E^*_{0\varphi} \\ -E_{0\vartheta}E^*_{0\varphi} - E_{0\varphi}E^*_{0\vartheta} \\ \mathrm{i}(E_{0\varphi}E^*_{0\vartheta} - E_{0\vartheta}E^*_{0\varphi}) \end{bmatrix} = \frac{1}{2}\sqrt{\frac{\varepsilon}{\mu}} \begin{bmatrix} E_{0\vartheta}E^*_{0\vartheta} + E_{0\varphi}E^*_{0\varphi} \\ E_{0\vartheta}E^*_{0\vartheta} - E_{0\varphi}E^*_{0\varphi} \\ -2\,\mathrm{Re}(E_{0\vartheta}E^*_{0\varphi}) \\ 2\mathrm{Im}(E_{0\vartheta}E^*_{0\varphi}) \end{bmatrix}, \tag{1.54}$$

where

$$\mathbf{D} = \begin{bmatrix} 1 & 0 & 0 & 1 \\ 1 & 0 & 0 & -1 \\ 0 & -1 & -1 & 0 \\ 0 & -\mathrm{i} & \mathrm{i} & 0 \end{bmatrix}. \tag{1.55}$$

The converse relationship is

$$\mathbf{J} = \mathbf{D}^{-1}\mathbf{I}, \tag{1.56}$$

where the inverse matrix $\mathbf{D}^{-1}$ is given by

$$\mathbf{D}^{-1} = \frac{1}{2}\begin{bmatrix} 1 & 1 & 0 & 0 \\ 0 & 0 & -1 & \mathrm{i} \\ 0 & 0 & -1 & -\mathrm{i} \\ 1 & -1 & 0 & 0 \end{bmatrix}. \tag{1.57}$$

Since the Stokes parameters are real-valued and have the dimension of monochromatic energy flux, they can be measured directly with suitable optical instruments. Furthermore, they form a complete set of quantities needed to characterize a plane electromagnetic wave, inasmuch as it is subject to practical analysis. This means that (i) any other observable quantity is a linear combination of the four Stokes parameters, and (ii) it is impossible to distinguish between two plane waves with the same values of the Stokes parameters using a traditional optical device (the so-called principle of optical equivalence). Indeed, the two complex amplitudes $E_{0\vartheta} = a_\vartheta \exp(\mathrm{i}\Delta_\vartheta)$ and $E_{0\varphi} = a_\varphi \exp(\mathrm{i}\Delta_\varphi)$ are characterized by four real numbers: the non-negative amplitudes a_ϑ and a_φ and the phases Δ_ϑ and $\Delta_\varphi = \Delta_\vartheta - \Delta$. The Stokes parameters carry information about the amplitudes and the phase difference Δ, but not about Δ_ϑ. The latter is the only quantity that could be used to distinguish different waves with the same a_ϑ, a_φ, and Δ (and thus the same Stokes parameters), but it vanishes when a field vector component is multiplied by the complex conjugate value of the same or another field vector component; cf. Eqs. (1.52) and (1.54).

The first Stokes parameter, I, is the intensity introduced in the previous section; the explicit definition given in Eq. (1.54) is applicable to a homogeneous, nonabsorbing medium. The Stokes parameters Q, U, and V describe the polarization state of the wave. The ellipsometric interpretation of the Stokes parameters will be the subject of the following section. The reader can easily verify that the Stokes parameters of a plane monochromatic wave are not completely independent but rather are related by the quadratic identity

$$I^2 \equiv Q^2 + U^2 + V^2. \tag{1.58}$$

We will see later, however, that this identity may not hold for a quasi-monochromatic beam of light. Because one usually must deal with relative rather than absolute intensities, the constant factor $\frac{1}{2}\sqrt{\varepsilon/\mu}$ is often unimportant and will be omitted in all cases where this does not generate confusion.

The coherency matrix and the Stokes vector are not the only representations of polarization and not always the most convenient ones. Two other frequently used representations are the real so-called modified Stokes column vector given by

$$\mathbf{I}^{\mathrm{MS}} = \begin{bmatrix} I_{\mathrm{v}} \\ I_{\mathrm{h}} \\ U \\ V \end{bmatrix} = \mathbf{B}\mathbf{I} = \begin{bmatrix} \frac{1}{2}(I+Q) \\ \frac{1}{2}(I-Q) \\ U \\ V \end{bmatrix} \tag{1.59}$$

and the complex circular-polarization column vector defined as

$$\mathbf{I}^{\mathrm{CP}} = \begin{bmatrix} I_2 \\ I_0 \\ I_{-0} \\ I_{-2} \end{bmatrix} = \mathbf{A}\mathbf{I} = \frac{1}{2}\begin{bmatrix} Q + \mathrm{i}U \\ I + V \\ I - V \\ Q - \mathrm{i}U \end{bmatrix}, \tag{1.60}$$

where

$$\mathbf{B} = \begin{bmatrix} 1/2 & 1/2 & 0 & 0 \\ 1/2 & -1/2 & 0 & 0 \\ 0 & 0 & 1 & 0 \\ 0 & 0 & 0 & 1 \end{bmatrix}, \tag{1.61}$$

$$\mathbf{A} = \frac{1}{2}\begin{bmatrix} 0 & 1 & \mathrm{i} & 0 \\ 1 & 0 & 0 & 1 \\ 1 & 0 & 0 & -1 \\ 0 & 1 & -\mathrm{i} & 0 \end{bmatrix}. \tag{1.62}$$

It is easy to verify that

$$\mathbf{I} = \mathbf{B}^{-1}\mathbf{I}^{\mathrm{MS}} \tag{1.63}$$

and

$$\mathbf{I} = \mathbf{A}^{-1}\mathbf{I}^{\mathrm{CP}}, \tag{1.64}$$

where

$$\mathbf{B}^{-1} = \begin{bmatrix} 1 & 1 & 0 & 0 \\ 1 & -1 & 0 & 0 \\ 0 & 0 & 1 & 0 \\ 0 & 0 & 0 & 1 \end{bmatrix} \tag{1.65}$$

and

$$\mathbf{A}^{-1} = \begin{bmatrix} 0 & 1 & 1 & 0 \\ 1 & 0 & 0 & 1 \\ -\mathrm{i} & 0 & 0 & \mathrm{i} \\ 0 & 1 & -1 & 0 \end{bmatrix}. \tag{1.66}$$

1.4 Ellipsometric interpretation of Stokes parameters

In this section we show how the Stokes parameters can be used to derive the ellipsometric characteristics of the plane electromagnetic wave given by Eq. (1.51).

Writing

$$E_{0\vartheta} = a_\vartheta \exp(\mathrm{i}\Delta_\vartheta), \tag{1.67}$$

$$E_{0\varphi} = a_\varphi \exp(\mathrm{i}\Delta_\varphi) \tag{1.68}$$

with real non-negative amplitudes a_ϑ and a_φ and real phases Δ_ϑ and Δ_φ, using Eq. (1.54), and omitting the factor $\frac{1}{2}\sqrt{\varepsilon/\mu}$ we obtain for the Stokes parameters

$$I = a_\vartheta^2 + a_\varphi^2, \tag{1.69}$$

$$Q = a_\vartheta^2 - a_\varphi^2, \tag{1.70}$$

$$U = -2a_\vartheta a_\varphi \cos\Delta, \tag{1.71}$$

$$V = 2a_\vartheta a_\varphi \sin\Delta, \tag{1.72}$$

where

$$\Delta = \Delta_\vartheta - \Delta_\varphi. \tag{1.73}$$

Substituting Eqs. (1.67) and (1.68) in Eq. (1.51), we have for the real electric vector

$$E_\vartheta(\mathbf{r}, t) = a_\vartheta \cos(\delta_\vartheta - \omega t), \tag{1.74}$$

$$E_\varphi(\mathbf{r}, t) = a_\varphi \cos(\delta_\varphi - \omega t), \tag{1.75}$$

where

$$\delta_\vartheta = \Delta_\vartheta + k\hat{\mathbf{n}}\cdot\mathbf{r}, \qquad \delta_\varphi = \Delta_\varphi + k\hat{\mathbf{n}}\cdot\mathbf{r}. \tag{1.76}$$

At any fixed point O in space, the endpoint of the real electric vector given by Eqs. (1.74)–(1.76) describes an ellipse with specific major and minor axes and orientation (see the top panel of Fig. 1.3). The major axis of the ellipse makes an angle ζ with the positive direction of the φ-axis such that $\zeta \in [0, \pi)$. By definition, this orientation angle is obtained by rotating the φ-axis in the *clockwise* direction when looking in the direction of propagation, until it is directed along the major axis of the ellipse. The ellipticity is defined as the ratio of the minor to the major axes of the ellipse and is usually expressed as $|\tan\beta|$, where $\beta \in [-\pi/4, \pi/4]$. By definition, β is positive when the real electric vector at O rotates clockwise, as viewed by an observer looking in the direction of propagation. The polarization for positive β is called right-handed, as opposed to the left-handed polarization corresponding to the anti-clockwise rotation of the electric vector.

To express the orientation ζ of the ellipse and the ellipticity $|\tan\beta|$ in terms of the Stokes parameters, we first write the equations representing the rotation of the real electric vector at O in the form

$$E_q(\mathbf{r}, t) = a\sin\beta \sin(\delta - \omega t), \tag{1.77}$$

$$E_p(\mathbf{r}, t) = a\cos\beta \cos(\delta - \omega t), \tag{1.78}$$

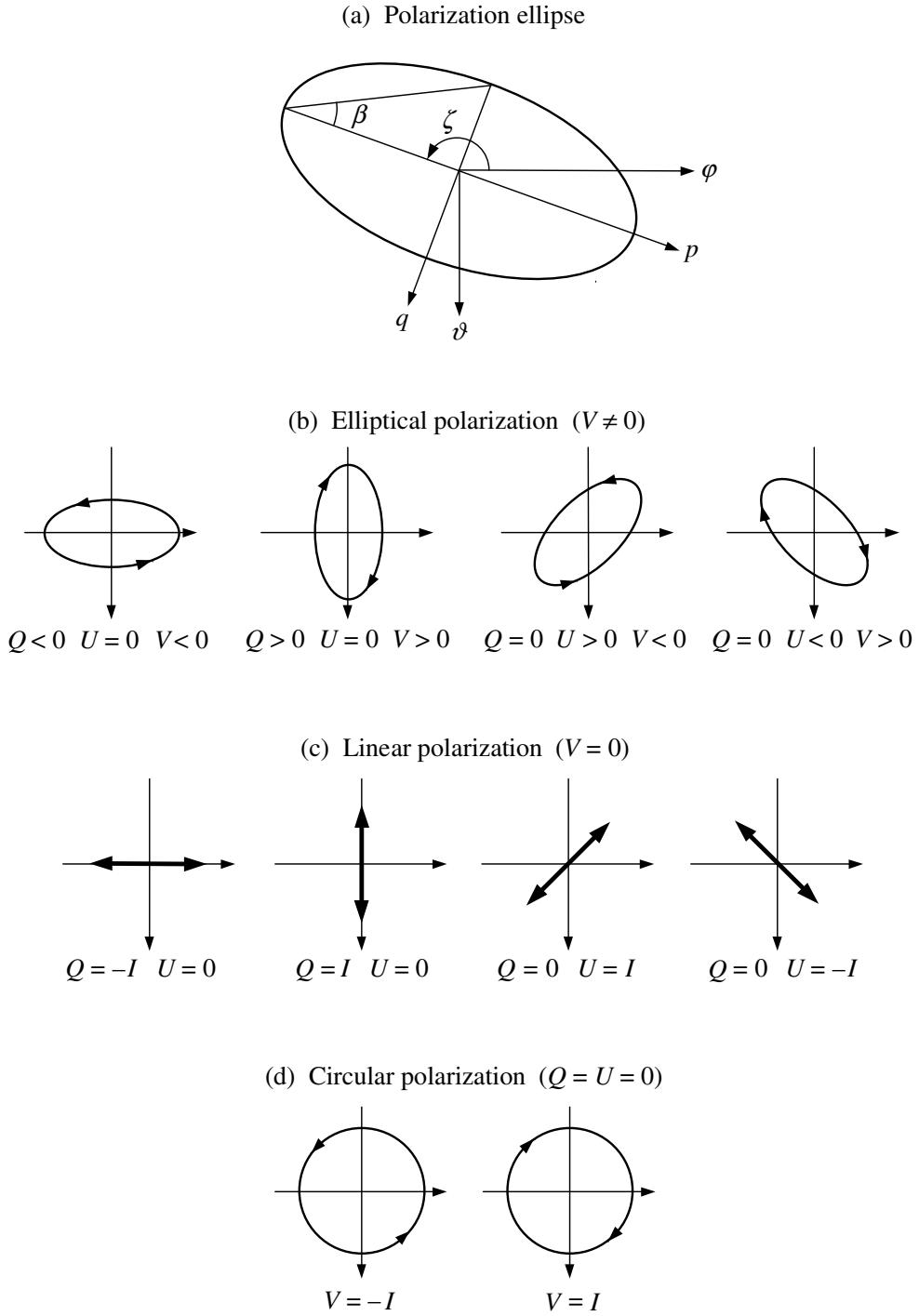

Figure 1.3. Ellipse described by the tip of the real electric vector at a fixed point O in space (upper panel) and particular cases of elliptical, linear, and circular polarization. The plane electromagnetic wave propagates in the direction $\hat{\boldsymbol{\vartheta}}\times\hat{\boldsymbol{\varphi}}$ (i.e., towards the reader).

where E_p and E_q are the electric field components along the major and minor axes of the ellipse, respectively (Fig. 1.3). One easily verifies that a positive (negative) β

indeed corresponds to the right-handed (left-handed) polarization. The connection between Eqs. (1.74)–(1.75) and Eqs. (1.77)–(1.78) can be established by using the simple transformation rule for rotation of a two-dimensional coordinate system:

$$E_\vartheta(\mathbf{r},t) = -E_q(\mathbf{r},t)\cos\zeta + E_p(\mathbf{r},t)\sin\zeta, \tag{1.79}$$

$$E_\varphi(\mathbf{r},t) = -E_q(\mathbf{r},t)\sin\zeta - E_p(\mathbf{r},t)\cos\zeta. \tag{1.80}$$

By equating the coefficients of $\cos\omega t$ and $\sin\omega t$ in the expanded Eqs. (1.74) and (1.79) and those in the expanded Eqs. (1.75) and (1.80), we obtain

$$a_\vartheta \cos\delta_\vartheta = -a\sin\beta\sin\delta\cos\zeta + a\cos\beta\cos\delta\sin\zeta, \tag{1.81}$$

$$a_\vartheta \sin\delta_\vartheta = a\sin\beta\cos\delta\cos\zeta + a\cos\beta\sin\delta\sin\zeta, \tag{1.82}$$

$$a_\varphi \cos\delta_\varphi = -a\sin\beta\sin\delta\sin\zeta - a\cos\beta\cos\delta\cos\zeta, \tag{1.83}$$

$$a_\varphi \sin\delta_\varphi = a\sin\beta\cos\delta\sin\zeta - a\cos\beta\sin\delta\cos\zeta. \tag{1.84}$$

Squaring and adding Eqs. (1.81) and (1.82) and Eqs. (1.83) and (1.84) gives

$$a_\vartheta^2 = a^2(\sin^2\beta\cos^2\zeta + \cos^2\beta\sin^2\zeta), \tag{1.85}$$

$$a_\varphi^2 = a^2(\sin^2\beta\sin^2\zeta + \cos^2\beta\cos^2\zeta). \tag{1.86}$$

Multiplying Eqs. (1.81) and (1.83) and Eqs. (1.82) and (1.84) and adding yields

$$a_\vartheta a_\varphi \cos\Delta = -\tfrac{1}{2}a^2\cos2\beta\sin2\zeta. \tag{1.87}$$

Similarly, multiplying Eqs. (1.82) and (1.83) and Eqs. (1.81) and (1.84) and subtracting gives

$$a_\vartheta a_\varphi \sin\Delta = -\tfrac{1}{2}a^2\sin2\beta. \tag{1.88}$$

Comparing Eqs. (1.69)–(1.72) with Eqs. (1.85)–(1.88), we finally derive

$$I = a^2, \tag{1.89}$$

$$Q = -I\cos2\beta\cos2\zeta, \tag{1.90}$$

$$U = I\cos2\beta\sin2\zeta, \tag{1.91}$$

$$V = -I\sin2\beta. \tag{1.92}$$

The parameters of the polarization ellipse are thus expressed in terms of the Stokes parameters as follows. The major and minor axes are given by $\sqrt{I}\cos\beta$ and $\sqrt{I}\,|\sin\beta|$, respectively (cf. Eqs. (1.77) and (1.78)). Equations (1.90) and (1.91) yield

$$\tan2\zeta = -\frac{U}{Q}. \tag{1.93}$$

Because $|\beta| \le \pi/4$, we have $\cos2\beta \ge 0$ so that $\cos2\zeta$ has the same sign as $-Q$.

Therefore, from the different values of ζ that satisfy Eq. (1.93) but differ by $\pi/2$, we must choose the one that makes the sign of $\cos 2\zeta$ the same as that of $-Q$. The ellipticity and handedness follow from

$$\tan 2\beta = -\frac{V}{\sqrt{Q^2 + U^2}}. \tag{1.94}$$

Thus, the polarization is left-handed if V is positive and right-handed if V is negative (Fig. 1.3).

The electromagnetic wave becomes linearly polarized when $\beta = 0$; then the electric vector vibrates along a line making an angle ζ with the φ-axis (cf. Fig. 1.3) and $V = 0$. Furthermore, if $\zeta = 0$ or $\zeta = \pi/2$ then U vanishes as well. This explains the usefulness of the modified Stokes representation of polarization given by Eq. (1.59) in situations involving linearly polarized light, as follows. The modified Stokes vector then has only one non-zero element and is equal to $[I\ 0\ 0\ 0]^{\mathrm{T}}$ if $\zeta = \pi/2$ (the electric vector vibrates along the ϑ-axis, i.e., in the meridional plane) or to $[0\ I\ 0\ 0]^{\mathrm{T}}$ if $\zeta = 0$ (the electric vector vibrates along the φ-axis, i.e., in the plane perpendicular to the meridional plane), where T indicates the transpose of a matrix.

If, however, $\beta = \pm\pi/4$, then both Q and U vanish, and the electric vector describes a circle either in the clockwise direction ($\beta = \pi/4$, $V = -I$) or the anticlockwise direction ($\beta = -\pi/4$, $V = I$), as viewed by an observer looking in the direction of propagation (Fig. 1.3). In this case the electromagnetic wave is circularly polarized; the circular-polarization vector $\mathbf{l}^{\mathrm{CP}}$ has only one non-zero element and takes the values $[0\ 0\ I\ 0]^{\mathrm{T}}$ and $[0\ I\ 0\ 0]^{\mathrm{T}}$, respectively (see Eq. (1.60)).

The polarization ellipse, along with a designation of the rotation direction (right- or left-handed), fully describes the temporal evolution of the real electric vector at a fixed point in space. This evolution can also be visualized by plotting the curve, in (ϑ, φ, t) coordinates, described by the tip of the electric vector as a function of time. For example, in the case of an elliptically polarized plane wave with right-handed polarization the curve is a right-handed helix with an elliptical projection onto the $\vartheta\varphi$-plane centered around the t-axis (Fig. 1.4(a)). The pitch of the helix is simply $2\pi/\omega$, where ω is the angular frequency of the wave. Another way to visualize a plane wave is to fix a moment in time and draw a three-dimensional curve in (ϑ, φ, s) coordinates described by the tip of the electric vector as a function of a spatial coordinate $s = \mathbf{r} \cdot \hat{\mathbf{n}}$ oriented along the direction of propagation $\hat{\mathbf{n}}$. According to Eqs. (1.74)–(1.76), the electric field is the same for all position–time combinations with constant $ks - \omega t$. Therefore, at any instant of time (say, $t = 0$) the locus of the points described by the tip of the electric vector originating at different points on the s-axis is also a helix, with the same projection onto the $\vartheta\varphi$-plane as the respective helix in the (ϑ, φ, t) coordinates but with opposite handedness. For example, for the wave with right-handed elliptical polarization shown in Fig. 1.4(a), the respective curve in the (ϑ, φ, s) coordinates is a left-handed elliptical helix, shown in Fig.

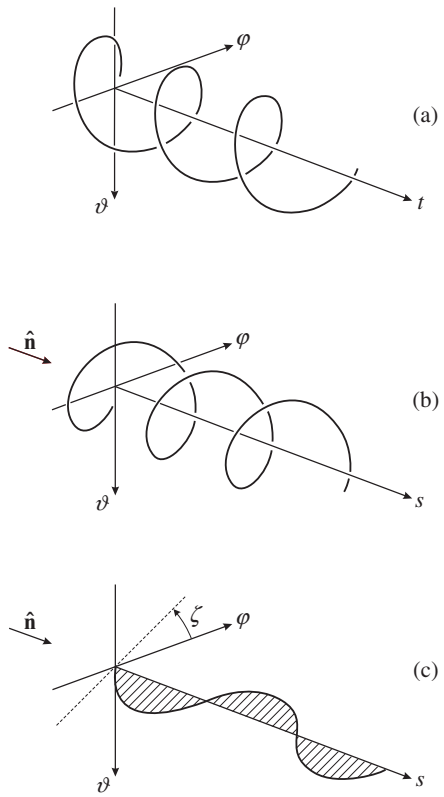

Figure 1.4. (a) The helix described by the tip of the real electric vector of a plane electromagnetic wave with right-handed polarization in (ϑ, φ, t) coordinates at a fixed point in space. (b) As in (a), but in (ϑ, φ, s) coordinates at a fixed moment in time. (c) As in (b), but for a linearly polarized wave.

1.4(b). The pitch of this helix is the wavelength λ. It is now clear that the propagation of the wave in time and space can be represented by progressive movement in time of the helix shown in Fig. 1.4(b) in the direction of $\hat{\mathbf{n}}$ with the speed of light. With increasing time, the intersection of the helix with any plane s = constant describes a right-handed vibration ellipse. In the case of a circularly polarized wave, the elliptical helix becomes a helix with a circular projection onto the $\vartheta\varphi$-plane. If the wave is linearly polarized, then the helix degenerates into a simple sinusoidal curve in the plane making an angle ζ with the φ-axis (Fig. 1.4(c)).

1.5 Rotation transformation rule for Stokes parameters

The Stokes parameters of a plane electromagnetic wave are always defined with respect to a reference plane containing the direction of wave propagation. If the reference plane is rotated about the direction of propagation then the Stokes parameters are modified according to a rotation transformation rule, which can be derived as follows. Consider a rotation of the coordinate axes ϑ and φ through an angle $0 \le \eta < 2\pi$ in

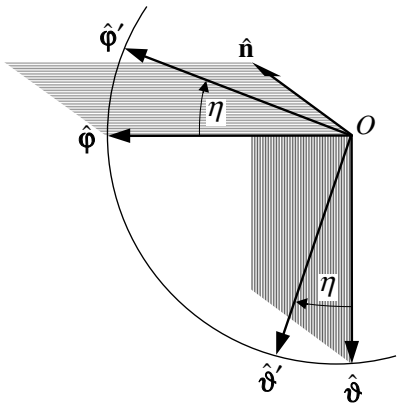

Figure 1.5. Rotation of the ϑ- and φ-axes through an angle $\eta \geq 0$ around $\hat{\mathbf{n}}$ in the clockwise direction when looking in the direction of propagation.

the *clockwise* direction when looking in the direction of propagation (Fig. 1.5). The transformation rule for rotation of a two-dimensional coordinate system yields

$$E'_{0\vartheta} = E_{0\vartheta}\cos\eta + E_{0\varphi}\sin\eta, \tag{1.95}$$

$$E'_{0\varphi} = -E_{0\vartheta}\sin\eta + E_{0\varphi}\cos\eta, \tag{1.96}$$

where the primes denote the electric field vector components with respect to the new reference frame. It then follows from Eq. (1.54) that the rotation transformation rule for the Stokes parameters is

$$\mathbf{I}' = \begin{bmatrix} I' \\ Q' \\ U' \\ V' \end{bmatrix} = \mathbf{L}(\eta)\mathbf{I} = \begin{bmatrix} 1 & 0 & 0 & 0 \\ 0 & \cos 2\eta & -\sin 2\eta & 0 \\ 0 & \sin 2\eta & \cos 2\eta & 0 \\ 0 & 0 & 0 & 1 \end{bmatrix} \begin{bmatrix} I \\ Q \\ U \\ V \end{bmatrix}, \tag{1.97}$$

where $\mathbf{L}(\eta)$ is called the Stokes rotation matrix for angle η. It is obvious that a $\eta = \pi$ rotation does not change the Stokes parameters.

Because

$$(\mathbf{I}^{\mathrm{MS}})' = \mathbf{B}\mathbf{I}' = \mathbf{B}\mathbf{L}(\eta)\mathbf{I} = \mathbf{B}\mathbf{L}(\eta)\mathbf{B}^{-1}\mathbf{I}^{\mathrm{MS}}, \tag{1.98}$$

the rotation matrix for the modified Stokes vector is given by

$$\mathbf{L}^{\mathrm{MS}}(\eta) = \mathbf{B}\mathbf{L}(\eta)\mathbf{B}^{-1} = \begin{bmatrix} \cos^2\eta & \sin^2\eta & -\frac{1}{2}\sin 2\eta & 0 \\ \sin^2\eta & \cos^2\eta & \frac{1}{2}\sin 2\eta & 0 \\ \sin 2\eta & -\sin 2\eta & \cos 2\eta & 0 \\ 0 & 0 & 0 & 1 \end{bmatrix}. \tag{1.99}$$

Similarly, for the circular polarization representation,

$$(\mathbf{I}^{\mathrm{CP}})' = \mathbf{A}\mathbf{I}' = \mathbf{A}\mathbf{L}(\eta)\mathbf{I} = \mathbf{A}\mathbf{L}(\eta)\mathbf{A}^{-1}\mathbf{I}^{\mathrm{CP}}, \tag{1.100}$$

and the corresponding rotation matrix is diagonal (Hovenier and van der Mee 1983):

$$\mathbf{L}^{\mathrm{CP}}(\eta) = \mathbf{A}\mathbf{L}(\eta)\mathbf{A}^{-1} = \begin{bmatrix} \exp(\mathrm{i}2\eta) & 0 & 0 & 0 \\ 0 & 1 & 0 & 0 \\ 0 & 0 & 1 & 0 \\ 0 & 0 & 0 & \exp(-\mathrm{i}2\eta) \end{bmatrix}. \tag{1.101}$$

1.6 Quasi-monochromatic light and incoherent addition of Stokes parameters

The definition of a monochromatic plane electromagnetic wave given by Eqs. (1.51) and (1.67)–(1.68) implies that the complex amplitude $\mathbf{E}_0$ and, therefore, the quantities a_ϑ, a_φ, Δ_ϑ, and Δ_φ are constant. In reality, these quantities often fluctuate in time. Although the typical frequency of these fluctuations is much smaller than the angular frequency ω, it is still so high that most optical devices are incapable of tracing the instantaneous values of the Stokes parameters but rather measure averages of the Stokes parameters over a relatively long period of time. Therefore, we must modify the definition of the Stokes parameters for such *quasi-monochromatic* beam of light as follows:

$$I = \langle E_{0\vartheta} E^*_{0\vartheta} \rangle + \langle E_{0\varphi} E^*_{0\varphi} \rangle = \langle a^2_\vartheta \rangle + \langle a^2_\varphi \rangle, \tag{1.102}$$

$$Q = \langle E_{0\vartheta} E^*_{0\vartheta} \rangle - \langle E_{0\varphi} E^*_{0\varphi} \rangle = \langle a^2_\vartheta \rangle - \langle a^2_\varphi \rangle, \tag{1.103}$$

$$U = -\langle E_{0\vartheta} E^*_{0\varphi} \rangle - \langle E_{0\varphi} E^*_{0\vartheta} \rangle = -2\langle a_\vartheta a_\varphi \cos\Delta \rangle, \tag{1.104}$$

$$V = \mathrm{i}\langle E_{0\varphi} E^*_{0\vartheta} \rangle - \mathrm{i}\langle E_{0\vartheta} E^*_{0\varphi} \rangle = 2\langle a_\vartheta a_\varphi \sin\Delta \rangle, \tag{1.105}$$

where we have omitted the common factor $\frac{1}{2}\sqrt{\varepsilon/\mu}$ and

$$\langle f \rangle = \frac{1}{T} \int_t^{t+T} \mathrm{d}t' f(t') \tag{1.106}$$

denotes the average over a time interval T long compared with the typical period of fluctuation.

The identity (1.58) is not valid, in general, for a quasi-monochromatic beam. Indeed, now we have

$$\begin{aligned} & I^2 - Q^2 - U^2 - V^2 \\ & = 4[\langle a^2_\vartheta \rangle \langle a^2_\varphi \rangle - \langle a_\vartheta a_\varphi \cos\Delta \rangle^2 - \langle a_\vartheta a_\varphi \sin\Delta \rangle^2] \\ & = \frac{4}{T^2} \int_t^{t+T} \mathrm{d}t' \int_t^{t+T} \mathrm{d}t'' \{ [a_\vartheta(t')]^2 [a_\varphi(t'')]^2 \\ & \qquad - a_\vartheta(t') a_\varphi(t') \cos[\Delta(t')] a_\vartheta(t'') a_\varphi(t'') \cos[\Delta(t'')] \\ & \qquad - a_\vartheta(t') a_\varphi(t') \sin[\Delta(t')] a_\vartheta(t'') a_\varphi(t'') \sin[\Delta(t'')] \} \end{aligned}$$

$$
\begin{aligned}
&= \frac{4}{T^2}\int_t^{t+T} \mathrm{d}t' \int_t^{t+T} \mathrm{d}t''\{[a_\vartheta(t')]^2[a_\varphi(t'')]^2 \\
&\qquad\qquad -a_\vartheta(t')a_\varphi(t')a_\vartheta(t'')a_\varphi(t'')\cos[\Delta(t')-\Delta(t'')]\} \\
&= \frac{2}{T^2}\int_t^{t+T} \mathrm{d}t' \int_t^{t+T} \mathrm{d}t''\{[a_\vartheta(t')]^2[a_\varphi(t'')]^2+[a_\vartheta(t'')]^2[a_\varphi(t')]^2 \\
&\qquad\qquad -2a_\vartheta(t')a_\varphi(t')a_\vartheta(t'')a_\varphi(t'')\cos[\Delta(t')-\Delta(t'')]\} \\
&\geq \frac{2}{T^2}\int_t^{t+T} \mathrm{d}t' \int_t^{t+T} \mathrm{d}t''\{[a_\vartheta(t')]^2[a_\varphi(t'')]^2+[a_\vartheta(t'')]^2[a_\varphi(t')]^2 \\
&\qquad\qquad -2a_\vartheta(t')a_\varphi(t')a_\vartheta(t'')a_\varphi(t'')\} \\
&= \frac{2}{T^2}\int_t^{t+T} \mathrm{d}t' \int_t^{t+T} \mathrm{d}t''[a_\vartheta(t')a_\varphi(t'')-a_\vartheta(t'')a_\varphi(t')]^2 \\
&\geq 0\,,
\end{aligned}
$$

thereby yielding

$$I^2 \geq Q^2+U^2+V^2. \tag{1.107}$$

The equality holds only if the ratio $a_\vartheta(t)/a_\varphi(t)$ of the real amplitudes and the phase difference $\Delta(t)$ are independent of time, which means that $E_{0\vartheta}(t)$ and $E_{0\varphi}(t)$ are completely correlated. In this case the beam is said to be fully (or completely) polarized. This definition includes a monochromatic wave, but is, of course, more general. However, if $a_\vartheta(t)$, $a_\varphi(t)$, $\Delta_\vartheta(t)$, and $\Delta_\varphi(t)$ are totally uncorrelated and $\langle a_\vartheta^2\rangle = \langle a_\varphi^2\rangle$, then $Q = U = V = 0$, and the quasi-monochromatic beam of light is said to be unpolarized (or natural). This means that the parameters of the vibration ellipse traced by the endpoint of the electric vector fluctuate in such a way that there is no preferred vibration ellipse.

When two or more quasi-monochromatic beams propagating in the same direction are mixed incoherently (i.e., there is no permanent phase relationship between the separate beams), the Stokes vector of the mixture is equal to the sum of the Stokes vectors of the individual beams:

$$\mathbf{I} = \sum_n \mathbf{I}_n, \tag{1.108}$$

where n numbers the beams. Indeed, inserting Eqs. (1.67) and (1.68) in Eq. (1.54), we obtain for the total intensity

$$
\begin{aligned}
I &= \sum_n\sum_m \langle a_{\vartheta n}a_{\vartheta m}\exp[\mathrm{i}(\Delta_{\vartheta n}-\Delta_{\vartheta m})]+a_{\varphi n}a_{\varphi m}\exp[\mathrm{i}(\Delta_{\varphi n}-\Delta_{\varphi m})]\rangle \\
&= \sum_n I_n + \sum_n\sum_{m\neq n}\langle a_{\vartheta n}a_{\vartheta m}\exp[\mathrm{i}(\Delta_{\vartheta n}-\Delta_{\vartheta m})]+a_{\varphi n}a_{\varphi m}\exp[\mathrm{i}(\Delta_{\varphi n}-\Delta_{\varphi m})]\rangle.
\end{aligned} \tag{1.109}
$$

Since the phases of different beams are uncorrelated, the second term on the right-

hand side of the relation above vanishes. Hence

$$I = \sum_n I_n, \tag{1.110}$$

and similarly for Q, U, and V. Of course, this additivity rule also applies to the coherency matrix $\boldsymbol{\rho}$, the modified Stokes vector $\mathbf{I}^{\rm MS}$, and the circular-polarization vector $\mathbf{I}^{\rm CP}$. An important example demonstrating the application of Eq. (1.108) is the scattering of light by a small volume element containing randomly positioned particles. The phases of the individual waves scattered by the particles depend on the positions of the particles. Therefore, if the distribution of the particles is sufficiently random then the individual scattered waves will be incoherent and the Stokes vectors of the individual waves will add. The additivity of the Stokes parameters allows us to generalize the principle of optical equivalence (Section 1.3) to quasi-monochromatic light as follows: it is impossible by means of a traditional optical instrument to distinguish between various incoherent mixtures of quasi-monochromatic beams that form a beam with the same Stokes parameters (I, Q, U, V). For example, there is only one kind of unpolarized light, although it can be composed of quasi-monochromatic beams in an infinite variety of optically indistinguishable ways.

In view of the general inequality (1.107), it is always possible *mathematically* to decompose any quasi-monochromatic beam into two parts, one unpolarized, with a Stokes vector

$$[I - \sqrt{Q^2 + U^2 + V^2} \quad 0 \quad 0 \quad 0]^{\rm T},$$

and one fully polarized, with a Stokes vector

$$[\sqrt{Q^2 + U^2 + V^2} \quad Q \quad U \quad V]^{\rm T}.$$

Thus, the intensity of the fully polarized component is $\sqrt{Q^2 + U^2 + V^2}$, so that the degree of (elliptical) polarization of the quasi-monochromatic beam is

$$P = \frac{\sqrt{Q^2 + U^2 + V^2}}{I}. \tag{1.111}$$

We further define the degree of linear polarization as

$$P_{\rm L} = \frac{\sqrt{Q^2 + U^2}}{I} \tag{1.112}$$

and the degree of circular polarization as

$$P_{\rm C} = \frac{V}{I}. \tag{1.113}$$

P vanishes for unpolarized light and is equal to unity for fully polarized light. For a partially polarized beam $(0 < P < 1)$ with $V \neq 0$, the sign of V indicates the preferen-

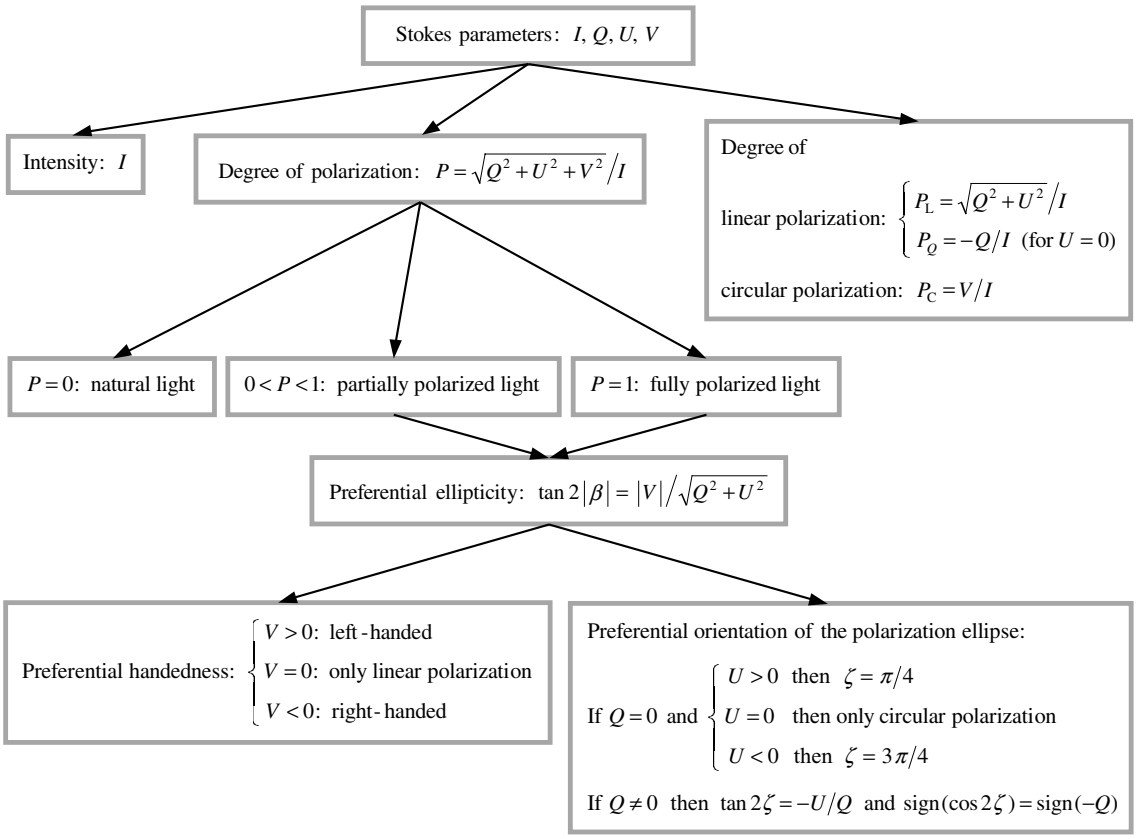

Figure 1.6. Analysis of a quasi-monochromatic beam with Stokes parameters I, Q, U, and V.

tial handedness of the vibration ellipses described by the endpoint of the electric vector: a positive V indicates left-handed polarization and a negative V indicates right-handed polarization. By analogy with Eqs. (1.93) and (1.94), the quantities $-U/Q$ and $|V|/\sqrt{Q^2+U^2}$ may be interpreted as specifying the preferential orientation and ellipticity of the vibration ellipse. Unlike the Stokes parameters, these quantities are not additive. In view of the rotation transformation rule (1.97), P, $P_{\rm L}$, and $P_{\rm C}$ are invariant with respect to rotations of the reference frame around the direction of propagation. When $U=0$, the ratio

$$P_Q=-\frac{Q}{I} \tag{1.114}$$

is also called the degree of linear polarization (or the *signed* degree of linear polarization). P_Q is positive when the vibrations of the electric vector in the φ-direction (i.e., the direction perpendicular to the meridional plane of the beam) dominate those in the ϑ-direction and is negative otherwise. The standard polarimetric analysis of a general quasi-monochromatic beam with Stokes parameters I, Q, U, and V is summarized in Fig. 1.6 (after Hovenier *et al*. 2005).

Further reading

Excellent treatments of classical electrodynamics and optics are provided by Stratton (1941), Kong (1990), Jackson (1998), and Born and Wolf (1999). The optical properties of bulk matter and their measurement are discussed in Chapters 9 and 10 of Bohren and Huffman (1983) as well as in the comprehensive handbook edited by Palik and Ghosh (1997). Several books are entirely devoted to polarization, for example Shurcliff (1962), Clarke and Grainger (1971), Azzam and Bashara (1977), Kliger *et al*. (1990), Collett (1992), and Brosseau (1998). In Pye (2001), numerous manifestations of polarization in science and nature are discussed.

Chapter 2

Scattering, absorption, and emission of electromagnetic radiation by an arbitrary finite particle

The presence of an object with a refractive index different from that of the surrounding medium changes the electromagnetic field that would otherwise exist in an unbounded homogeneous space. The difference of the total field in the presence of the object and the original field that would exist in the absence of the object can be thought of as the field *scattered* by the object. In other words, the total field is equal to the vector sum of the *incident* (original) field and the *scattered* field.

The angular distribution and polarization of the scattered field depend on the polarization and directional characteristics of the incident field as well as on such properties of the scatterer as its size relative to the wavelength and its shape, composition, and orientation. Therefore, in practice one usually must solve the scattering problem anew every time some or all of these input parameters change. It is appropriate, however, to consider first the general mathematical description of the scattering process without making any detailed assumptions about the scattering object except that it is composed of a linear and isotropic material. Hence the goal of this chapter is to establish a basic theoretical framework underlying more specific problems discussed in the following chapters.

2.1 Volume integral equation

Consider a finite scattering object in the form of a single body or a fixed aggregate embedded in an infinite, homogeneous, linear, isotropic, and nonabsorbing medium (Fig. 2.1(a)). Mathematically, this is equivalent to dividing all space into two mutually disjoint regions, the finite interior region $V_{\rm INT}$ occupied by the scattering object and the infinite exterior region $V_{\rm EXT}$. The region $V_{\rm INT}$ is filled with an isotropic, linear, and possibly inhomogeneous material.

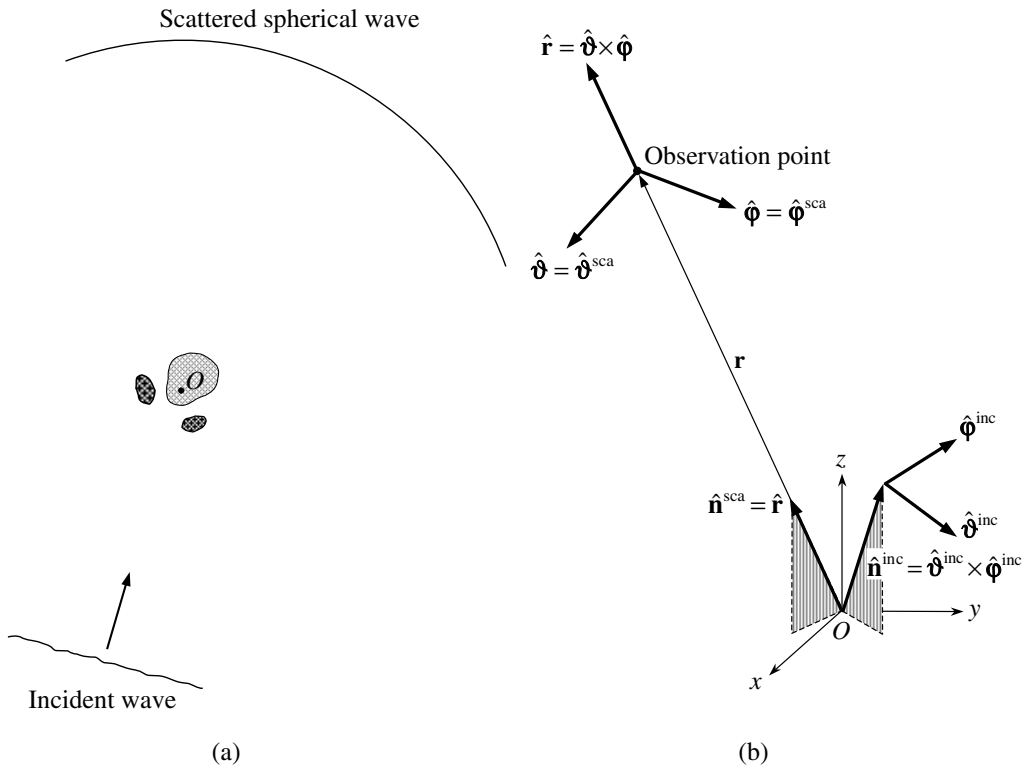

Figure 2.1. Schematic representation of the electromagnetic scattering problem. The unshaded exterior region V_{EXT} is unbounded in all directions and the shaded areas collectively constitute the interior region V_{INT}.

It is well known that optical properties of bulk substances in solid or liquid phase are qualitatively different from those of their constituent atoms and molecules when the latter are isolated. This may cause a problem when one applies the concept of bulk optical constants to a very small particle because either the optical constants determined for bulk matter provide an inaccurate estimate or the particle is so small that the entire concept of optical constants loses its validity. We will therefore assume that the individual bodies forming the scattering object are sufficiently large that they can still be characterized by optical constants appropriate to bulk matter. According to Huffman (1988), this implies that each body is larger than approximately 50 Å.

The monochromatic Maxwell curl equations (1.18) and (1.20) describing the scattering problem can be rewritten as follows:

$$\left.\begin{aligned} \nabla \times \mathbf{E}(\mathbf{r}) &= \mathrm{i}\omega\mu_1 \mathbf{H}(\mathbf{r}) \\ \nabla \times \mathbf{H}(\mathbf{r}) &= -\mathrm{i}\omega\varepsilon_1 \mathbf{E}(\mathbf{r}) \end{aligned}\right\} \qquad \mathbf{r} \in V_{\mathrm{EXT}}, \tag{2.1}$$

$$\left.\begin{aligned} \nabla \times \mathbf{E}(\mathbf{r}) &= \mathrm{i}\omega\mu_2(\mathbf{r}) \mathbf{H}(\mathbf{r}) \\ \nabla \times \mathbf{H}(\mathbf{r}) &= -\mathrm{i}\omega\varepsilon_2(\mathbf{r}) \mathbf{E}(\mathbf{r}) \end{aligned}\right\} \qquad \mathbf{r} \in V_{\mathrm{INT}}, \tag{2.2}$$

where the subscripts 1 and 2 refer to the exterior and interior regions, respectively. Since the first relations in Eqs. (2.1) and (2.2) yield the magnetic field provided that

the electric field is known everywhere, we will look for the solution of Eqs. (2.1) and (2.2) in terms of only the electric field. Assuming that the host medium and the scattering object are nonmagnetic, i.e., $\mu_2(\mathbf{r}) \equiv \mu_1 = \mu_0$, where μ_0 is the permeability of a vacuum, we easily derive the following vector wave equations:

$$\nabla\times\nabla\times\mathbf{E}(\mathbf{r}) - k_1^2\mathbf{E}(\mathbf{r}) = 0, \qquad \mathbf{r}\in V_{\rm EXT}, \tag{2.3}$$

$$\nabla\times\nabla\times\mathbf{E}(\mathbf{r}) - k_2^2(\mathbf{r})\mathbf{E}(\mathbf{r}) = 0, \qquad \mathbf{r}\in V_{\rm INT}, \tag{2.4}$$

where $k_1 = \omega\sqrt{\varepsilon_1\mu_0}$ and $k_2(\mathbf{r}) = \omega\sqrt{\varepsilon_2(\mathbf{r})\mu_0}$ are the wave numbers of the exterior and interior regions, respectively. The permittivity for the interior region is regarded as a function of $\mathbf{r}$, to provide for the general case where the scattering object is inhomogeneous. Equations (2.3) and (2.4) can be rewritten as the single inhomogeneous differential equation

$$\nabla\times\nabla\times\mathbf{E}(\mathbf{r}) - k_1^2\mathbf{E}(\mathbf{r}) = \mathbf{j}(\mathbf{r}), \qquad \mathbf{r}\in V_{\rm EXT}\cup V_{\rm INT}, \tag{2.5}$$

where

$$\mathbf{j}(\mathbf{r}) = k_1^2[\tilde{m}^2(\mathbf{r}) - 1]\,\mathbf{E}(\mathbf{r}), \tag{2.6a}$$

$$\tilde{m}(\mathbf{r}) = \begin{cases} 1, & \mathbf{r}\in V_{\rm EXT}, \\ m(\mathbf{r}) = k_2(\mathbf{r})/k_1 = m_2(\mathbf{r})/m_1, & \mathbf{r}\in V_{\rm INT}, \end{cases} \tag{2.6b}$$

and $m(\mathbf{r})$ is the refractive index of the interior relative to that of the exterior. The forcing function $\mathbf{j}(\mathbf{r})$ obviously vanishes everywhere outside the interior region.

Any solution of an inhomogeneous linear differential equation can be divided into two parts: (i) a solution of the respective homogeneous equation with the right-hand side identically equal to zero and (ii) a particular solution of the inhomogeneous equation. Thus, the first part satisfies the equation

$$\nabla\times\nabla\times\mathbf{E}^{\rm inc}(\mathbf{r}) - k_1^2\mathbf{E}^{\rm inc}(\mathbf{r}) = 0, \qquad \mathbf{r}\in V_{\rm EXT}\cup V_{\rm INT}, \tag{2.7}$$

and describes the field that would exist in the absence of the scattering object, i.e., the *incident field.* The physically appropriate particular solution of Eq. (2.5) must give the *scattered field* $\mathbf{E}^{\rm sca}(\mathbf{r})$ generated by the forcing function $\mathbf{j}(\mathbf{r})$. Obviously, of all possible particular solutions of Eq. (2.5) we must choose the one that vanishes at large distances from the scattering object and ensures energy conservation.

To find $\mathbf{E}^{\rm sca}(\mathbf{r})$, we first introduce the free space dyadic Green's function $\ddot{G}(\mathbf{r},\mathbf{r}')$ as a dyadic (Cartesian tensor) satisfying the differential equation

$$\nabla\times\nabla\times\ddot{G}(\mathbf{r},\mathbf{r}') - k_1^2\ddot{G}(\mathbf{r},\mathbf{r}') = \ddot{I}\delta(\mathbf{r}-\mathbf{r}'), \tag{2.8}$$

where $\ddot{I}$ is the identity dyadic and $\delta(\mathbf{r}-\mathbf{r}') = \delta(x-x')\delta(y-y')\delta(z-z')$ is the three-dimensional Dirac delta function. Note that the result of a dyadic operating on a vector is another vector (see, e.g., Appendix 3 of Van Bladel 1964). This operation may be thought of as a 3×3 matrix representing the dyadic multiplying a column matrix consisting of the initial vector components, thereby producing another column matrix consisting of the resulting vector components. The components of both vectors must

be specified in the same coordinate system. From a coordinate-free standpoint, a dyadic can be introduced as a sum of so-called dyads, each dyad being the result of a dyadic product of two vectors $\mathbf{a}\otimes\mathbf{b}$ such that the operation $(\mathbf{a}\otimes\mathbf{b})\cdot\mathbf{c}$ yields the vector $\mathbf{a}(\mathbf{b}\cdot\mathbf{c})$ and the operation $\mathbf{c}\cdot(\mathbf{a}\otimes\mathbf{b})$ yields the vector $(\mathbf{c}\cdot\mathbf{a})\mathbf{b}$. Any dyadic can be represented as a sum of at most nine dyads. The vector product $(\mathbf{a}\otimes\mathbf{b})\times\mathbf{c}$ is defined as a dyad $\mathbf{a}\otimes(\mathbf{b}\times\mathbf{c})$, and $\mathbf{c}\times(\mathbf{a}\otimes\mathbf{b})$ yields $(\mathbf{c}\times\mathbf{a})\otimes\mathbf{b}$. The dot product of dyads $\mathbf{a}\otimes\mathbf{b}$ and $\mathbf{c}\otimes\mathbf{d}$ yields the dyad $(\mathbf{b}\cdot\mathbf{c})(\mathbf{a}\otimes\mathbf{d})$.

Taking into account that

$$\nabla\times[\ddot{G}(\mathbf{r},\mathbf{r}')\cdot\mathbf{j}(\mathbf{r}')]=[\nabla\times\ddot{G}(\mathbf{r},\mathbf{r}')]\cdot\mathbf{j}(\mathbf{r}'),$$

we get

$$\nabla\times\nabla\times[\ddot{G}(\mathbf{r},\mathbf{r}')\cdot\mathbf{j}(\mathbf{r}')]-k_1^2[\ddot{G}(\mathbf{r},\mathbf{r}')\cdot\mathbf{j}(\mathbf{r}')]=\ddot{I}\cdot\mathbf{j}(\mathbf{r}')\delta(\mathbf{r}-\mathbf{r}'). \tag{2.9}$$

We integrate both sides of this equation over the entire space to obtain

$$(\nabla\times\nabla\times\ddot{I}-k_1^2\ddot{I})\cdot\int_{V_{\mathrm{INT}}\cup V_{\mathrm{EXT}}}\mathrm{d}\mathbf{r}'\ddot{G}(\mathbf{r},\mathbf{r}')\cdot\mathbf{j}(\mathbf{r}')=\mathbf{j}(\mathbf{r}). \tag{2.10}$$

Comparison with Eq. (2.5) now shows that

$$\mathbf{E}^{\mathrm{sca}}(\mathbf{r})=\int_{V_{\mathrm{INT}}}\mathrm{d}\mathbf{r}'\ddot{G}(\mathbf{r},\mathbf{r}')\cdot\mathbf{j}(\mathbf{r}'),\qquad \mathbf{r}\in V_{\mathrm{INT}}\cup V_{\mathrm{EXT}}, \tag{2.11}$$

where we have taken into account that $\mathbf{j}(\mathbf{r})$ vanishes everywhere outside V_{INT}. We will see in the following section that this particular solution of Eq. (2.5) indeed vanishes at infinity and ensures energy conservation and is therefore the physically appropriate particular solution. Hence, the complete solution of Eq. (2.5) is

$$\mathbf{E}(\mathbf{r})=\mathbf{E}^{\mathrm{inc}}(\mathbf{r})+\int_{V_{\mathrm{INT}}}\mathrm{d}\mathbf{r}'\ddot{G}(\mathbf{r},\mathbf{r}')\cdot\mathbf{j}(\mathbf{r}'),\qquad \mathbf{r}\in V_{\mathrm{INT}}\cup V_{\mathrm{EXT}}. \tag{2.12}$$

To find the free space dyadic Green's function $\ddot{G}(\mathbf{r},\mathbf{r}')$, we first express it in terms of a scalar Green's function $g(\mathbf{r},\mathbf{r}')$ as follows:

$$\ddot{G}(\mathbf{r},\mathbf{r}')=\left(\ddot{I}+\frac{1}{k_1^2}\nabla\otimes\nabla\right)g(\mathbf{r},\mathbf{r}'). \tag{2.13}$$

Inserting Eq. (2.13) into Eq. (2.8) and noticing that

$$\nabla\times[\nabla\times(\nabla\otimes\nabla)]=\nabla\times[(\nabla\times\nabla)\otimes\nabla]=0,$$
$$\nabla\times\nabla\times(\ddot{I}g)=\nabla\otimes\nabla g-\ddot{I}\,\nabla^2 g,$$

we obtain the following differential equation for g:

$$(\nabla^2+k_1^2)g(\mathbf{r},\mathbf{r}')=-\delta(\mathbf{r}-\mathbf{r}'). \tag{2.14}$$

The well-known solution of this equation representing so-called *outgoing* waves (i.e., satisfying the condition $\lim_{k_1|\mathbf{r}-\mathbf{r}'|\to\infty}g(\mathbf{r},\mathbf{r}')=0$) is

$$g(\mathbf{r},\mathbf{r}') = \frac{\mathrm{e}^{\mathrm{i}k_1|\mathbf{r}-\mathbf{r}'|}}{4\pi|\mathbf{r}-\mathbf{r}'|} \tag{2.15}$$

(e.g., Jackson 1998, p. 427). Hence, Eqs. (2.6), (2.12), (2.13), and (2.15) finally yield (Shifrin 1968; Saxon 1955b)

$$\begin{aligned}\mathbf{E}(\mathbf{r}) &= \mathbf{E}^{\mathrm{inc}}(\mathbf{r}) + k_1^2 \int_{V_{\mathrm{INT}}} \mathrm{d}\mathbf{r}'\, \ddot{G}(\mathbf{r},\mathbf{r}')\cdot\mathbf{E}(\mathbf{r}')\,[m^2(\mathbf{r}')-1] \\ &= \mathbf{E}^{\mathrm{inc}}(\mathbf{r}) + k_1^2\left(\ddot{I} + \frac{1}{k_1^2}\nabla\otimes\nabla\right)\cdot\int_{V_{\mathrm{INT}}} \mathrm{d}\mathbf{r}'\,[m^2(\mathbf{r}')-1]\,\mathbf{E}(\mathbf{r}')\,\frac{\mathrm{e}^{\mathrm{i}k_1|\mathbf{r}-\mathbf{r}'|}}{4\pi|\mathbf{r}-\mathbf{r}'|}, \\ &\qquad \mathbf{r}\in V_{\mathrm{INT}}\cup V_{\mathrm{EXT}}.\end{aligned} \tag{2.16}$$

Equation (2.16) expresses the total electric field everywhere in space in terms of the incident field and the total field inside the scattering object. Since the latter is not known in general, one must solve Eq. (2.16) either numerically or analytically. As a first step, the internal field can be approximated by the incident field. This is the gist of the so-called Rayleigh–Gans approximation otherwise known as the Rayleigh–Debye or Born approximation (van de Hulst 1957; Ishimaru 1997). The total field computed in the Rayleigh-Gans approximation can be substituted in the integral on the right-hand side of Eq. (2.16) in order to compute an improved approximation, and this iterative process can be continued until the total field converges within a given numerical accuracy. Although this procedure can be rather involved, it shows that in the final analysis the total electric field can be expressed in terms of the incident field as follows:

$$\mathbf{E}(\mathbf{r}) = \mathbf{E}^{\mathrm{inc}}(\mathbf{r}) + \int_{V_{\mathrm{INT}}} \mathrm{d}\mathbf{r}'\,\ddot{G}(\mathbf{r},\mathbf{r}')\cdot\int_{V_{\mathrm{INT}}} \mathrm{d}\mathbf{r}''\,\ddot{T}(\mathbf{r}',\mathbf{r}'')\cdot\mathbf{E}^{\mathrm{inc}}(\mathbf{r}''), \qquad \mathbf{r}\in V_{\mathrm{INT}}\cup V_{\mathrm{EXT}}, \tag{2.17}$$

where $\ddot{T}$ is the so-called dyadic transition operator (Tsang *et al*. 1985). Substituting Eq. (2.17) in Eq. (2.16), we derive the following integral equation for $\ddot{T}$:

$$\begin{aligned}\ddot{T}(\mathbf{r},\mathbf{r}') &= k_1^2[m^2(\mathbf{r})-1]\delta(\mathbf{r}-\mathbf{r}')\ddot{I} \\ &\quad + k_1^2[m^2(\mathbf{r})-1]\int_{V_{\mathrm{INT}}} \mathrm{d}\mathbf{r}''\,\ddot{G}(\mathbf{r},\mathbf{r}'')\cdot\ddot{T}(\mathbf{r}'',\mathbf{r}'), \qquad \mathbf{r},\mathbf{r}'\in V_{\mathrm{INT}}.\end{aligned} \tag{2.18}$$

Equations of this type appear in the quantum theory of scattering and are called Lippmann-Schwinger equations (Lippmann and Schwinger 1950; Newton 1966).

2.2 Scattering in the far-field zone

Let us now choose an arbitrary point O close to the geometrical center of the scattering object as the common origin of all position (radius) vectors (Figs. 2.1(a), (b)). Usually one is interested in calculating the scattered field in the so-called far-field

zone. Specifically, let us assume that $k_1 r \gg 1$ and that r is much greater than any linear dimension of the scattering object ($r \gg r'$ for any $\mathbf{r}' \in V_{\rm INT}$). Since

$$|\mathbf{r}-\mathbf{r}'| = r\sqrt{1-2\frac{\hat{\mathbf{r}}\cdot\mathbf{r}'}{r}+\frac{r'^2}{r^2}} \approx r-\hat{\mathbf{r}}\cdot\mathbf{r}'+\frac{r'^2}{2r}, \tag{2.19}$$

where $\hat{\mathbf{r}} = \mathbf{r}/r$ is the unit vector in the direction of $\mathbf{r}$ (Fig. 2.1(b)), we have

$$g(\mathbf{r},\mathbf{r}') \approx \frac{\mathrm{e}^{\mathrm{i}k_1 r}}{4\pi r}\mathrm{e}^{-\mathrm{i}k_1\hat{\mathbf{r}}\cdot\mathbf{r}'},$$

where it is also assumed that $k_1 r'^2/2r \ll 1$. Therefore,

$$\ddot{G}(\mathbf{r},\mathbf{r}') \approx (\ddot{I}-\hat{\mathbf{r}}\otimes\hat{\mathbf{r}})\frac{\mathrm{e}^{\mathrm{i}k_1 r}}{4\pi r}\mathrm{e}^{-\mathrm{i}k_1\hat{\mathbf{r}}\cdot\mathbf{r}'}. \tag{2.20}$$

In deriving Eq. (2.20), we have taken into account that in spherical coordinates, defined in Section 1.3, centered at the origin,

$$\nabla = \hat{\mathbf{r}}\frac{\partial}{\partial r}+\hat{\boldsymbol{\vartheta}}\frac{1}{r}\frac{\partial}{\partial\vartheta}+\hat{\boldsymbol{\varphi}}\frac{1}{r\sin\vartheta}\frac{\partial}{\partial\varphi}, \tag{2.21}$$

where the order of operator components relative to the unit basis vectors is essential because $\hat{\mathbf{r}}$, $\hat{\boldsymbol{\vartheta}}$, and $\hat{\boldsymbol{\varphi}}$ depend on ϑ and φ. Hence,

$$\mathbf{E}^{\rm sca}(\mathbf{r}) \approx \frac{\mathrm{e}^{\mathrm{i}k_1 r}}{r}\frac{k_1^2}{4\pi}(\ddot{I}-\hat{\mathbf{r}}\otimes\hat{\mathbf{r}})\cdot\int_{V_{\rm INT}}\mathrm{d}\mathbf{r}'[m^2(\mathbf{r}')-1]\,\mathbf{E}(\mathbf{r}')\mathrm{e}^{-\mathrm{i}k_1\hat{\mathbf{r}}\cdot\mathbf{r}'}. \tag{2.22}$$

This important formula shows that the scattered field at a large distance from the object behaves as an outgoing transverse spherical wave. Specifically, since the identity dyadic in the spherical coordinate system centered at the origin is given by

$$\ddot{I} = \hat{\mathbf{r}}\otimes\hat{\mathbf{r}}+\hat{\boldsymbol{\vartheta}}\otimes\hat{\boldsymbol{\vartheta}}+\hat{\boldsymbol{\varphi}}\otimes\hat{\boldsymbol{\varphi}},$$

the factor $\ddot{I}-\hat{\mathbf{r}}\otimes\hat{\mathbf{r}} = \hat{\boldsymbol{\vartheta}}\otimes\hat{\boldsymbol{\vartheta}}+\hat{\boldsymbol{\varphi}}\otimes\hat{\boldsymbol{\varphi}}$ ensures that the scattered wave in the far-field zone is transverse, i.e., the electric field vector is always perpendicular to the direction of propagation $\hat{\mathbf{r}}$:

$$\hat{\mathbf{r}}\cdot\mathbf{E}^{\rm sca}(\mathbf{r}) = 0. \tag{2.23}$$

Hence, only the ϑ- and φ-components of the electric vector of the scattered field are non-zero. Furthermore, the scattered field decays inversely with distance r from the scattering object. Equation (2.22) can be rewritten in the form

$$\mathbf{E}^{\rm sca}(\mathbf{r}) = \frac{\mathrm{e}^{\mathrm{i}k_1 r}}{r}\mathbf{E}_1^{\rm sca}(\hat{\mathbf{r}}), \qquad \hat{\mathbf{r}}\cdot\mathbf{E}_1^{\rm sca}(\hat{\mathbf{r}}) = 0, \tag{2.24}$$

where the vector $\mathbf{E}_1^{\rm sca}(\hat{\mathbf{r}})$ is independent of r and describes the angular distribution of the scattered radiation in the far-field zone. Obviously, this solution also obeys the

energy conservation law by making the total energy flux across a spherical surface of radius r independent of r.

Assuming that the incident field is a plane electromagnetic wave given by

$$\mathbf{E}^{\rm inc}(\mathbf{r}) = \mathbf{E}_0^{\rm inc} \exp({\rm i}k_1\hat{\mathbf{n}}^{\rm inc}\cdot\mathbf{r}) \tag{2.25}$$

and using Eq. (2.17), we derive for the far-field zone

$$\mathbf{E}^{\rm sca}(r\hat{\mathbf{n}}^{\rm sca}) = \frac{{\rm e}^{{\rm i}k_1 r}}{r}\vec{A}(\hat{\mathbf{n}}^{\rm sca},\hat{\mathbf{n}}^{\rm inc})\cdot\mathbf{E}_0^{\rm inc}, \tag{2.26}$$

where $\hat{\mathbf{n}}^{\rm sca} = \hat{\mathbf{r}}$ (Fig. 2.1(b)) and the scattering dyadic $\vec{A}$ is given by

$$\vec{A}(\hat{\mathbf{n}}^{\rm sca},\hat{\mathbf{n}}^{\rm inc}) = \frac{1}{4\pi}(\vec{I}-\hat{\mathbf{n}}^{\rm sca}\otimes\hat{\mathbf{n}}^{\rm sca})\cdot\int_{V_{\rm INT}} {\rm d}\mathbf{r}'\exp(-{\rm i}k_1\hat{\mathbf{n}}^{\rm sca}\cdot\mathbf{r}')$$
$$\times\int_{V_{\rm INT}} {\rm d}\mathbf{r}''\vec{T}(\mathbf{r}',\mathbf{r}'')\exp({\rm i}k_1\hat{\mathbf{n}}^{\rm inc}\cdot\mathbf{r}''). \tag{2.27}$$

The elements of the scattering dyadic have the dimension of length.

Equation (2.17) shows that if $\mathbf{E}_1^{\rm inc}(\mathbf{r})$ and $\mathbf{E}_2^{\rm inc}(\mathbf{r})$ are two different incident fields and $\mathbf{E}_1^{\rm sca}(\mathbf{r})$ and $\mathbf{E}_2^{\rm sca}(\mathbf{r})$ are the corresponding scattered fields, then $\mathbf{E}_1^{\rm sca}(\mathbf{r})+\mathbf{E}_2^{\rm sca}(\mathbf{r})$ is the scattered field corresponding to the incident field $\mathbf{E}_1^{\rm inc}(\mathbf{r})+\mathbf{E}_2^{\rm inc}(\mathbf{r})$. This result is, of course, a consequence of the linearity of Maxwell's equations (2.1) and (2.2) and constitutive relations (1.8)–(1.10) and a manifestation of the well-known principle of superposition: if two electromagnetic fields satisfy the Maxwell equations, then their sum also satisfies these equations. Therefore, although the scattering dyadic $\vec{A}$ describes the scattering of a plane electromagnetic wave, it can be used to compute the scattering of any incident field as long as the latter can be expanded in elementary plane waves.

It follows from Eqs. (2.23) and (2.27) that

$$\hat{\mathbf{n}}^{\rm sca}\cdot\vec{A}(\hat{\mathbf{n}}^{\rm sca},\hat{\mathbf{n}}^{\rm inc}) = 0. \tag{2.28}$$

However, because the incident field given by Eq. (2.25) is a transverse wave with electric vector perpendicular to the direction of propagation, the dot product $\vec{A}(\hat{\mathbf{n}}^{\rm sca},\hat{\mathbf{n}}^{\rm inc})\cdot\hat{\mathbf{n}}^{\rm inc}$ is not defined by Eq. (2.26). To complete the definition, we take this product to be zero:

$$\vec{A}(\hat{\mathbf{n}}^{\rm sca},\hat{\mathbf{n}}^{\rm inc})\cdot\hat{\mathbf{n}}^{\rm inc} = 0, \tag{2.29}$$

which means that one must retain only the part of the expression on the right-hand side of Eq. (2.27) that is transverse to the incidence direction. As a consequence of Eqs. (2.28) and (2.29), only four out of the nine components of the scattering dyadic are independent. It is therefore convenient to formulate the scattering problem in the spherical coordinate system centered at the origin and to introduce the 2×2 so-called amplitude scattering matrix $\mathbf{S}$, which describes the transformation of the ϑ- and φ-components of the incident plane wave into the ϑ- and φ-components of the scattered spherical wave:

$$\begin{bmatrix} E_{\vartheta}^{\rm sca}(r\hat{\mathbf{n}}^{\rm sca}) \\ E_{\varphi}^{\rm sca}(r\hat{\mathbf{n}}^{\rm sca}) \end{bmatrix} = \frac{e^{ik_1 r}}{r} \mathbf{S}(\hat{\mathbf{n}}^{\rm sca}, \hat{\mathbf{n}}^{\rm inc}) \begin{bmatrix} E_{0\vartheta}^{\rm inc} \\ E_{0\varphi}^{\rm inc} \end{bmatrix}. \tag{2.30}$$

The amplitude scattering matrix depends on the directions of incidence and scattering as well as on the size, morphology, composition, and orientation of the scattering object with respect to the coordinate system. As will be discussed in Section 2.11, it also depends on the choice of origin of the coordinate system inside the scattering object. If known, the amplitude scattering matrix gives the scattered and thus the total field, thereby providing a complete description of the scattering pattern in the far-field zone. The elements of the amplitude scattering matrix have the dimension of length and are expressed in terms of the scattering dyadic as follows:

$$S_{11} = \hat{\boldsymbol{\vartheta}}^{\rm sca} \cdot \vec{\vec{A}} \cdot \hat{\boldsymbol{\vartheta}}^{\rm inc}, \tag{2.31}$$

$$S_{12} = \hat{\boldsymbol{\vartheta}}^{\rm sca} \cdot \vec{\vec{A}} \cdot \hat{\boldsymbol{\varphi}}^{\rm inc}, \tag{2.32}$$

$$S_{21} = \hat{\boldsymbol{\varphi}}^{\rm sca} \cdot \vec{\vec{A}} \cdot \hat{\boldsymbol{\vartheta}}^{\rm inc}, \tag{2.33}$$

$$S_{22} = \hat{\boldsymbol{\varphi}}^{\rm sca} \cdot \vec{\vec{A}} \cdot \hat{\boldsymbol{\varphi}}^{\rm inc}. \tag{2.34}$$

We have pointed out in Section 1.3 that when a wave propagates along the z-axis, the ϑ- and φ-components of the electric field vector are determined by the specific choice of meridional plane. Therefore, the amplitude scattering matrix explicitly depends on $\varphi^{\rm inc}$ and $\varphi^{\rm sca}$ even when $\vartheta^{\rm inc} = 0$ or π and/or $\vartheta^{\rm sca} = 0$ or π.

2.3 Reciprocity

A fundamental property of the scattering dyadic is the reciprocity relation, which is a manifestation of the symmetry of the scattering process with respect to an inversion of time (Saxon 1955a). To derive the reciprocity relation, we first consider the scattering of a spherical incoming wave by an arbitrary finite object embedded in an infinite, homogeneous, nonabsorbing medium. In the far-field zone of the object, the total electric field is the sum of the incoming and scattered spherical waves:

$$\mathbf{E}(r\hat{\mathbf{r}}) = \frac{e^{-ik_1 r}}{r} \mathbf{E}^{\rm inc}(\hat{\mathbf{r}}) + \frac{e^{ik_1 r}}{r} \mathbf{E}^{\rm sca}(\hat{\mathbf{r}}), \tag{2.35}$$

where $\mathbf{E}^{\rm inc}(\hat{\mathbf{r}})$ and $\mathbf{E}^{\rm sca}(\hat{\mathbf{r}})$ are independent of r and

$$\hat{\mathbf{r}} \cdot \mathbf{E}^{\rm inc}(\hat{\mathbf{r}}) = 0, \tag{2.36}$$

$$\hat{\mathbf{r}} \cdot \mathbf{E}^{\rm sca}(\hat{\mathbf{r}}) = 0. \tag{2.37}$$

Equation (2.37) follows from Eq. (2.24), whereas Eq. (2.36) follows from the divergence condition

$$\nabla \cdot \mathbf{E}(\mathbf{r}) = 0 \tag{2.38}$$

(Eq. (1.17) with ε_1 = constant) and the following relations:

$$\nabla\cdot(f\mathbf{a}) = f\nabla\cdot\mathbf{a} + (\nabla f)\cdot\mathbf{a}, \tag{2.39}$$

$$\nabla\frac{\mathrm{e}^{\pm\mathrm{i}k_1 r}}{r} = -\left(\frac{1}{r}\mp\mathrm{i}k_1\right)\frac{\mathrm{e}^{\pm\mathrm{i}k_1 r}}{r}\hat{\mathbf{r}}, \tag{2.40}$$

$$\nabla\cdot\left[\frac{\mathrm{e}^{-\mathrm{i}k_1 r}}{r}\mathbf{E}^{\mathrm{inc}}(\hat{\mathbf{r}})\right] = \frac{\mathrm{e}^{-\mathrm{i}k_1 r}}{r}\nabla\cdot\mathbf{E}^{\mathrm{inc}}(\hat{\mathbf{r}}) - \left(\frac{1}{r}+\mathrm{i}k_1\right)\frac{\mathrm{e}^{-\mathrm{i}k_1 r}}{r}\hat{\mathbf{r}}\cdot\mathbf{E}^{\mathrm{inc}}(\hat{\mathbf{r}}) = 0, \tag{2.41}$$

$$\nabla\cdot\mathbf{E}^{\mathrm{inc}}(\hat{\mathbf{r}}) \underset{r\to\infty}{=} O(r^{-1}). \tag{2.42}$$

The latter is a consequence of Eq. (2.21) and the fact that $\mathbf{E}^{\mathrm{inc}}(\hat{\mathbf{r}})$ is independent of r.

Because of the linearity of the Maxwell equations and by analogy with Eq. (2.26), the outgoing spherical wave must be linearly related to the incoming spherical wave. Following Saxon (1955a), we express this relationship in terms of the so-called scattering tensor $\ddot{S}$ as follows:

$$\mathbf{E}^{\mathrm{sca}}(\hat{\mathbf{r}}) = -\int_{4\pi}\mathrm{d}\hat{\mathbf{r}}'\,\ddot{S}(\hat{\mathbf{r}},\hat{\mathbf{r}}')\cdot\mathbf{E}^{\mathrm{inc}}(-\hat{\mathbf{r}}'), \tag{2.43}$$

where

$$\int_{4\pi}\mathrm{d}\hat{\mathbf{r}}' = \int_0^{2\pi}\mathrm{d}\varphi'\int_0^{\pi}\mathrm{d}\vartheta'\sin\vartheta'. \tag{2.44}$$

In view of Eq. (2.37), we have

$$\hat{\mathbf{r}}\cdot\ddot{S}(\hat{\mathbf{r}},\hat{\mathbf{r}}') = 0. \tag{2.45}$$

Since $\mathbf{E}^{\mathrm{inc}}(\hat{\mathbf{r}})$ is transverse, the product $\ddot{S}(\hat{\mathbf{r}},\hat{\mathbf{r}}')\cdot\hat{\mathbf{r}}'$ remains undefined by Eq. (2.43). Therefore, we will complete the definition of the scattering tensor by taking this product to be zero:

$$\ddot{S}(\hat{\mathbf{r}},\hat{\mathbf{r}}')\cdot\hat{\mathbf{r}}' = 0. \tag{2.46}$$

As a consequence of Eqs. (2.45) and (2.46), $\ddot{S}$ has only four independent components.

The derivation of the reciprocity relation for the scattering tensor starts from the fact that if $\mathbf{E}_1$ and $\mathbf{E}_2$ are any two solutions of the source-free Maxwell equations (but with the same harmonic time dependence) then

$$r^2\int_{4\pi}\mathrm{d}\hat{\mathbf{r}}\,\hat{\mathbf{r}}\cdot\{\mathbf{E}_2(r\hat{\mathbf{r}})\times[\nabla\times\mathbf{E}_1(r\hat{\mathbf{r}})] - \mathbf{E}_1(r\hat{\mathbf{r}})\times[\nabla\times\mathbf{E}_2(r\hat{\mathbf{r}})]\} \underset{r\to\infty}{=} 0. \tag{2.47}$$

Indeed, using Eqs. (1.26), (2.1), and (2.2), it can easily be established that $\nabla\cdot(\mathbf{E}_2\times\mathbf{H}_1 - \mathbf{E}_1\times\mathbf{H}_2)$ vanishes identically everywhere in space. Integrating $\nabla\cdot(\mathbf{E}_2\times\mathbf{H}_1 - \mathbf{E}_1\times\mathbf{H}_2)$ over all space and applying the Gauss theorem then yields Eq. (2.47). We now take $\mathbf{E}_1$ and $\mathbf{E}_2$ to be superpositions of incoming and outgoing spherical waves:

$$\mathbf{E}_j(r\hat{\mathbf{r}}) \underset{r\to\infty}{=} \frac{\mathrm{e}^{-\mathrm{i}k_1 r}}{r}\mathbf{E}_j^{\mathrm{inc}}(\hat{\mathbf{r}}) + \frac{\mathrm{e}^{\mathrm{i}k_1 r}}{r}\mathbf{E}_j^{\mathrm{sca}}(\hat{\mathbf{r}}), \qquad j = 1, 2. \tag{2.48}$$

Taking into account Eq. (1.40), (2.36), (2.37), and (2.40) and the formulas

$$\nabla\times(f\mathbf{a}) = (\nabla f)\times\mathbf{a} + f(\nabla\times\mathbf{a}), \tag{2.49}$$

$$\nabla\times\mathbf{E}_{1,2}^{\mathrm{inc,sca}}(\hat{\mathbf{r}}) \underset{r\to\infty}{=} O(r^{-1}), \tag{2.50}$$

cf. Eq. (2.21), we derive the following after some algebra:

$$\int_{4\pi} \mathrm{d}\hat{\mathbf{r}}[\mathbf{E}_2^{\mathrm{inc}}(\hat{\mathbf{r}})\cdot\mathbf{E}_1^{\mathrm{sca}}(\hat{\mathbf{r}}) - \mathbf{E}_1^{\mathrm{inc}}(\hat{\mathbf{r}})\cdot\mathbf{E}_2^{\mathrm{sca}}(\hat{\mathbf{r}})] = 0. \tag{2.51}$$

Using Eq. (2.43) to express the outgoing waves in terms of the incoming waves, we then have

$$\int_{4\pi} \mathrm{d}\hat{\mathbf{r}} \int_{4\pi} \mathrm{d}\hat{\mathbf{r}}'[\mathbf{E}_2^{\mathrm{inc}}(\hat{\mathbf{r}})\cdot\vec{S}(\hat{\mathbf{r}},\hat{\mathbf{r}}')\cdot\mathbf{E}_1^{\mathrm{inc}}(-\hat{\mathbf{r}}') - \mathbf{E}_1^{\mathrm{inc}}(\hat{\mathbf{r}})\cdot\vec{S}(\hat{\mathbf{r}},\hat{\mathbf{r}}')\cdot\mathbf{E}_2^{\mathrm{inc}}(-\hat{\mathbf{r}}')] = 0. \tag{2.52}$$

Replacing $\hat{\mathbf{r}}$ by $-\hat{\mathbf{r}}'$ and $\hat{\mathbf{r}}'$ by $-\hat{\mathbf{r}}$ in the last term and transposing the tensor product according to the identity

$$\mathbf{a}\cdot\vec{B}\cdot\mathbf{c} = \mathbf{c}\cdot\vec{B}^{\mathrm{T}}\cdot\mathbf{a}$$

we derive

$$\int_{4\pi} \mathrm{d}\hat{\mathbf{r}} \int_{4\pi} \mathrm{d}\hat{\mathbf{r}}'\mathbf{E}_2^{\mathrm{inc}}(\hat{\mathbf{r}})\cdot[\vec{S}(\hat{\mathbf{r}},\hat{\mathbf{r}}') - \vec{S}^{\mathrm{T}}(-\hat{\mathbf{r}}',-\hat{\mathbf{r}})]\cdot\mathbf{E}_1^{\mathrm{inc}}(-\hat{\mathbf{r}}') = 0, \tag{2.53}$$

where T denotes the transposed tensor:

$$(\vec{S}^{\mathrm{T}})_{ij} = \vec{S}_{ji}. \tag{2.54}$$

Since $\mathbf{E}_1^{\mathrm{inc}}$ and $\mathbf{E}_2^{\mathrm{inc}}$ are arbitrary, we finally have

$$\vec{S}(\hat{\mathbf{r}},\hat{\mathbf{r}}') = \vec{S}^{\mathrm{T}}(-\hat{\mathbf{r}}',-\hat{\mathbf{r}}). \tag{2.55}$$

This is the reciprocity condition for the scattering tensor.

It should be remarked that in deriving Eq. (2.47) we assumed, as almost everywhere else in this book, that the permeability, permittivity, and conductivity are scalars. However, it is easily checked that Eq. (2.47) and thus the reciprocity condition (2.55) remain valid even when the permeability, permittivity, and conductivity of the scattering object are tensors, provided that all these tensors are symmetric. If any of these tensors is not symmetric, then Eq. (2.55) may become invalid (Dolginov *et al.* 1995; Lacoste and van Tiggelen 1999).

We now use Eq. (2.55) to derive the reciprocity relation for the scattering dyadic $\vec{A}$ by considering the case in which the scattering object is illuminated by a plane wave incident along the direction $\hat{\mathbf{n}}^{\mathrm{inc}}$. As follows from Eqs. (2.24) and (2.25), the total electric field in the far-field zone is given by

$$\mathbf{E}(r\hat{\mathbf{n}}^{\rm sca}) = \mathbf{E}_0^{\rm inc}\exp({\rm i}k_1 r\hat{\mathbf{n}}^{\rm inc}\cdot\hat{\mathbf{n}}^{\rm sca}) + \mathbf{E}_1^{\rm sca}(\hat{\mathbf{n}}^{\rm sca})\frac{{\rm e}^{{\rm i}k_1 r}}{r}. \tag{2.56}$$

Representing the incident plane wave as a superposition of incoming and outgoing spherical waves,

$$\exp({\rm i}k_1 r\hat{\mathbf{n}}^{\rm inc}\cdot\hat{\mathbf{n}}^{\rm sca}) \underset{k_1 r\to\infty}{=} \frac{{\rm i}2\pi}{k_1}\left[\delta(\hat{\mathbf{n}}^{\rm inc}+\hat{\mathbf{n}}^{\rm sca})\frac{{\rm e}^{-{\rm i}k_1 r}}{r} - \delta(\hat{\mathbf{n}}^{\rm inc}-\hat{\mathbf{n}}^{\rm sca})\frac{{\rm e}^{{\rm i}k_1 r}}{r}\right] \tag{2.57}$$

(see Appendix A), where

$$\delta(\hat{\mathbf{n}}^{\rm inc}\pm\hat{\mathbf{n}}^{\rm sca}) = \delta(\cos\vartheta^{\rm inc}\pm\cos\vartheta^{\rm sca})\,\delta(\varphi^{\rm inc}\pm\varphi^{\rm sca}) \tag{2.58}$$

is the solid-angle Dirac delta function, we derive

$$\begin{aligned}\mathbf{E}(r\hat{\mathbf{n}}^{\rm sca}) \underset{k_1 r\to\infty}{=}& \frac{{\rm i}2\pi}{k_1}\mathbf{E}_0^{\rm inc}\,\delta(\hat{\mathbf{n}}^{\rm inc}+\hat{\mathbf{n}}^{\rm sca})\frac{{\rm e}^{-{\rm i}k_1 r}}{r}\\ &+\left[\mathbf{E}_1^{\rm sca}(\hat{\mathbf{n}}^{\rm sca}) - \frac{{\rm i}2\pi}{k_1}\delta(\hat{\mathbf{n}}^{\rm inc}-\hat{\mathbf{n}}^{\rm sca})\mathbf{E}_0^{\rm inc}\right]\frac{{\rm e}^{{\rm i}k_1 r}}{r}.\end{aligned} \tag{2.59}$$

Considering this a special form of Eq. (2.35) and recalling the definition of the scattering tensor, Eq. (2.43), we have

$$\mathbf{E}_1^{\rm sca}(\hat{\mathbf{n}}^{\rm sca}) = \frac{{\rm i}2\pi}{k_1}[\delta(\hat{\mathbf{n}}^{\rm inc}-\hat{\mathbf{n}}^{\rm sca})\mathbf{E}_0^{\rm inc} - \ddot{S}(\hat{\mathbf{n}}^{\rm sca},\hat{\mathbf{n}}^{\rm inc})\cdot\mathbf{E}_0^{\rm inc}]. \tag{2.60}$$

It now follows from the definition of the scattering dyadic, Eqs. (2.26), (2.28), and (2.29), that

$$\ddot{A}(\hat{\mathbf{n}}^{\rm sca},\hat{\mathbf{n}}^{\rm inc}) = \frac{{\rm i}2\pi}{k_1}[(\ddot{I}-\hat{\mathbf{n}}^{\rm inc}\otimes\hat{\mathbf{n}}^{\rm inc})\,\delta(\hat{\mathbf{n}}^{\rm inc}-\hat{\mathbf{n}}^{\rm sca}) - \ddot{S}(\hat{\mathbf{n}}^{\rm sca},\hat{\mathbf{n}}^{\rm inc})]. \tag{2.61}$$

Finally, from Eqs. (2.55) and (2.61) we derive the reciprocity relation for the scattering dyadic:

$$\ddot{A}(-\hat{\mathbf{n}}^{\rm inc},-\hat{\mathbf{n}}^{\rm sca}) = \ddot{A}^{\rm T}(\hat{\mathbf{n}}^{\rm sca},\hat{\mathbf{n}}^{\rm inc}). \tag{2.62}$$

The reciprocity relation for the amplitude scattering matrix follows from Eqs. (2.31)–(2.34) and (2.62) and the unit vector identities

$$\hat{\boldsymbol{\vartheta}}(-\hat{\mathbf{n}}) = \hat{\boldsymbol{\vartheta}}(\hat{\mathbf{n}}), \qquad \hat{\boldsymbol{\varphi}}(-\hat{\mathbf{n}}) = -\hat{\boldsymbol{\varphi}}(\hat{\mathbf{n}}). \tag{2.63}$$

Simple algebra gives

$$\mathbf{S}(-\hat{\mathbf{n}}^{\rm inc},-\hat{\mathbf{n}}^{\rm sca}) = \begin{bmatrix} S_{11}(\hat{\mathbf{n}}^{\rm sca},\hat{\mathbf{n}}^{\rm inc}) & -S_{21}(\hat{\mathbf{n}}^{\rm sca},\hat{\mathbf{n}}^{\rm inc}) \\ -S_{12}(\hat{\mathbf{n}}^{\rm sca},\hat{\mathbf{n}}^{\rm inc}) & S_{22}(\hat{\mathbf{n}}^{\rm sca},\hat{\mathbf{n}}^{\rm inc}) \end{bmatrix}. \tag{2.64}$$

An interesting consequence of reciprocity is the so-called backscattering theorem, which directly follows from Eq. (2.64) after substituting $\hat{\mathbf{n}}^{\rm inc} = \hat{\mathbf{n}}$ and $\hat{\mathbf{n}}^{\rm sca} = -\hat{\mathbf{n}}$:

$$S_{21}(-\hat{\mathbf{n}}, \hat{\mathbf{n}}) = -S_{12}(-\hat{\mathbf{n}}, \hat{\mathbf{n}}) \tag{2.65}$$

(van de Hulst 1957, Section 5.32).

Because of the universal nature of reciprocity, Eqs. (2.62), (2.64), and (2.65) are important tests in computations or measurements of light scattering by small particles; violation of reciprocity means that the computations or measurements are incorrect or inaccurate. Alternatively, the use of reciprocity can substantially shorten the required computer time or reduce the measurement effort because one may calculate or measure light scattering for only half of the scattering geometries and then use Eqs. (2.62) and (2.64) for the reciprocal geometries. Reciprocity plays a fundamental role in the phenomenon of coherent backscattering of light from discrete random media discussed in Section 3.4 (e.g., Mishchenko 1992b; van Tiggelen and Maynard 1997).

2.4 Reference frames and particle orientation

It is often convenient to specify the orientation of the scattering object using the same fixed reference frame that is used to specify the directions and states of polarization of the incident and scattered waves. In what follows, we will refer to this reference frame as the laboratory coordinate system and denote it by L. Although the spatial orientation of the laboratory coordinate system is, in principle, arbitrary, it can often be chosen in such a way that it most adequately represents the geometry of the scattering medium or the physical mechanism of particle orientation. In order to describe the orientation of the scattering object with respect to the laboratory reference frame, we introduce a right-handed coordinate system P affixed to the particle and having the same origin inside the particle as L. This coordinate system will be called the particle reference frame. The orientation of the particle with respect to L is specified by three Euler angles of rotation, α, β, and γ, which transform the laboratory coordinate system $L\{x, y, z\}$ into the particle coordinate system $P\{x', y', z'\}$, as shown in Fig. 2.2. The three consecutive Euler rotations are performed as follows:

- rotation of the laboratory coordinate system about the z-axis through an angle $\alpha \in [0, 2\pi)$, reorienting the y-axis in such a way that it coincides with the line of nodes (i.e., the line formed by the intersection of the xy- and $x'y'$- planes);
- rotation about the new y-axis through an angle $\beta \in [0, \pi]$;
- rotation about the z'- axis through an angle $\gamma \in [0, 2\pi)$.

An angle of rotation is positive if the rotation is performed in the *clockwise* direction when one is looking in the positive direction of the rotation axis.

As we will see in Chapters 5 and 6, most of the available analytical and numerical techniques assume that (or become especially efficient when) the scattering problem is solved in the particle reference frame with coordinate axes directed along the axes of particle symmetry. This implies that the incidence and scattering directions and polarization reference planes must also be specified with respect to the particle refer-

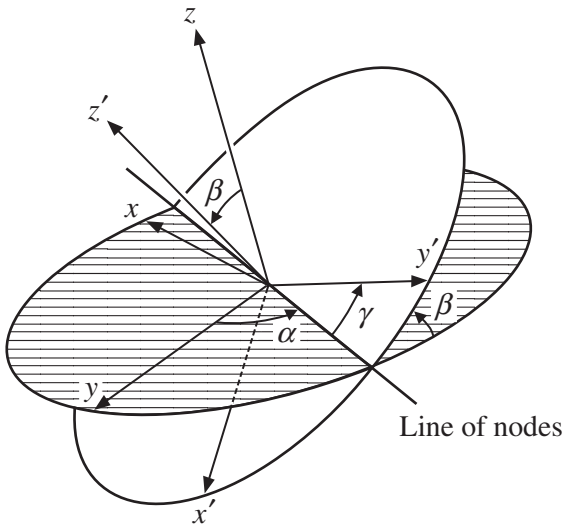

Figure 2.2. Euler angles of rotation α, β, and γ transforming the laboratory coordinate system $L\{x, y, z\}$ into the particle coordinate system $P\{x', y', z'\}$.

ence frame. Therefore, in order to solve the scattering problem with respect to the laboratory reference frame, one must first determine the illumination and scattering directions with respect to the particle reference frame for a given orientation of the particle relative to the laboratory reference frame, then solve the scattering problem in the particle reference frame, and finally perform the backward transition to the laboratory reference frame. In this section we derive general formulas describing this procedure (Mishchenko 2000).

Consider a monochromatic plane electromagnetic wave with electric field vector

$$\mathbf{E}^{\rm inc}(\mathbf{r}) = (E_{0\vartheta L}^{\rm inc}\hat{\boldsymbol{\vartheta}}_L^{\rm inc} + E_{0\varphi L}^{\rm inc}\hat{\boldsymbol{\varphi}}_L^{\rm inc})\exp(\mathrm{i}k_1\hat{\mathbf{n}}^{\rm inc}\cdot\mathbf{r}) \tag{2.66}$$

incident upon a nonspherical particle in a direction $\hat{\mathbf{n}}^{\rm inc}$, where $\mathbf{r}$ is the position (radius) vector connecting the origin of the laboratory coordinate system and the observation point and the index L labels unit vectors and electric field vector components computed in the laboratory reference frame. In the far-field region, the scattered field vector components are given by

$$\begin{bmatrix} E_{\vartheta L}^{\rm sca}(r\hat{\mathbf{n}}^{\rm sca}) \\ E_{\varphi L}^{\rm sca}(r\hat{\mathbf{n}}^{\rm sca}) \end{bmatrix} = \frac{\exp(\mathrm{i}k_1 r)}{r}\mathbf{S}^L(\hat{\mathbf{n}}^{\rm sca}, \hat{\mathbf{n}}^{\rm inc}; \alpha, \beta, \gamma)\begin{bmatrix} E_{0\vartheta L}^{\rm inc} \\ E_{0\varphi L}^{\rm inc} \end{bmatrix}, \tag{2.67}$$

where $\mathbf{S}^L$ is the 2×2 amplitude scattering matrix in the laboratory reference frame. The amplitude scattering matrix depends on the directions of incidence and scattering as well as on the orientation of the scattering particle with respect to the laboratory reference frame as specified by the Euler angles of rotation α, β, and γ.

Assume now that one of the available analytical or numerical techniques can be efficiently used to find the amplitude scattering matrix with respect to the particle

reference frame. This matrix will be denoted by $\mathbf{S}^P$ and relates the incident and scattered field vector components computed in the particle reference frame for the same incidence and scattering directions:

$$\begin{bmatrix} E_{\vartheta P}^{\rm sca}(r\hat{\mathbf{n}}^{\rm sca}) \\ E_{\varphi P}^{\rm sca}(r\hat{\mathbf{n}}^{\rm sca}) \end{bmatrix} = \frac{\exp({\rm i}k_1 r)}{r} \mathbf{S}^P(\hat{\mathbf{n}}^{\rm sca}, \hat{\mathbf{n}}^{\rm inc}) \begin{bmatrix} E_{0\vartheta P}^{\rm inc} \\ E_{0\varphi P}^{\rm inc} \end{bmatrix}. \tag{2.68}$$

The amplitude scattering matrix with respect to the laboratory reference frame can be expressed in terms of the matrix $\mathbf{S}^P$ as follows. Denote by $\mathbf{t}$ a 2×2 matrix that transforms the electric field vector components of a transverse electromagnetic wave computed in the laboratory reference frame into those computed in the particle reference frame:

$$\begin{bmatrix} E_{\vartheta P}(\vartheta_P, \varphi_P) \\ E_{\varphi P}(\vartheta_P, \varphi_P) \end{bmatrix} = \mathbf{t}(\hat{\mathbf{n}}; \alpha, \beta, \gamma) \begin{bmatrix} E_{\vartheta L}(\vartheta_L, \varphi_L) \\ E_{\varphi L}(\vartheta_L, \varphi_L) \end{bmatrix}, \tag{2.69}$$

where $\hat{\mathbf{n}}$ is a unit vector in the direction of light propagation; (ϑ_L, φ_L) and (ϑ_P, φ_P) specify this direction with respect to the laboratory and particle reference frames, respectively. The $\mathbf{t}$ matrix depends on $\hat{\mathbf{n}}$ as well as on the orientation of the particle relative to the laboratory reference frame, specified by the Euler angles α, β, and γ. The inverse transformation is

$$\begin{bmatrix} E_{\vartheta L}(\vartheta_L, \varphi_L) \\ E_{\varphi L}(\vartheta_L, \varphi_L) \end{bmatrix} = \mathbf{t}^{-1}(\hat{\mathbf{n}}; \alpha, \beta, \gamma) \begin{bmatrix} E_{\vartheta P}(\vartheta_P, \varphi_P) \\ E_{\varphi P}(\vartheta_P, \varphi_P) \end{bmatrix}, \tag{2.70}$$

where

$$\mathbf{t}(\hat{\mathbf{n}}; \alpha, \beta, \gamma)\, \mathbf{t}^{-1}(\hat{\mathbf{n}}; \alpha, \beta, \gamma) = \begin{bmatrix} 1 & 0 \\ 0 & 1 \end{bmatrix}. \tag{2.71}$$

We then easily derive

$$\mathbf{S}^L(\vartheta_L^{\rm sca}, \varphi_L^{\rm sca}; \vartheta_L^{\rm inc}, \varphi_L^{\rm inc}; \alpha, \beta, \gamma) = \mathbf{t}^{-1}(\hat{\mathbf{n}}^{\rm sca}; \alpha, \beta, \gamma) \times \mathbf{S}^P(\vartheta_P^{\rm sca}, \varphi_P^{\rm sca}; \vartheta_P^{\rm inc}, \varphi_P^{\rm inc})\, \mathbf{t}(\hat{\mathbf{n}}^{\rm inc}; \alpha, \beta, \gamma). \tag{2.72}$$

To determine the matrix $\mathbf{t}$, we proceed as follows. Denote by $\boldsymbol{\alpha}$ a 3×2 matrix that transforms the ϑ and φ components of the electric field vector into its x, y, and z components,

$$\begin{bmatrix} E_x \\ E_y \\ E_z \end{bmatrix} = \boldsymbol{\alpha}(\vartheta, \varphi) \begin{bmatrix} E_\vartheta \\ E_\varphi \end{bmatrix}, \tag{2.73}$$

and by $\boldsymbol{\beta}$ a 3×3 matrix that expresses the x, y, and z components of a vector in the particle coordinate system in terms of the x, y, and z components of the same vector in the laboratory coordinate system,

$$\begin{bmatrix} E_{xP} \\ E_{yP} \\ E_{zP} \end{bmatrix} = \boldsymbol{\beta}(\alpha, \beta, \gamma) \begin{bmatrix} E_{xL} \\ E_{yL} \\ E_{zL} \end{bmatrix}. \tag{2.74}$$

We then have

$$\mathbf{t}(\hat{\mathbf{n}}; \alpha, \beta, \gamma) = \boldsymbol{\alpha}^{-1}(\vartheta_P, \varphi_P)\, \boldsymbol{\beta}(\alpha, \beta, \gamma)\, \boldsymbol{\alpha}(\vartheta_L, \varphi_L), \tag{2.75}$$

where $\boldsymbol{\alpha}^{-1}(\vartheta_P, \varphi_P)$ is a suitable left inverse of $\boldsymbol{\alpha}(\vartheta_P, \varphi_P)$.

The matrices entering the right-hand side of Eq. (2.75) are as follows (Arfken and Weber 1995, pp. 118 and 189):

$$\boldsymbol{\alpha}(\vartheta, \varphi) = \begin{bmatrix} \cos\vartheta\cos\varphi & -\sin\varphi \\ \cos\vartheta\sin\varphi & \cos\varphi \\ -\sin\vartheta & 0 \end{bmatrix}, \tag{2.76}$$

$$\boldsymbol{\alpha}^{-1}(\vartheta, \varphi) = \begin{bmatrix} \cos\vartheta\cos\varphi & \cos\vartheta\sin\varphi & -\sin\vartheta \\ -\sin\varphi & \cos\varphi & 0 \end{bmatrix}, \tag{2.77}$$

$$\boldsymbol{\beta}(\alpha, \beta, \gamma) = \begin{bmatrix} \cos\alpha\cos\beta\cos\gamma - \sin\alpha\sin\gamma & \sin\alpha\cos\beta\cos\gamma + \cos\alpha\sin\gamma & -\sin\beta\cos\gamma \\ -\cos\alpha\cos\beta\sin\gamma - \sin\alpha\cos\gamma & -\sin\alpha\cos\beta\sin\gamma + \cos\alpha\cos\gamma & \sin\beta\sin\gamma \\ \cos\alpha\sin\beta & \sin\alpha\sin\beta & \cos\beta \end{bmatrix}. \tag{2.78}$$

To express the angles ϑ_P and φ_P in terms of the angles ϑ_L and φ_L, we rewrite Eq. (2.74) as

$$\begin{bmatrix} \sin\vartheta_P\cos\varphi_P \\ \sin\vartheta_P\sin\varphi_P \\ \cos\vartheta_P \end{bmatrix} = \boldsymbol{\beta}(\alpha, \beta, \gamma) \begin{bmatrix} \sin\vartheta_L\cos\varphi_L \\ \sin\vartheta_L\sin\varphi_L \\ \cos\vartheta_L \end{bmatrix}, \tag{2.79}$$

where (ϑ_L, φ_L) and (ϑ_P, φ_P) are spherical angular coordinates of an arbitrary unit vector in the laboratory and particle reference frames, respectively. Equations (2.78) and (2.79) and simple algebra then give

$$\cos\vartheta_P = \cos\vartheta_L\cos\beta + \sin\vartheta_L\sin\beta\cos(\varphi_L - \alpha), \tag{2.80}$$

$$\begin{aligned}\cos\varphi_P = \frac{1}{\sin\vartheta_P}[&\cos\beta\cos\gamma\sin\vartheta_L\cos(\varphi_L - \alpha) \\ &+ \sin\gamma\sin\vartheta_L\sin(\varphi_L - \alpha) - \sin\beta\cos\gamma\cos\vartheta_L],\end{aligned} \tag{2.81}$$

$$\begin{aligned}\sin\varphi_P = \frac{1}{\sin\vartheta_P}[&-\cos\beta\sin\gamma\sin\vartheta_L\cos(\varphi_L - \alpha) \\ &+ \cos\gamma\sin\vartheta_L\sin(\varphi_L - \alpha) + \sin\beta\sin\gamma\cos\vartheta_L].\end{aligned} \tag{2.82}$$

One easily verifies that if $\alpha = 0$, $\beta = 0$, and $\gamma = 0$ (i.e., the particle reference

frame coincides with the laboratory reference frame), then $\vartheta_P = \vartheta_L$, $\varphi_P = \varphi_L$,

$$\mathbf{t}(\hat{\mathbf{n}}; \alpha = 0, \beta = 0, \gamma = 0) \equiv \begin{bmatrix} 1 & 0 \\ 0 & 1 \end{bmatrix}, \tag{2.83}$$

and

$$\mathbf{S}^L(\vartheta_L^{\rm sca}, \varphi_L^{\rm sca}; \vartheta_L^{\rm inc}, \varphi_L^{\rm inc}; 0, 0, 0) = \mathbf{S}^P(\vartheta_P^{\rm sca}, \varphi_P^{\rm sca}; \vartheta_P^{\rm inc}, \varphi_P^{\rm inc}). \tag{2.84}$$

For rotationally symmetric particles, it is often advantageous to choose the particle coordinate system such that its z-axis is directed along the axis of particle symmetry. In this case the orientation of the particle with respect to the laboratory coordinate system is independent of the Euler angle γ, so that we can set $\gamma = 0$ and get instead of Eqs. (2.78), (2.81), and (2.82)

$$\boldsymbol{\beta}(\alpha, \beta, \gamma = 0) = \begin{bmatrix} \cos\alpha\cos\beta & \sin\alpha\cos\beta & -\sin\beta \\ -\sin\alpha & \cos\alpha & 0 \\ \cos\alpha\sin\beta & \sin\alpha\sin\beta & \cos\beta \end{bmatrix}, \tag{2.85}$$

$$\cos\varphi_P = \frac{1}{\sin\vartheta_P}[\cos\beta\sin\vartheta_L\cos(\varphi_L - \alpha) - \sin\beta\cos\vartheta_L], \tag{2.86}$$

$$\sin\varphi_P = \frac{\sin\vartheta_L\sin(\varphi_L - \alpha)}{\sin\vartheta_P}. \tag{2.87}$$

In summary, the numerical scheme for computing the amplitude scattering matrix for given $\vartheta_L^{\rm inc}$, $\varphi_L^{\rm inc}$, $\vartheta_L^{\rm sca}$, $\varphi_L^{\rm sca}$, α, β, and γ is as follows:

- calculation of $\vartheta_P^{\rm inc}$, $\varphi_P^{\rm inc}$, $\vartheta_P^{\rm sca}$, and $\varphi_P^{\rm sca}$ via Eqs. (2.80)–(2.82);
- calculation of the matrix $\boldsymbol{\beta}(\alpha, \beta, \gamma)$ via Eq. (2.78);
- calculation of the matrices $\boldsymbol{\alpha}(\vartheta_L^{\rm inc}, \varphi_L^{\rm inc})$, $\boldsymbol{\alpha}(\vartheta_L^{\rm sca}, \varphi_L^{\rm sca})$, $\boldsymbol{\alpha}^{-1}(\vartheta_P^{\rm inc}, \varphi_P^{\rm inc})$, and $\boldsymbol{\alpha}^{-1}(\vartheta_P^{\rm sca}, \varphi_P^{\rm sca})$ via Eqs. (2.76) and (2.77);
- calculation of the matrices $\mathbf{t}(\hat{\mathbf{n}}^{\rm inc}; \alpha, \beta, \gamma)$ and $\mathbf{t}^{-1}(\hat{\mathbf{n}}^{\rm sca}; \alpha, \beta, \gamma)$ via Eq. (2.75);
- calculation of the matrix $\mathbf{S}^P(\vartheta_P^{\rm sca}, \varphi_P^{\rm sca}; \vartheta_P^{\rm inc}, \varphi_P^{\rm inc})$ using one of the available analytical or numerical techniques;
- calculation of the matrix $\mathbf{S}^L(\vartheta_L^{\rm sca}, \varphi_L^{\rm sca}; \vartheta_L^{\rm inc}, \varphi_L^{\rm inc}; \alpha, \beta, \gamma)$ via Eq. (2.72).

We finally remark that because the particle reference frame can, in principle, be chosen arbitrarily, Eq. (2.72) can be considered as a general rotation transformation law expressing the amplitude scattering matrix in the original coordinate system in terms of the amplitude scattering matrix computed in a rotated coordinate system.

2.5 Poynting vector of the total field

Although the knowledge of the amplitude scattering matrix provides a complete de-

scription of the monochromatic scattering process in the far-field zone, measurement of the amplitude scattering matrix is a very complicated experimental problem involving the determination of both the amplitude and the phase of the incident and scattered waves. Measuring the phase is especially difficult, and only a handful of such experiments have been performed, all using the microwave analog technique (Gustafson 2000). The majority of other experiments have dealt with quasi-monochromatic rather than monochromatic light and involved measurements of derivative quantities having the dimension of energy flux rather than the electric field itself. It is therefore useful to characterize the scattering process using quantities that are easier to measure and are encountered more often, even though they may provide a less complete description of the scattering pattern in some cases. These quantities will be introduced in this and the following sections.

We begin by writing the time-averaged Poynting vector $\langle \mathbf{S}(\mathbf{r}) \rangle$ at any point in the far-field zone as the sum of three terms:

$$\langle \mathbf{S}(\mathbf{r}) \rangle = \tfrac{1}{2} \mathrm{Re}[\mathbf{E}(\mathbf{r}) \times \mathbf{H}^*(\mathbf{r})] = \langle \mathbf{S}^{\mathrm{inc}}(\mathbf{r}) \rangle + \langle \mathbf{S}^{\mathrm{sca}}(\mathbf{r}) \rangle + \langle \mathbf{S}^{\mathrm{ext}}(\mathbf{r}) \rangle, \tag{2.88}$$

where

$$\langle \mathbf{S}^{\mathrm{inc}}(\mathbf{r}) \rangle = \tfrac{1}{2} \mathrm{Re}\{\mathbf{E}^{\mathrm{inc}}(\mathbf{r}) \times [\mathbf{H}^{\mathrm{inc}}(\mathbf{r})]^*\} \tag{2.89}$$

and

$$\langle \mathbf{S}^{\mathrm{sca}}(\mathbf{r}) \rangle = \tfrac{1}{2} \mathrm{Re}\{\mathbf{E}^{\mathrm{sca}}(\mathbf{r}) \times [\mathbf{H}^{\mathrm{sca}}(\mathbf{r})]^*\} \tag{2.90}$$

are Poynting vectors associated with the incident and the scattered fields, respectively, whereas

$$\langle \mathbf{S}^{\mathrm{ext}}(\mathbf{r}) \rangle = \tfrac{1}{2} \mathrm{Re}\{\mathbf{E}^{\mathrm{inc}}(\mathbf{r}) \times [\mathbf{H}^{\mathrm{sca}}(\mathbf{r})]^* + \mathbf{E}^{\mathrm{sca}}(\mathbf{r}) \times [\mathbf{H}^{\mathrm{inc}}(\mathbf{r})]^*\} \tag{2.91}$$

can be interpreted as a term caused by interaction between the incident and the scattered fields. Let us consider a scattering object illuminated by a plane electromagnetic wave. Recalling Eqs. (1.36), (1.38), (1.42), (2.25), and (2.57), we have for the incident wave in the far-field zone of the scattering particle

$$\begin{aligned} \mathbf{E}^{\mathrm{inc}}(\mathbf{r}) &= \mathbf{E}_0^{\mathrm{inc}} \exp(\mathrm{i}k_1 \hat{\mathbf{n}}^{\mathrm{inc}} \cdot \mathbf{r}) \\ &\underset{k_1 r \to \infty}{=} \frac{\mathrm{i}2\pi}{k_1} \left[\delta(\hat{\mathbf{n}}^{\mathrm{inc}} + \hat{\mathbf{r}}) \frac{\mathrm{e}^{-\mathrm{i}k_1 r}}{r} - \delta(\hat{\mathbf{n}}^{\mathrm{inc}} - \hat{\mathbf{r}}) \frac{\mathrm{e}^{\mathrm{i}k_1 r}}{r} \right] \mathbf{E}_0^{\mathrm{inc}}, \qquad \mathbf{E}_0^{\mathrm{inc}} \cdot \hat{\mathbf{n}}^{\mathrm{inc}} = 0, \end{aligned} \tag{2.92}$$

$$\begin{aligned} \mathbf{H}^{\mathrm{inc}}(\mathbf{r}) &= \sqrt{\frac{\varepsilon_1}{\mu_0}} \exp(\mathrm{i}k_1 \hat{\mathbf{n}}^{\mathrm{inc}} \cdot \mathbf{r})\, \hat{\mathbf{n}}^{\mathrm{inc}} \times \mathbf{E}_0^{\mathrm{inc}} \\ &\underset{k_1 r \to \infty}{=} \frac{\mathrm{i}2\pi}{k_1} \left[\delta(\hat{\mathbf{n}}^{\mathrm{inc}} + \hat{\mathbf{r}}) \frac{\mathrm{e}^{-\mathrm{i}k_1 r}}{r} - \delta(\hat{\mathbf{n}}^{\mathrm{inc}} - \hat{\mathbf{r}}) \frac{\mathrm{e}^{\mathrm{i}k_1 r}}{r} \right] \sqrt{\frac{\varepsilon_1}{\mu_0}}\, \hat{\mathbf{n}}^{\mathrm{inc}} \times \mathbf{E}_0^{\mathrm{inc}}, \end{aligned} \tag{2.93}$$

where $\mathbf{r} = r\hat{\mathbf{r}}$ is the radius vector connecting the particle and the observation point. The first relation of Eq. (2.1) and Eqs. (2.23), (2.24), (2.40), and (2.49)–(2.50) give for the scattered wave:

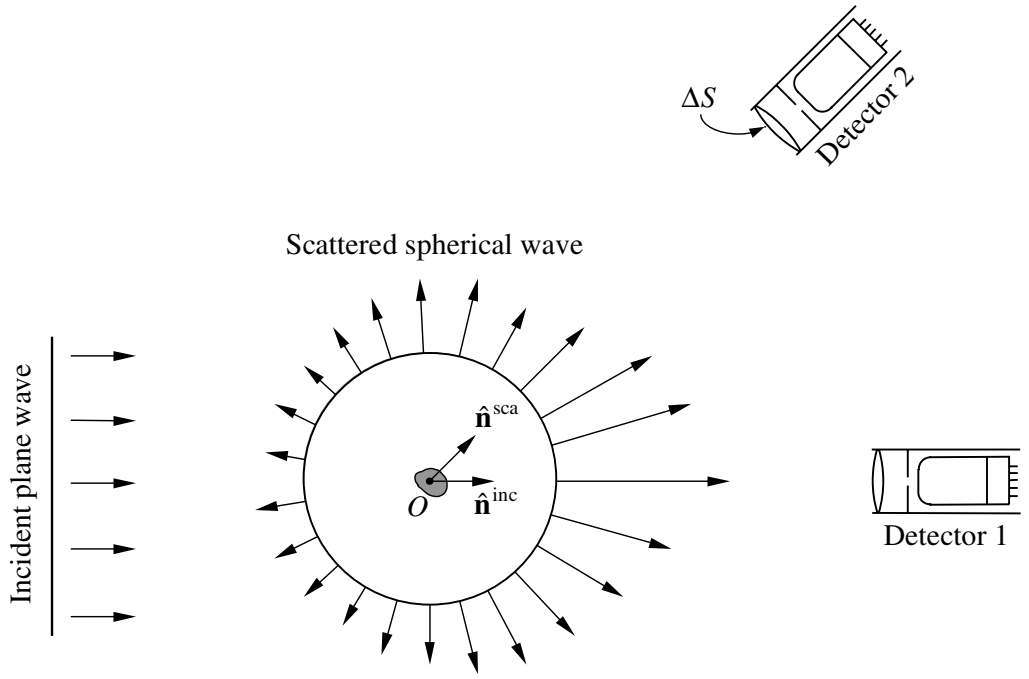

Figure 2.3. The response of the collimated detector depends on the line of sight.

$$\mathbf{E}^{\rm sca}(\mathbf{r}) \underset{k_1 r\to\infty}{=} \frac{e^{ik_1 r}}{r}\mathbf{E}_1^{\rm sca}(\hat{\mathbf{r}}), \qquad \mathbf{E}_1^{\rm sca}(\hat{\mathbf{r}})\cdot\hat{\mathbf{r}} = 0, \tag{2.94}$$

$$\mathbf{H}^{\rm sca}(\mathbf{r}) \underset{k_1 r\to\infty}{=} \sqrt{\frac{\varepsilon_1}{\mu_0}}\,\frac{e^{ik_1 r}}{r}\hat{\mathbf{r}}\times\mathbf{E}_1^{\rm sca}(\hat{\mathbf{r}}). \tag{2.95}$$

Consider now a well-collimated detector of electromagnetic radiation placed at a distance r from the particle in the far-field zone, with its surface ΔS aligned normal to and centered on the straight line extending from the particle in the direction of the unit vector $\hat{\mathbf{n}}^{\rm inc}$ (Fig. 2.3). We assume that the dimension of the detector surface is much greater than any dimension of the scattering object and the wavelength but much smaller than r. Furthermore, we assume that $\Delta S/r^2$ is smaller than the detector solid-angle field of view Ω so that all radiation scattered by the particle and impinging on ΔS is detected. Obviously, the term $\langle \mathbf{S}^{\rm inc}(\mathbf{r})\rangle$ does not contribute to the detected signal unless $\hat{\mathbf{r}} = \hat{\mathbf{n}}^{\rm inc}$. From Eqs. (2.88)–(2.95), it is straightforward to show that the total electromagnetic power received by the detector is

$$\begin{aligned} W_{\Delta S}(\hat{\mathbf{n}}^{\rm sca}) &= \int_{\Delta S} dS\,\hat{\mathbf{r}}\cdot\langle \mathbf{S}(\mathbf{r})\rangle \\ &\approx \frac{1}{2}\sqrt{\frac{\varepsilon_1}{\mu_0}}\,\frac{\Delta S}{r^2}\,|\mathbf{E}_1^{\rm sca}(\hat{\mathbf{n}}^{\rm sca})|^2 \end{aligned} \tag{2.96}$$

when $\hat{\mathbf{n}}^{\rm sca} \neq \hat{\mathbf{n}}^{\rm inc}$, whereas for the exact forward-scattering direction

$$
\begin{aligned}
W_{\Delta S}(\hat{\mathbf{n}}^{\rm inc}) &= \int_{\Delta S} {\rm d}S \hat{\mathbf{n}}^{\rm inc} \cdot \langle \mathbf{S}(\mathbf{r}) \rangle \\
&= \frac{1}{2} \Delta S \sqrt{\frac{\varepsilon_1}{\mu_0}} |\mathbf{E}_0^{\rm inc}|^2 + \int_{\Delta S} {\rm d}S \hat{\mathbf{n}}^{\rm inc} \cdot [\langle \mathbf{S}^{\rm sca}(\mathbf{r}) \rangle + \langle \mathbf{S}^{\rm ext}(\mathbf{r}) \rangle] \\
&\approx \frac{1}{2} \Delta S \sqrt{\frac{\varepsilon_1}{\mu_0}} \left[|\mathbf{E}_0^{\rm inc}|^2 + \frac{1}{r^2} |\mathbf{E}_1^{\rm sca}(\hat{\mathbf{n}}^{\rm inc})|^2 \right] + r^2 \int_{\Delta \Omega} {\rm d}\hat{\mathbf{r}} \hat{\mathbf{n}}^{\rm inc} \cdot \langle \mathbf{S}^{\rm ext}(r\mathbf{r}) \rangle \\
&\approx \frac{1}{2} \Delta S \sqrt{\frac{\varepsilon_1}{\mu_0}} \left[|\mathbf{E}_0^{\rm inc}|^2 + \frac{1}{r^2} |\mathbf{E}_1^{\rm sca}(\hat{\mathbf{n}}^{\rm inc})|^2 \right] - \frac{2\pi}{k_1} \sqrt{\frac{\varepsilon_1}{\mu_0}} \, {\rm Im}[\mathbf{E}_1^{\rm sca}(\hat{\mathbf{n}}^{\rm inc}) \cdot \mathbf{E}_0^{\rm inc*}] \\
&= \frac{1}{2} \Delta S \sqrt{\frac{\varepsilon_1}{\mu_0}} |\mathbf{E}_0^{\rm inc}|^2 - \frac{2\pi}{k_1} \sqrt{\frac{\varepsilon_1}{\mu_0}} \, {\rm Im}[\mathbf{E}_1^{\rm sca}(\hat{\mathbf{n}}^{\rm inc}) \cdot \mathbf{E}_0^{\rm inc*}] + O(r^{-2}), \qquad (2.97)
\end{aligned}
$$

where $\Delta\Omega = \Delta S / r^2$ is the solid angle element centered at the direction $\hat{\mathbf{n}}^{\rm inc}$ and formed by the detector surface at the distance r from the particle. The term $\frac{1}{2} \Delta S \sqrt{\varepsilon_1 / \mu_0} \, |\mathbf{E}_0^{\rm inc}|^2$ on the right-hand side of Eq. (2.97) is proportional to the detector area ΔS and is equal to the electromagnetic power that would be received by detector 1 in the absence of the scattering particle, whereas $-(2\pi/k_1)\sqrt{\varepsilon_1/\mu_0} \, {\rm Im}[\mathbf{E}_1^{\rm sca}(\hat{\mathbf{n}}^{\rm inc}) \cdot \mathbf{E}_0^{\rm inc*}]$ is an attenuation term independent of ΔS, caused by interposing the particle between the light source and the detector. Thus, a well-collimated detector located in the far-field zone and having its surface ΔS aligned normal to the exact forward-scattering direction (i.e., $\hat{\mathbf{n}}^{\rm sca} = \hat{\mathbf{n}}^{\rm inc}$, detector 1 in Fig. 2.3) measures the power of the incident light attenuated by interference of the incident and the scattered fields plus a relatively small contribution from the scattered light, whereas a detector with surface aligned normal to any other scattering direction (i.e., $\hat{\mathbf{n}}^{\rm sca} \neq \hat{\mathbf{n}}^{\rm inc}$, detector 2 in Fig. 2.3) "sees" only the scattered light. These are two fundamental features of electromagnetic scattering by a small particle. Equation (2.97) is a representation of the so-called optical theorem and will be further discussed in Section 2.8.

2.6 Phase matrix

In the thought experiment described in the previous section and shown schematically in Fig. 2.3, it is assumed that the detectors can measure only the total electromagnetic power and that they make no distinction between electromagnetic waves with different states of polarization. Many detectors of electromagnetic energy are indeed polarization-insensitive. However, by interposing a polarizer between the source of light and the scattering particle one can generate incident light with a specific state of polarization, whereas interposing a polarizer between the scattering particle and the detector enables the detector to measure the power corresponding to a particular polarization component of the scattered light. By repeating the measurement for a num-

ber of different combinations of the polarizers one can, in principle, determine the specific prescription for the transformation of a complete set of polarization characteristics of the incident light into that of the scattered light, *provided that both sets of characteristics have the same dimension of energy flux* (Section 8.1). As we saw in Chapter 1, convenient complete sets of polarization characteristics having the dimension of monochromatic energy flux are the coherency and the Stokes vectors. So we will now assume that the device shown schematically in Fig. 2.3 can (i) generate incident light with different (but physically realizable) combinations of coherency or Stokes vector components, and (ii) measure the electromagnetic power associated with any component of the coherency vector or the Stokes vector and equal to the integral of the component over the surface ΔS of the collimated detector aligned normal to the direction of propagation $\hat{\mathbf{r}}$. The component itself is then found by dividing the measured power by ΔS.

To derive the relationship between the polarization characteristics of the incident and the scattered waves for scattering directions *away from the incidence direction* ($\hat{\mathbf{r}} \neq \hat{\mathbf{n}}^{\rm inc}$), we first define the respective coherency vectors (cf. Eqs. (1.53), (2.24), and (2.25)):

$$\mathbf{J}^{\rm inc} = \frac{1}{2}\sqrt{\frac{\varepsilon_1}{\mu_0}} \begin{bmatrix} E_{0\vartheta}^{\rm inc} E_{0\vartheta}^{\rm inc*} \\ E_{0\vartheta}^{\rm inc} E_{0\varphi}^{\rm inc*} \\ E_{0\varphi}^{\rm inc} E_{0\vartheta}^{\rm inc*} \\ E_{0\varphi}^{\rm inc} E_{0\varphi}^{\rm inc*} \end{bmatrix}, \tag{2.98}$$

$$\begin{aligned} \mathbf{J}^{\rm sca}(r\hat{\mathbf{n}}^{\rm sca}) &= \frac{1}{2}\sqrt{\frac{\varepsilon_1}{\mu_0}} \begin{bmatrix} E_{\vartheta}^{\rm sca}(r\hat{\mathbf{n}}^{\rm sca})[E_{\vartheta}^{\rm sca}(r\hat{\mathbf{n}}^{\rm sca})]^* \\ E_{\vartheta}^{\rm sca}(r\hat{\mathbf{n}}^{\rm sca})[E_{\varphi}^{\rm sca}(r\hat{\mathbf{n}}^{\rm sca})]^* \\ E_{\varphi}^{\rm sca}(r\hat{\mathbf{n}}^{\rm sca})[E_{\vartheta}^{\rm sca}(r\hat{\mathbf{n}}^{\rm sca})]^* \\ E_{\varphi}^{\rm sca}(r\hat{\mathbf{n}}^{\rm sca})[E_{\varphi}^{\rm sca}(r\hat{\mathbf{n}}^{\rm sca})]^* \end{bmatrix} \\ &= \frac{1}{r^2}\frac{1}{2}\sqrt{\frac{\varepsilon_1}{\mu_0}} \begin{bmatrix} E_{1\vartheta}^{\rm sca}(\hat{\mathbf{n}}^{\rm sca})[E_{1\vartheta}^{\rm sca}(\hat{\mathbf{n}}^{\rm sca})]^* \\ E_{1\vartheta}^{\rm sca}(\hat{\mathbf{n}}^{\rm sca})[E_{1\varphi}^{\rm sca}(\hat{\mathbf{n}}^{\rm sca})]^* \\ E_{1\varphi}^{\rm sca}(\hat{\mathbf{n}}^{\rm sca})[E_{1\vartheta}^{\rm sca}(\hat{\mathbf{n}}^{\rm sca})]^* \\ E_{1\varphi}^{\rm sca}(\hat{\mathbf{n}}^{\rm sca})[E_{1\varphi}^{\rm sca}(\hat{\mathbf{n}}^{\rm sca})]^* \end{bmatrix}. \end{aligned} \tag{2.99}$$

Equation (2.30) and simple algebra lead to the following formula describing the transformation of the coherency vector of the incident wave into that of the scattered wave:

$$\mathbf{J}^{\rm sca}(r\hat{\mathbf{n}}^{\rm sca}) = \frac{1}{r^2}\mathbf{Z}^J(\hat{\mathbf{n}}^{\rm sca}, \hat{\mathbf{n}}^{\rm inc})\mathbf{J}^{\rm inc}, \tag{2.100}$$

where the elements of the coherency phase matrix $\mathbf{Z}^J(\hat{\mathbf{n}}^{\rm sca}, \hat{\mathbf{n}}^{\rm inc})$ are quadratic combinations of the elements of the amplitude scattering matrix $\mathbf{S}(\hat{\mathbf{n}}^{\rm sca}, \hat{\mathbf{n}}^{\rm inc})$:

$$\mathbf{Z}^J = \begin{bmatrix} |S_{11}|^2 & S_{11}S_{12}^* & S_{12}S_{11}^* & |S_{12}|^2 \\ S_{11}S_{21}^* & S_{11}S_{22}^* & S_{12}S_{21}^* & S_{12}S_{22}^* \\ S_{21}S_{11}^* & S_{21}S_{12}^* & S_{22}S_{11}^* & S_{22}S_{12}^* \\ |S_{21}|^2 & S_{21}S_{22}^* & S_{22}S_{21}^* & |S_{22}|^2 \end{bmatrix}. \tag{2.101}$$

Analogously, the Stokes phase matrix $\mathbf{Z}$ describes the transformation of the Stokes vector of the incident wave into that of the scattered wave,

$$\mathbf{I}^{\rm sca}(r\hat{\mathbf{n}}^{\rm sca}) = \frac{1}{r^2}\mathbf{Z}(\hat{\mathbf{n}}^{\rm sca}, \hat{\mathbf{n}}^{\rm inc})\mathbf{I}^{\rm inc}, \tag{2.102}$$

and is given by

$$\mathbf{Z}(\hat{\mathbf{n}}^{\rm sca}, \hat{\mathbf{n}}^{\rm inc}) = \mathbf{D}\mathbf{Z}^J(\hat{\mathbf{n}}^{\rm sca}, \hat{\mathbf{n}}^{\rm inc})\mathbf{D}^{-1}, \tag{2.103}$$

where

$$\mathbf{I}^{\rm inc} = \mathbf{D}\mathbf{J}^{\rm inc} = \frac{1}{2}\sqrt{\frac{\varepsilon_1}{\mu_0}} \begin{bmatrix} E_{0\vartheta}^{\rm inc}E_{0\vartheta}^{\rm inc*} + E_{0\varphi}^{\rm inc}E_{0\varphi}^{\rm inc*} \\ E_{0\vartheta}^{\rm inc}E_{0\vartheta}^{\rm inc*} - E_{0\varphi}^{\rm inc}E_{0\varphi}^{\rm inc*} \\ -E_{0\vartheta}^{\rm inc}E_{0\varphi}^{\rm inc*} - E_{0\varphi}^{\rm inc}E_{0\vartheta}^{\rm inc*} \\ \mathrm{i}(E_{0\varphi}^{\rm inc}E_{0\vartheta}^{\rm inc*} - E_{0\vartheta}^{\rm inc}E_{0\varphi}^{\rm inc*}) \end{bmatrix} \tag{2.104}$$

and

$$\mathbf{I}^{\rm sca}(r\hat{\mathbf{n}}^{\rm sca}) = \mathbf{D}\mathbf{J}^{\rm sca}(r\hat{\mathbf{n}}^{\rm sca}) = \frac{1}{r^2}\frac{1}{2}\sqrt{\frac{\varepsilon_1}{\mu_0}} \begin{bmatrix} E_{1\vartheta}^{\rm sca}E_{1\vartheta}^{\rm sca*} + E_{1\varphi}^{\rm sca}E_{1\varphi}^{\rm sca*} \\ E_{1\vartheta}^{\rm sca}E_{1\vartheta}^{\rm sca*} - E_{1\varphi}^{\rm sca}E_{1\varphi}^{\rm sca*} \\ -E_{1\vartheta}^{\rm sca}E_{1\varphi}^{\rm sca*} - E_{1\varphi}^{\rm sca}E_{1\vartheta}^{\rm sca*} \\ \mathrm{i}(E_{1\varphi}^{\rm sca}E_{1\vartheta}^{\rm sca*} - E_{1\vartheta}^{\rm sca}E_{1\varphi}^{\rm sca*}) \end{bmatrix} \tag{2.105}$$

(cf. Eq. (1.54)); the matrices $\mathbf{D}$ and $\mathbf{D}^{-1}$ were defined by Eqs. (1.55) and (1.57), respectively. Explicit formulas for the elements of the Stokes phase matrix in terms of the amplitude scattering matrix elements follow from Eqs. (2.101) and (2.103):

$$Z_{11} = \tfrac{1}{2}(|S_{11}|^2 + |S_{12}|^2 + |S_{21}|^2 + |S_{22}|^2), \tag{2.106}$$

$$Z_{12} = \tfrac{1}{2}(|S_{11}|^2 - |S_{12}|^2 + |S_{21}|^2 - |S_{22}|^2), \tag{2.107}$$

$$Z_{13} = -\mathrm{Re}(S_{11}S_{12}^* + S_{22}S_{21}^*), \tag{2.108}$$

$$Z_{14} = -\mathrm{Im}(S_{11}S_{12}^* - S_{22}S_{21}^*), \tag{2.109}$$

$$Z_{21} = \tfrac{1}{2}(|S_{11}|^2 + |S_{12}|^2 - |S_{21}|^2 - |S_{22}|^2), \tag{2.110}$$

$$Z_{22} = \tfrac{1}{2}(|S_{11}|^2 - |S_{12}|^2 - |S_{21}|^2 + |S_{22}|^2), \tag{2.111}$$

$$Z_{23} = -\mathrm{Re}(S_{11}S_{12}^* - S_{22}S_{21}^*), \tag{2.112}$$

$$Z_{24} = -\mathrm{Im}(S_{11}S_{12}^* + S_{22}S_{21}^*), \tag{2.113}$$

$$Z_{31} = -\mathrm{Re}(S_{11}S_{21}^* + S_{22}S_{12}^*), \tag{2.114}$$

$$Z_{32} = -\mathrm{Re}(S_{11}S_{21}^* - S_{22}S_{12}^*), \tag{2.115}$$

$$Z_{33} = \mathrm{Re}(S_{11}S_{22}^* + S_{12}S_{21}^*), \tag{2.116}$$

$$Z_{34} = \mathrm{Im}(S_{11}S_{22}^* + S_{21}S_{12}^*), \tag{2.117}$$

$$Z_{41} = -\mathrm{Im}(S_{21}S_{11}^* + S_{22}S_{12}^*), \tag{2.118}$$

$$Z_{42} = -\mathrm{Im}(S_{21}S_{11}^* - S_{22}S_{12}^*), \tag{2.119}$$

$$Z_{43} = \mathrm{Im}(S_{22}S_{11}^* - S_{12}S_{21}^*), \tag{2.120}$$

$$Z_{44} = \mathrm{Re}(S_{22}S_{11}^* - S_{12}S_{21}^*). \tag{2.121}$$

Finally, the modified Stokes and circular-polarization phase matrices are given by

$$\mathbf{Z}^{\mathrm{MS}}(\hat{\mathbf{n}}^{\mathrm{sca}}, \hat{\mathbf{n}}^{\mathrm{inc}}) = \mathbf{B}\mathbf{Z}(\hat{\mathbf{n}}^{\mathrm{sca}}, \hat{\mathbf{n}}^{\mathrm{inc}})\mathbf{B}^{-1} \tag{2.122}$$

and

$$\mathbf{Z}^{\mathrm{CP}}(\hat{\mathbf{n}}^{\mathrm{sca}}, \hat{\mathbf{n}}^{\mathrm{inc}}) = \mathbf{A}\mathbf{Z}(\hat{\mathbf{n}}^{\mathrm{sca}}, \hat{\mathbf{n}}^{\mathrm{inc}})\mathbf{A}^{-1}, \tag{2.123}$$

respectively (see Eqs. (1.59)–(1.66)). The elements of all phase matrices have the same dimension of area. The matrices $\mathbf{Z}$ and $\mathbf{Z}^{\mathrm{MS}}$ are real-valued. Like the amplitude scattering matrix, the phase matrices explicitly depend on φ^{inc} and φ^{sca} even when the incident and/or scattered light propagates along the z-axis.

Up to this point we have considered the scattering of only monochromatic plane waves. However, it is obvious that Eqs. (2.100) and (2.102) remain valid even when the incident radiation is a parallel quasi-monochromatic beam of light, provided that the coherency and Stokes vectors entering these equations are averages over a time interval long compared with the period of fluctuations (Section 1.6). Hence, the phase matrix concept is quite useful even in the more general situations involving quasi-monochromatic light.

In general, all 16 elements of any of the phase matrices introduced above are nonzero. However, the phase matrix elements of a single particle are expressed in terms of only seven independent real numbers resulting from the four moduli $|S_{ij}|$ $(i, j = 1,2)$ and three differences in phase between S_{ij}. Therefore, only seven of the phase matrix elements are actually independent, and there must be nine unique relations among the 16 phase matrix elements. Furthermore, the specific mathematical structure of the phase matrix can also be used to derive many useful linear and quadratic inequalities for the phase matrix elements. Two important inequalities are $Z_{11} \geq 0$ (this property follows directly from Eq. (2.106)) and $|Z_{ij}| \leq Z_{11}$ $(i, j = 1, \ldots, 4)$. The reader is referred to Hovenier *et al*. (1986), Cloude and Pottier (1996), and Hovenier and van der Mee (1996, 2000) for a review of this subject and a discussion of how the general properties of the phase matrix can be used for testing the results of theoretical computations and laboratory measurements.

From Eqs. (2.106)–(2.121) and (2.64) we derive the reciprocity relation for the Stokes phase matrix:

$$\mathbf{Z}(-\hat{\mathbf{n}}^{\rm inc}, -\hat{\mathbf{n}}^{\rm sca}) = \mathbf{\Delta}_3[\mathbf{Z}(\hat{\mathbf{n}}^{\rm sca}, \hat{\mathbf{n}}^{\rm inc})]^{\rm T}\mathbf{\Delta}_3, \tag{2.124}$$

where

$$\mathbf{\Delta}_3 = \mathbf{\Delta}_3^{\rm T} = \mathbf{\Delta}_3^{-1} = \begin{bmatrix} 1 & 0 & 0 & 0 \\ 0 & 1 & 0 & 0 \\ 0 & 0 & -1 & 0 \\ 0 & 0 & 0 & 1 \end{bmatrix} \tag{2.125}$$

and T denotes the transpose of a matrix, as before. The reciprocity relations for other phase matrices can be obtained easily from Eqs. (2.103), (2.122), and (2.123):

$$\begin{aligned} \mathbf{Z}^J(-\hat{\mathbf{n}}^{\rm inc}, -\hat{\mathbf{n}}^{\rm sca}) &= \mathbf{D}^{-1}\mathbf{Z}(-\hat{\mathbf{n}}^{\rm inc}, -\hat{\mathbf{n}}^{\rm sca})\mathbf{D} \\ &= \mathbf{D}^{-1}\mathbf{\Delta}_3[\mathbf{Z}(\hat{\mathbf{n}}^{\rm sca}, \hat{\mathbf{n}}^{\rm inc})]^{\rm T}\mathbf{\Delta}_3\mathbf{D} \\ &= \mathbf{D}^{-1}\mathbf{\Delta}_3[\mathbf{D}\mathbf{Z}^J(\hat{\mathbf{n}}^{\rm sca}, \hat{\mathbf{n}}^{\rm inc})\mathbf{D}^{-1}]^{\rm T}\mathbf{\Delta}_3\mathbf{D} \\ &= \mathbf{D}^{-1}\mathbf{\Delta}_3[\mathbf{D}^{-1}]^{\rm T}[\mathbf{Z}^J(\hat{\mathbf{n}}^{\rm sca}, \hat{\mathbf{n}}^{\rm inc})]^{\rm T}\mathbf{D}^{\rm T}\mathbf{\Delta}_3\mathbf{D} \\ &= \mathbf{\Delta}_{23}[\mathbf{Z}^J(\hat{\mathbf{n}}^{\rm sca}, \hat{\mathbf{n}}^{\rm inc})]^{\rm T}\mathbf{\Delta}_{23}, \end{aligned} \tag{2.126}$$

$$\begin{aligned} \mathbf{Z}^{\rm MS}(-\hat{\mathbf{n}}^{\rm inc}, -\hat{\mathbf{n}}^{\rm sca}) &= \mathbf{B}\mathbf{Z}(-\hat{\mathbf{n}}^{\rm inc}, -\hat{\mathbf{n}}^{\rm sca})\mathbf{B}^{-1} \\ &= \mathbf{B}\mathbf{\Delta}_3[\mathbf{Z}(\hat{\mathbf{n}}^{\rm sca}, \hat{\mathbf{n}}^{\rm inc})]^{\rm T}\mathbf{\Delta}_3\mathbf{B}^{-1} \\ &= \mathbf{B}\mathbf{\Delta}_3[\mathbf{B}^{-1}\mathbf{Z}^{\rm MS}(\hat{\mathbf{n}}^{\rm sca}, \hat{\mathbf{n}}^{\rm inc})\mathbf{B}]^{\rm T}\mathbf{\Delta}_3\mathbf{B}^{-1} \\ &= \mathbf{B}\mathbf{\Delta}_3\mathbf{B}^{\rm T}[\mathbf{Z}^{\rm MS}(\hat{\mathbf{n}}^{\rm sca}, \hat{\mathbf{n}}^{\rm inc})]^{\rm T}[\mathbf{B}^{-1}]^{\rm T}\mathbf{\Delta}_3\mathbf{B}^{-1} \\ &= \mathbf{\Delta}^{\rm MS}[\mathbf{Z}^{\rm MS}(\hat{\mathbf{n}}^{\rm sca}, \hat{\mathbf{n}}^{\rm inc})]^{\rm T}[\mathbf{\Delta}^{\rm MS}]^{-1}, \end{aligned} \tag{2.127}$$

$$\begin{aligned} \mathbf{Z}^{\rm CP}(-\hat{\mathbf{n}}^{\rm inc}, -\hat{\mathbf{n}}^{\rm sca}) &= \mathbf{A}\mathbf{\Delta}_3\mathbf{A}^{\rm T}[\mathbf{Z}^{\rm CP}(\hat{\mathbf{n}}^{\rm sca}, \hat{\mathbf{n}}^{\rm inc})]^{\rm T}[\mathbf{A}^{-1}]^{\rm T}\mathbf{\Delta}_3\mathbf{A}^{-1} \\ &= [\mathbf{Z}^{\rm CP}(\hat{\mathbf{n}}^{\rm sca}, \hat{\mathbf{n}}^{\rm inc})]^{\rm T}, \end{aligned} \tag{2.128}$$

where

$$\mathbf{\Delta}_{23} = \mathbf{\Delta}_{23}^{\rm T} = \mathbf{\Delta}_{23}^{-1} = \begin{bmatrix} 1 & 0 & 0 & 0 \\ 0 & -1 & 0 & 0 \\ 0 & 0 & -1 & 0 \\ 0 & 0 & 0 & 1 \end{bmatrix}, \tag{2.129}$$

$$\mathbf{\Delta}^{\rm MS} = [\mathbf{\Delta}^{\rm MS}]^{\rm T} = \begin{bmatrix} 1/2 & 0 & 0 & 0 \\ 0 & 1/2 & 0 & 0 \\ 0 & 0 & -1 & 0 \\ 0 & 0 & 0 & 1 \end{bmatrix}, \quad [\mathbf{\Delta}^{\rm MS}]^{-1} = \begin{bmatrix} 2 & 0 & 0 & 0 \\ 0 & 2 & 0 & 0 \\ 0 & 0 & -1 & 0 \\ 0 & 0 & 0 & 1 \end{bmatrix}. \tag{2.130}$$

The backscattering theorem, Eq. (2.65), along with Eqs. (2.106), (2.111), (2.116), and (2.121), leads to the following general property of the backscattering Stokes phase

matrix (Mishchenko *et al.* 2000b):

$$Z_{11}(-\hat{\mathbf{n}}, \hat{\mathbf{n}}) - Z_{22}(-\hat{\mathbf{n}}, \hat{\mathbf{n}}) + Z_{33}(-\hat{\mathbf{n}}, \hat{\mathbf{n}}) - Z_{44}(-\hat{\mathbf{n}}, \hat{\mathbf{n}}) = 0. \tag{2.131}$$

Electromagnetic scattering most typically produces light with polarization characteristics different from those of the incident beam. If the incident beam is unpolarized, i.e., $\mathbf{I}^{\rm inc} = [I^{\rm inc}\ 0\ 0\ 0]^{\rm T}$, the scattered light generally has at least one non-zero Stokes parameter other than intensity:

$$I^{\rm sca} = Z_{11} I^{\rm inc}, \quad Q^{\rm sca} = Z_{21} I^{\rm inc}, \quad U^{\rm sca} = Z_{31} I^{\rm inc}, \quad V^{\rm sca} = Z_{41} I^{\rm inc}. \tag{2.132}$$

This phenomenon is traditionally called "polarization" and results in scattered light with non-zero degree of polarization, see Eq. (1.111),

$$P = \frac{\sqrt{Z_{21}^2 + Z_{31}^2 + Z_{41}^2}}{Z_{11}}. \tag{2.133}$$

Obviously, if the incident light is unpolarized, then the element Z_{11} determines the angular distribution of the scattered intensity. When the incident beam is linearly polarized, i.e., $\mathbf{I}^{\rm inc} = [I^{\rm inc}\ Q^{\rm inc}\ U^{\rm inc}\ 0]^{\rm T}$, the scattered light may become elliptically polarized ($V^{\rm sca} \neq 0$). Conversely, when the incident light is circularly polarized, i.e., $\mathbf{I}^{\rm inc} = [I^{\rm inc}\ 0\ 0\ V^{\rm inc}]^{\rm T}$, the scattered light may become partially linearly polarized ($Q^{\rm sca} \neq 0$ and/or $U^{\rm sca} \neq 0$). A general feature of scattering by a single particle is that if the incident beam is fully polarized ($P^{\rm inc} = 1$) then the scattered light is also fully polarized. Hovenier *et al.* (1986) gave a proof of this property based on the general mathematical structure of the Stokes phase matrix. Thus, a single particle does not depolarize fully polarized incident light. We will see later, however, that single scattering by a collection of non-identical nonspherical particles (including particles of the same kind but with different orientations) can result in depolarization of the incident polarized light, and this is another important property of electromagnetic scattering.

2.7 Extinction matrix

Let us now consider the special case of the *exact forward-scattering direction* ($\hat{\mathbf{r}} = \hat{\mathbf{n}}^{\rm inc}$). As in Section 2.6, we begin by defining the coherency vector of the total field for $\hat{\mathbf{r}}$ very close to $\hat{\mathbf{n}}^{\rm inc}$ as

$$\mathbf{J}(r\hat{\mathbf{r}}) = \frac{1}{2}\sqrt{\frac{\varepsilon_1}{\mu_0}} \begin{bmatrix} E_\vartheta(r\hat{\mathbf{r}})[E_\vartheta(r\hat{\mathbf{r}})]^* \\ E_\vartheta(r\hat{\mathbf{r}})[E_\varphi(r\hat{\mathbf{r}})]^* \\ E_\varphi(r\hat{\mathbf{r}})[E_\vartheta(r\hat{\mathbf{r}})]^* \\ E_\varphi(r\hat{\mathbf{r}})[E_\varphi(r\hat{\mathbf{r}})]^* \end{bmatrix}, \tag{2.134}$$

where the total electric field is

$$\mathbf{E}(r\hat{\mathbf{r}}) = \mathbf{E}^{\rm inc}(r\hat{\mathbf{r}}) + \mathbf{E}^{\rm sca}(r\hat{\mathbf{r}}). \tag{2.135}$$

Integrating the elements of $\mathbf{J}(r\hat{\mathbf{r}})$ over the surface of the collimated detector aligned normal to $\hat{\mathbf{n}}^{\rm inc}$ and using Eqs. (2.92), (2.94), and (2.98), we derive after rather lengthy algebraic manipulations

$$\mathbf{J}(r\hat{\mathbf{n}}^{\rm inc})\Delta S = \mathbf{J}^{\rm inc}\Delta S - \mathbf{K}^{J}(\hat{\mathbf{n}}^{\rm inc})\mathbf{J}^{\rm inc} + O(r^{-2}), \tag{2.136}$$

where the elements of the 4×4 so-called coherency extinction matrix $\mathbf{K}^{J}(\vartheta^{\rm inc}, \varphi^{\rm inc})$ are expressed in terms of the elements of the forward-scattering amplitude matrix $\mathbf{S}(\vartheta^{\rm inc}, \varphi^{\rm inc}; \vartheta^{\rm inc}, \varphi^{\rm inc})$ as follows:

$$\mathbf{K}^{J} = \frac{\mathrm{i}2\pi}{k_1}\begin{bmatrix} S_{11}^{*} - S_{11} & S_{12}^{*} & -S_{12} & 0 \\ S_{21}^{*} & S_{22}^{*} - S_{11} & 0 & -S_{12} \\ -S_{21} & 0 & S_{11}^{*} - S_{22} & S_{12}^{*} \\ 0 & -S_{21} & S_{21}^{*} & S_{22}^{*} - S_{22} \end{bmatrix}. \tag{2.137}$$

Switching again to Stokes parameters, we have

$$\mathbf{I}(r\hat{\mathbf{n}}^{\rm inc})\Delta S = \mathbf{I}^{\rm inc}\Delta S - \mathbf{K}(\hat{\mathbf{n}}^{\rm inc})\mathbf{I}^{\rm inc} + O(r^{-2}), \tag{2.138}$$

where $\mathbf{I}(r\hat{\mathbf{n}}^{\rm inc}) = \mathbf{D}\mathbf{J}(r\hat{\mathbf{n}}^{\rm inc})$. The Stokes extinction matrix is given by

$$\mathbf{K}(\hat{\mathbf{n}}^{\rm inc}) = \mathbf{D}\mathbf{K}^{J}(\hat{\mathbf{n}}^{\rm inc})\mathbf{D}^{-1}. \tag{2.139}$$

The explicit formulas for the elements of this matrix in terms of the elements of the matrix $\mathbf{S}(\vartheta^{\rm inc}, \varphi^{\rm inc}; \vartheta^{\rm inc}, \varphi^{\rm inc})$ are as follows:

$$K_{jj} = \frac{2\pi}{k_1}\mathrm{Im}(S_{11} + S_{22}), \qquad j = 1, ..., 4, \tag{2.140}$$

$$K_{12} = K_{21} = \frac{2\pi}{k_1}\mathrm{Im}(S_{11} - S_{22}), \tag{2.141}$$

$$K_{13} = K_{31} = -\frac{2\pi}{k_1}\mathrm{Im}(S_{12} + S_{21}), \tag{2.142}$$

$$K_{14} = K_{41} = \frac{2\pi}{k_1}\mathrm{Re}(S_{21} - S_{12}), \tag{2.143}$$

$$K_{23} = -K_{32} = \frac{2\pi}{k_1}\mathrm{Im}(S_{21} - S_{12}), \tag{2.144}$$

$$K_{24} = -K_{42} = -\frac{2\pi}{k_1}\mathrm{Re}(S_{12} + S_{21}), \tag{2.145}$$

$$K_{34} = -K_{43} = \frac{2\pi}{k_1}\mathrm{Re}(S_{22} - S_{11}). \tag{2.146}$$

Thus, only seven elements of the Stokes extinction matrix are independent. It is easy to verify that this is also true of the coherency extinction matrix. The elements of both matrices have the dimension of area and explicitly depend on $\varphi^{\rm inc}$ even when the incident wave propagates along the *z*-axis.

Equations (2.136) and (2.138) represent the most general form of the optical theorem. They show that the presence of the scattering particle changes not only the total power of the electromagnetic radiation received by the detector facing the incident wave (detector 1 in Fig. 2.3) but also, perhaps, its state of polarization. This phenomenon is called dichroism and results from different attenuation rates for different polarization components of the incident wave. Obviously, Eqs. (2.136) and (2.138) remain valid if the incident radiation is a parallel quasi-monochromatic beam of light rather than a monochromatic plane wave.

From Eqs. (2.64) and (2.140)–(2.146) we obtain the reciprocity relation for the Stokes extinction matrix:

$$\mathbf{K}(-\hat{\mathbf{n}}^{\rm inc}) = \mathbf{\Delta}_3[\mathbf{K}(\hat{\mathbf{n}}^{\rm inc})]^{\rm T}\mathbf{\Delta}_3, \tag{2.147a}$$

where the matrix $\mathbf{\Delta}_3$ is given by Eq. (2.125). It is also easy to derive a related symmetry property:

$$\mathbf{K}(-\hat{\mathbf{n}}^{\rm inc}) = \begin{bmatrix} K_{11}(\hat{\mathbf{n}}^{\rm inc}) & K_{12}(\hat{\mathbf{n}}^{\rm inc}) & -K_{13}(\hat{\mathbf{n}}^{\rm inc}) & K_{14}(\hat{\mathbf{n}}^{\rm inc}) \\ K_{21}(\hat{\mathbf{n}}^{\rm inc}) & K_{22}(\hat{\mathbf{n}}^{\rm inc}) & K_{23}(\hat{\mathbf{n}}^{\rm inc}) & -K_{24}(\hat{\mathbf{n}}^{\rm inc}) \\ -K_{31}(\hat{\mathbf{n}}^{\rm inc}) & K_{32}(\hat{\mathbf{n}}^{\rm inc}) & K_{33}(\hat{\mathbf{n}}^{\rm inc}) & K_{34}(\hat{\mathbf{n}}^{\rm inc}) \\ K_{41}(\hat{\mathbf{n}}^{\rm inc}) & -K_{42}(\hat{\mathbf{n}}^{\rm inc}) & K_{43}(\hat{\mathbf{n}}^{\rm inc}) & K_{44}(\hat{\mathbf{n}}^{\rm inc}) \end{bmatrix}. \tag{2.147b}$$

In other words, the only effect of reversing the direction of propagation is to change the sign of four elements of the Stokes extinction matrix. The modified Stokes and circular-polarization extinction matrices are given by

$$\mathbf{K}^{\rm MS}(\hat{\mathbf{n}}^{\rm inc}) = \mathbf{B}\mathbf{K}(\hat{\mathbf{n}}^{\rm inc})\mathbf{B}^{-1}, \tag{2.148}$$

$$\mathbf{K}^{\rm CP}(\hat{\mathbf{n}}^{\rm inc}) = \mathbf{A}\mathbf{K}(\hat{\mathbf{n}}^{\rm inc})\mathbf{A}^{-1}. \tag{2.149}$$

Reciprocity relations for the matrices $\mathbf{K}^{J}(\hat{\mathbf{n}}^{\rm inc})$, $\mathbf{K}^{\rm MS}(\hat{\mathbf{n}}^{\rm inc})$, and $\mathbf{K}^{\rm CP}(\hat{\mathbf{n}}^{\rm inc})$ can be derived from Eq. (2.147a) by analogy with Eqs. (2.126)–(2.128):

$$\mathbf{K}^{J}(-\hat{\mathbf{n}}^{\rm inc}) = \mathbf{\Delta}_{23}[\mathbf{K}^{J}(\hat{\mathbf{n}}^{\rm inc})]^{\rm T}\mathbf{\Delta}_{23}, \tag{2.150}$$

$$\mathbf{K}^{\rm MS}(-\hat{\mathbf{n}}^{\rm inc}) = \mathbf{\Delta}^{\rm MS}[\mathbf{K}^{\rm MS}(\hat{\mathbf{n}}^{\rm inc})]^{\rm T}[\mathbf{\Delta}^{\rm MS}]^{-1}, \tag{2.151}$$

$$\mathbf{K}^{\rm CP}(-\hat{\mathbf{n}}^{\rm inc}) = [\mathbf{K}^{\rm CP}(\hat{\mathbf{n}}^{\rm inc})]^{\rm T}. \tag{2.152}$$

2.8 Extinction, scattering, and absorption cross sections

Knowledge of the total electromagnetic field in the far-field zone also allows us to calculate such important optical characteristics of the scattering object as the total

scattering, absorption, and extinction cross sections. These optical cross sections are defined as follows. The product of the scattering cross section $C_{\rm sca}$ and the incident monochromatic energy flux gives the total monochromatic power removed from the incident wave as a result of scattering of the incident radiation in all directions. Analogously, the product of the absorption cross section $C_{\rm abs}$ and the incident monochromatic energy flux gives the total monochromatic power removed from the incident wave as a result of absorption of light by the object. Of course, the absorbed electromagnetic energy does not disappear but, rather, is converted into other forms of energy. Finally, the extinction cross section $C_{\rm ext}$ is the sum of the scattering and absorption cross sections and, when multiplied by the incident monochromatic energy flux, gives the total monochromatic power removed from the incident light by the combined effect of scattering and absorption.

To determine the total optical cross sections, we surround the object by an imaginary sphere of radius r large enough to be in the far-field zone. Since the surrounding medium is assumed to be nonabsorbing, the net rate at which the electromagnetic energy crosses the surface S of the sphere is always non-negative and is equal to the power absorbed by the particle:

$$W^{\rm abs} = -\int_S {\rm d}S \langle \mathbf{S}(\mathbf{r}) \rangle \cdot \hat{\mathbf{r}} = -r^2 \int_{4\pi} {\rm d}\hat{\mathbf{r}} \langle \mathbf{S}(\mathbf{r}) \rangle \cdot \hat{\mathbf{r}} \tag{2.153}$$

(see Eq. (1.31)). According to Eq. (2.88), $W^{\rm abs}$ can be written as a combination of three terms:

$$W^{\rm abs} = W^{\rm inc} - W^{\rm sca} + W^{\rm ext}, \tag{2.154}$$

where

$$W^{\rm inc} = -r^2 \int_{4\pi} {\rm d}\hat{\mathbf{r}} \langle \mathbf{S}^{\rm inc}(\mathbf{r}) \rangle \cdot \hat{\mathbf{r}}, \qquad W^{\rm sca} = r^2 \int_{4\pi} {\rm d}\hat{\mathbf{r}} \langle \mathbf{S}^{\rm sca}(\mathbf{r}) \rangle \cdot \hat{\mathbf{r}},$$

$$W^{\rm ext} = -r^2 \int_{4\pi} {\rm d}\hat{\mathbf{r}} \langle \mathbf{S}^{\rm ext}(\mathbf{r}) \rangle \cdot \hat{\mathbf{r}}. \tag{2.155}$$

$W^{\rm inc}$ vanishes identically because the surrounding medium is nonabsorbing and $\mathbf{S}^{\rm inc}(\mathbf{r})$ is a constant vector independent of $\mathbf{r}$, whereas $W^{\rm sca}$ is the rate at which the scattered energy crosses the surface S in the outward direction. Therefore, $W^{\rm ext}$ is equal to the sum of the energy scattering rate and the energy absorption rate:

$$W^{\rm ext} = W^{\rm sca} + W^{\rm abs}. \tag{2.156}$$

Inserting Eqs. (2.90)–(2.95) in Eq. (2.155) and recalling the definitions of the extinction and scattering cross sections, we derive after some algebra

$$C_{\rm ext} = \frac{W^{\rm ext}}{\frac{1}{2}\sqrt{\varepsilon_1/\mu_0}\,|\mathbf{E}_0^{\rm inc}|^2} = \frac{4\pi}{k_1|\mathbf{E}_0^{\rm inc}|^2}\,{\rm Im}[\mathbf{E}_1^{\rm sca}(\hat{\mathbf{n}}^{\rm inc})\cdot\mathbf{E}_0^{\rm inc*}], \tag{2.157}$$

$$C_{\rm sca} = \frac{W^{\rm sca}}{\frac{1}{2}\sqrt{\varepsilon_1/\mu_0}\,|\mathbf{E}_0^{\rm inc}|^2} = \frac{1}{|\mathbf{E}_0^{\rm inc}|^2}\int_{4\pi} d\hat{\mathbf{r}}\,|\mathbf{E}_1^{\rm sca}(\hat{\mathbf{r}})|^2. \tag{2.158}$$

In view of Eqs. (2.24), (2.30), (2.102), (2.104), (2.105), and (2.140)–(2.146), Eqs. (2.157) and (2.158) can be rewritten as

$$C_{\rm ext} = \frac{1}{I^{\rm inc}}[K_{11}(\hat{\mathbf{n}}^{\rm inc})I^{\rm inc} + K_{12}(\hat{\mathbf{n}}^{\rm inc})Q^{\rm inc} + K_{13}(\hat{\mathbf{n}}^{\rm inc})U^{\rm inc} + K_{14}(\hat{\mathbf{n}}^{\rm inc})V^{\rm inc}], \tag{2.159}$$

$$\begin{aligned} C_{\rm sca} &= \frac{r^2}{I^{\rm inc}}\int_{4\pi} d\hat{\mathbf{r}}\, I^{\rm sca}(r\hat{\mathbf{r}}) \\ &= \frac{1}{I^{\rm inc}}\int_{4\pi} d\hat{\mathbf{r}}[Z_{11}(\hat{\mathbf{r}}, \hat{\mathbf{n}}^{\rm inc})I^{\rm inc} + Z_{12}(\hat{\mathbf{r}}, \hat{\mathbf{n}}^{\rm inc})Q^{\rm inc} \\ &\qquad + Z_{13}(\hat{\mathbf{r}}, \hat{\mathbf{n}}^{\rm inc})U^{\rm inc} + Z_{14}(\hat{\mathbf{r}}, \hat{\mathbf{n}}^{\rm inc})V^{\rm inc}]. \end{aligned} \tag{2.160}$$

The absorption cross section is equal to the difference of the extinction and scattering cross sections:

$$C_{\rm abs} = C_{\rm ext} - C_{\rm sca} \geq 0. \tag{2.161}$$

The single-scattering albedo is defined as the ratio of the scattering and extinction cross sections:

$$\varpi = \frac{C_{\rm sca}}{C_{\rm ext}} \leq 1. \tag{2.162}$$

This quantity is widely used in radiative transfer theory and is interpreted as the probability that a photon interacting with the particle will be scattered rather than absorbed. Obviously, $\varpi = 1$ for nonabsorbing particles. Equations (2.159) and (2.160) (and thus Eqs. (2.161) and (2.162)) also hold for quasi-monochromatic incident light provided that the elements of the Stokes vector entering these equations are averages over a time interval long compared with the period of fluctuations. All cross sections are inherently real-valued positive quantities and have the dimension of area. They depend on the direction, polarization state, and wavelength of the incident light as well as on the particle size, morphology, relative refractive index, and orientation with respect to the reference frame.

Equation (2.159) is another representation of the optical theorem and, along with Eqs. (2.140)–(2.143), shows that although extinction is the combined effect of absorption and scattering in all directions by the particle, it is determined only by the amplitude scattering matrix in the exact forward direction. This is a direct consequence of the fact that extinction results from interference between the incident and scattered light, Eq. (2.91), and the presence of delta-function terms in Eqs. (2.92) and (2.93). Having derived Eq. (2.157), we can now rewrite Eq. (2.97) in the form

$$W_{\Delta S}(\hat{\mathbf{n}}^{\rm inc}) = \frac{1}{2}\sqrt{\frac{\varepsilon_1}{\mu_0}}\,|\mathbf{E}_0^{\rm inc}|^2(\Delta S - C_{\rm ext}) + O(r^{-2}). \tag{2.163}$$

This shows that the extinction cross section is a well-defined, observable quantity and can be determined by measuring $W_{\Delta S}(\hat{\mathbf{n}}^{\text{inc}})$ with and without the particle interposed between the source of light and the detector. The net effect of the particle is to reduce the detector area by "casting a shadow" of area C_{ext}. Of course, this does not mean that C_{ext} is merely given by the area G of the particle geometrical projection on the detector surface. However, this geometrical interpretation of the extinction cross section illustrates the rationale for introducing the dimensionless efficiency factor for extinction as the ratio of the extinction cross section to the geometrical cross section:

$$Q_{\text{ext}} = \frac{C_{\text{ext}}}{G}. \tag{2.164}$$

We will see in later chapters that Q_{ext} can be considerably greater or much less than unity. The efficiency factors for scattering and absorption are defined analogously:

$$Q_{\text{sca}} = \frac{C_{\text{sca}}}{G}, \qquad Q_{\text{abs}} = \frac{C_{\text{abs}}}{G}. \tag{2.165}$$

The quantity

$$\begin{aligned}\frac{\mathrm{d}C_{\text{sca}}}{\mathrm{d}\Omega} &= \frac{I^{\text{sca}}(r\hat{\mathbf{r}})r^2}{I^{\text{inc}}} \\ &= \frac{1}{I^{\text{inc}}}[Z_{11}(\hat{\mathbf{r}}, \hat{\mathbf{n}}^{\text{inc}})I^{\text{inc}} + Z_{12}(\hat{\mathbf{r}}, \hat{\mathbf{n}}^{\text{inc}})Q^{\text{inc}} + Z_{13}(\hat{\mathbf{r}}, \hat{\mathbf{n}}^{\text{inc}})U^{\text{inc}} + Z_{14}(\hat{\mathbf{r}}, \hat{\mathbf{n}}^{\text{inc}})V^{\text{inc}}]\end{aligned} \tag{2.166}$$

also has the dimension of area and is called the differential scattering cross section; it describes the angular distribution of the scattered light and specifies the electromagnetic power scattered into unit solid angle about a given direction per unit incident intensity. (Note that the symbol $\mathrm{d}C_{\text{sca}}/\mathrm{d}\Omega$ should not be interpreted as the derivative of a function of Ω.) The differential scattering cross section depends on the polarization state of the incident light as well as on the incidence and scattering directions. Clearly,

$$C_{\text{sca}} = \int_{4\pi} \mathrm{d}\hat{\mathbf{r}} \frac{\mathrm{d}C_{\text{sca}}}{\mathrm{d}\Omega}$$

(cf. Eqs. (2.160) and (2.166)). A quantity related to the differential scattering cross section is the phase function $p(\hat{\mathbf{r}}, \hat{\mathbf{n}}^{\text{inc}})$ defined as

$$p(\hat{\mathbf{r}}, \hat{\mathbf{n}}^{\text{inc}}) = \frac{4\pi}{C_{\text{sca}}} \frac{\mathrm{d}C_{\text{sca}}}{\mathrm{d}\Omega}. \tag{2.167}$$

The convenience of the phase function is that it is dimensionless and normalized:

$$\frac{1}{4\pi} \int_{4\pi} \mathrm{d}\hat{\mathbf{r}} p(\hat{\mathbf{r}}, \hat{\mathbf{n}}^{\text{inc}}) = 1. \tag{2.168}$$

The asymmetry parameter $\langle\cos\Theta\rangle$ is defined as the average cosine of the scattering angle $\Theta = \arccos(\hat{\mathbf{r}}\cdot\hat{\mathbf{n}}^{\text{inc}})$ (i.e., the angle between the incidence and scattering directions):

$$\langle\cos\Theta\rangle = \frac{1}{4\pi}\int_{4\pi} \mathrm{d}\hat{\mathbf{r}}\, p(\hat{\mathbf{r}}, \hat{\mathbf{n}}^{\text{inc}})\hat{\mathbf{r}}\cdot\hat{\mathbf{n}}^{\text{inc}} = \frac{1}{C_{\text{sca}}}\int_{4\pi} \mathrm{d}\hat{\mathbf{r}}\frac{\mathrm{d}C_{\text{sca}}}{\mathrm{d}\Omega}\hat{\mathbf{r}}\cdot\hat{\mathbf{n}}^{\text{inc}}. \tag{2.169}$$

The asymmetry parameter is positive if the particle scatters more light toward the forward direction $(\Theta = 0)$, is negative if more light is scattered toward the backscattering direction $(\Theta = \pi)$, and vanishes if the scattering is symmetric with respect to the plane perpendicular to the incidence direction. Obviously, $\langle\cos\Theta\rangle \in [-1, +1]$. The limiting values correspond to the phase functions $4\pi\delta(\hat{\mathbf{r}} + \hat{\mathbf{n}}^{\text{inc}})$ and $4\pi\delta(\hat{\mathbf{r}} - \hat{\mathbf{n}}^{\text{inc}})$, respectively.

2.9 Radiation pressure and radiation torque

The scattering and absorption of an electromagnetic wave cause the transfer of momentum from the electromagnetic field to the scattering object. The resulting force, called radiation pressure, is used in laboratories to levitate and size small particles (Ashkin and Dziedzic 1980; Chýlek *et al*. 1992; Ashkin 2000) and affects the spatial distribution of interplanetary and interstellar dust grains (Il'in and Voshchinnikov 1998; Landgraf *et al*. 1999). If the amplitudes of the incident and scattered fields do not change in time, the force due to radiation pressure averaged over the period $2\pi/\omega$ of the time-harmonic incident wave is

$$\mathbf{F} = \int_S \mathrm{d}S\,\langle\vec{\vec{T}}_{\text{M}}(\mathbf{r})\rangle\cdot\hat{\mathbf{n}} \tag{2.170}$$

(Stratton 1941, Section 2.5; Jackson 1998, Section 6.7), where $\vec{\vec{T}}_{\text{M}}$ is the so-called Maxwell stress tensor, the integration is performed over a closed surface S surrounding the scattering object, and $\hat{\mathbf{n}}$ is the unit vector in the direction of the local outward normal to S. Assume, for simplicity, that the scattering object is surrounded by a vacuum. Then the instantaneous value of the Maxwell stress tensor is

$$\begin{aligned}\vec{\vec{T}}_{\text{M}} &= \varepsilon_0[\mathbf{E}\otimes\mathbf{E} + c^2\mathbf{B}\otimes\mathbf{B} - \tfrac{1}{2}(\mathbf{E}\cdot\mathbf{E} + c^2\mathbf{B}\cdot\mathbf{B})\vec{I}\,] \\ &= \varepsilon_0\mathbf{E}\otimes\mathbf{E} + \mu_0\mathbf{H}\otimes\mathbf{H} - \tfrac{1}{2}(\varepsilon_0\mathbf{E}\cdot\mathbf{E} + \mu_0\mathbf{H}\cdot\mathbf{H})\vec{I},\end{aligned} \tag{2.171}$$

where $c = 1/\sqrt{\varepsilon_0\mu_0}$ is the speed of light in a vacuum. By analogy with Eq. (1.24), we have for the time average of the Maxwell stress tensor

$$\langle\vec{\vec{T}}_{\text{M}}(\mathbf{r})\rangle = \tfrac{1}{2}\text{Re}[\varepsilon_0\mathbf{E}(\mathbf{r})\otimes\mathbf{E}^*(\mathbf{r}) + \mu_0\mathbf{H}(\mathbf{r})\otimes\mathbf{H}^*(\mathbf{r}) - \tfrac{1}{2}(\varepsilon_0|\mathbf{E}(\mathbf{r})|^2 + \mu_0|\mathbf{H}(\mathbf{r})|^2)\vec{I}\,]. \tag{2.172}$$

It is convenient to choose for S a sphere centered at the scattering object and having a radius r large enough to be in the far-field zone. Then Eq. (2.170) becomes

$$\mathbf{F} = r^2 \int_{4\pi} \mathrm{d}\hat{\mathbf{r}} \langle \vec{\vec{T}}_{\mathrm{M}}(r\hat{\mathbf{r}}) \rangle \cdot \hat{\mathbf{r}}. \tag{2.173}$$

The total electric and magnetic fields are vector sums of the respective incident and scattered fields given by Eqs. (2.92)–(2.95). Because the incident and scattered fields are transverse, the first and second terms in square brackets on the right-hand side of Eq. (2.172) do not contribute to the integral in Eq. (2.173). We thus have

$$\begin{aligned}\mathbf{F} = &-\frac{\varepsilon_0 r^2}{4} \mathrm{Re} \int_{4\pi} \mathrm{d}\hat{\mathbf{r}}\, \hat{\mathbf{r}} \{ |\mathbf{E}^{\mathrm{inc}}(\mathbf{r})|^2 + |\mathbf{E}^{\mathrm{sca}}(\mathbf{r})|^2 + \mathbf{E}^{\mathrm{inc}}(\mathbf{r}) \cdot [\mathbf{E}^{\mathrm{sca}}(\mathbf{r})]^* \\ &\qquad + \mathbf{E}^{\mathrm{sca}}(\mathbf{r}) \cdot [\mathbf{E}^{\mathrm{inc}}(\mathbf{r})]^* \} \\ &-\frac{\mu_0 r^2}{4} \mathrm{Re} \int_{4\pi} \mathrm{d}\hat{\mathbf{r}}\, \hat{\mathbf{r}} \{ |\mathbf{H}^{\mathrm{inc}}(\mathbf{r})|^2 + |\mathbf{H}^{\mathrm{sca}}(\mathbf{r})|^2 + \mathbf{H}^{\mathrm{inc}}(\mathbf{r}) \cdot [\mathbf{H}^{\mathrm{sca}}(\mathbf{r})]^* \\ &\qquad + \mathbf{H}^{\mathrm{sca}}(\mathbf{r}) \cdot [\mathbf{H}^{\mathrm{inc}}(\mathbf{r})]^* \}. \end{aligned} \tag{2.174}$$

The terms $|\mathbf{E}^{\mathrm{inc}}(\mathbf{r})|^2$ and $|\mathbf{H}^{\mathrm{inc}}(\mathbf{r})|^2$ are constants independent of $\mathbf{r}$, so their contribution to $\mathbf{F}$ is simply zero. The contribution of the remaining terms follows from Eqs. (2.92)–(2.95) and the vector identity $(\mathbf{a}\times\mathbf{b})\cdot(\mathbf{c}\times\mathbf{d}) = (\mathbf{a}\cdot\mathbf{c})(\mathbf{b}\cdot\mathbf{d}) - (\mathbf{a}\cdot\mathbf{d})(\mathbf{b}\cdot\mathbf{c})$:

$$\mathbf{F} = \frac{2\pi\varepsilon_0}{k_1} \hat{\mathbf{n}}^{\mathrm{inc}} \, \mathrm{Im}\{\mathbf{E}_1^{\mathrm{sca}}(\hat{\mathbf{n}}^{\mathrm{inc}}) \cdot \mathbf{E}_0^{\mathrm{inc}*}\} - \frac{\varepsilon_0}{2} \int_{4\pi} \mathrm{d}\hat{\mathbf{r}}\, \hat{\mathbf{r}} |\mathbf{E}_1^{\mathrm{sca}}(\hat{\mathbf{r}})|^2 \tag{2.175}$$

or, in view of Eqs. (2.102), (2.104), (2.105), (2.157), and (2.166),

$$\begin{aligned}\mathbf{F} &= \frac{1}{c} \hat{\mathbf{n}}^{\mathrm{inc}} C_{\mathrm{ext}} I^{\mathrm{inc}} - \frac{1}{c} \int_{4\pi} \mathrm{d}\hat{\mathbf{r}}\, \hat{\mathbf{r}} [Z_{11}(\hat{\mathbf{r}}, \hat{\mathbf{n}}^{\mathrm{inc}}) I^{\mathrm{inc}} + Z_{12}(\hat{\mathbf{r}}, \hat{\mathbf{n}}^{\mathrm{inc}}) Q^{\mathrm{inc}} \\ &\qquad + Z_{13}(\hat{\mathbf{r}}, \hat{\mathbf{n}}^{\mathrm{inc}}) U^{\mathrm{inc}} + Z_{14}(\hat{\mathbf{r}}, \hat{\mathbf{n}}^{\mathrm{inc}}) V^{\mathrm{inc}}] \\ &= \frac{1}{c} \hat{\mathbf{n}}^{\mathrm{inc}} C_{\mathrm{ext}} I^{\mathrm{inc}} - \frac{1}{c} I^{\mathrm{inc}} \int_{4\pi} \mathrm{d}\hat{\mathbf{r}}\, \hat{\mathbf{r}} \frac{\mathrm{d}C_{\mathrm{sca}}}{\mathrm{d}\Omega} \end{aligned} \tag{2.176}$$

(Mishchenko 2001).

Although the first term on the right-hand side of Eq. (2.176) represents a force in the direction of $\hat{\mathbf{n}}^{\mathrm{inc}}$, the direction of the total radiation force is different, in general, from the direction of propagation of the incident beam and depends on its polarization state because of the second term. The projection of the total force on any direction $\hat{\mathbf{n}}$ is simply the dot product $\mathbf{F}\cdot\hat{\mathbf{n}}$. In particular, the component of the force in the direction of propagation of the incident light is

$$\begin{aligned}\mathbf{F}\cdot\hat{\mathbf{n}}^{\mathrm{inc}} &= \frac{1}{c} C_{\mathrm{ext}} I^{\mathrm{inc}} - \frac{1}{c} I^{\mathrm{inc}} \int_{4\pi} \mathrm{d}\hat{\mathbf{r}}\, \hat{\mathbf{r}} \cdot \hat{\mathbf{n}}^{\mathrm{inc}} \frac{\mathrm{d}C_{\mathrm{sca}}}{\mathrm{d}\Omega} \\ &= \frac{1}{c} I^{\mathrm{inc}} (C_{\mathrm{ext}} - C_{\mathrm{sca}} \langle \cos\Theta \rangle) \end{aligned}$$

$$= \frac{1}{c} I^{\text{inc}} C_{\text{pr}} \tag{2.177}$$

(see Eq. (2.169)), where the quantity

$$C_{\text{pr}} = C_{\text{ext}} - C_{\text{sca}} \langle \cos\Theta \rangle \tag{2.178}$$

is called the radiation-pressure cross section. By analogy with Eqs. (2.164) and (2.165), we can define the radiation-pressure efficiency factor as

$$Q_{\text{pr}} = \frac{C_{\text{pr}}}{G}. \tag{2.179}$$

Although being the result of a lengthy rigorous derivation, Eq. (2.177) allows a transparent physical interpretation. A beam of light carries linear momentum as well as energy. The direction of the momentum is that of propagation, while the absolute value of the momentum is energy/(speed of light). Since the total momentum of the electromagnetic field and the scattering object must be constant, the radiation force exerted on the object is equal to the momentum removed from the total electromagnetic field per unit time. Consider the component of the force in the direction of incidence. The momentum removed from the incident beam per unit time is $C_{\text{ext}} I^{\text{inc}} / c$. Of this amount, the part proportional to C_{abs} is not replaced, whereas the part proportional to C_{sca} is to some extent replaced by the contribution due to the projection of the moment of the scattered light on the direction of incidence. This contribution is equal to the integral of $I^{\text{sca}} \cos\Theta / c$ over all scattering directions, or $I^{\text{inc}} C_{\text{sca}} \langle \cos\Theta \rangle / c$. Note that van de Hulst (1957) used similar arguments as an heuristic derivation of Eq. (2.177).

If the absolute temperature of the particle is above zero then light emitted by the particle in all directions causes an additional component of the radiation force. This component will be discussed in Section 2.10.

The radiation pressure is accompanied by the radiation torque exerted on the particle and given by

$$\begin{aligned} \mathbf{\Gamma} &= -\int_S \mathrm{d}S\, r\hat{\mathbf{r}} \cdot [\langle \vec{\vec{T}}_{\text{M}}(\mathbf{r}) \rangle \times \hat{\mathbf{r}}] \\ &= -r^3 \int_{4\pi} \mathrm{d}\hat{\mathbf{r}}\, \hat{\mathbf{r}} \cdot [\langle \vec{\vec{T}}_{\text{M}}(\mathbf{r}) \rangle \times \hat{\mathbf{r}}] \end{aligned} \tag{2.180}$$

(cf. p. 288 of Jackson 1998), where r is the radius of a sphere S centered inside the scattering particle and having its surface in the far-field zone. Since $\hat{\mathbf{r}} \cdot \vec{\vec{I}} \times \hat{\mathbf{r}}$ vanishes identically, only the first two terms in square brackets on the right-hand side of Eq. (2.172) contribute to the integrals in Eq. (2.180). The evaluation of this contribution is complicated because it requires the knowledge of not only the transverse component of the scattered electric and magnetic fields but also of the longitudinal component, which we have so far neglected because it decays faster than $1/r$. Marston and

Crichton (1984) computed $\mathbf{\Gamma}$ for homogeneous and isotropic spherical particles, whereas Draine and Weingartner (1996) derived a formula for $\mathbf{\Gamma}$ in the framework of the so-called discrete dipole approximation (see Section 6.5).

2.10 Thermal emission

If the particle's absolute temperature T is above zero, it can emit as well as scatter and absorb electromagnetic radiation. The emitted radiation in the far-field zone of the particle propagates in the radial direction, i.e., along the unit vector $\hat{\mathbf{r}} = \mathbf{r}/r$, where $\mathbf{r}$ is the position vector of the observation point with origin inside the particle. The energetic and polarization characteristics of the emitted radiation are described by a four-component Stokes emission column vector $\mathbf{K}_{\rm e}(\hat{\mathbf{r}}, T, \omega)$ defined in such a way that the net rate at which the emitted energy crosses a surface element ΔS normal to $\hat{\mathbf{r}}$ at a distance r from the particle at frequencies from ω to $\omega + \Delta\omega$ is

$$W^{\rm e} = \frac{1}{r^2} K_{\rm e1}(\hat{\mathbf{r}}, T, \omega)\Delta S \Delta\omega. \tag{2.181}$$

$K_{\rm e1}(\hat{\mathbf{r}}, T, \omega)$, the first component of the column vector, can also be interpreted as the amount of electromagnetic energy emitted by the particle in the direction $\hat{\mathbf{r}}$ per unit solid angle per unit frequency interval per unit time.

In order to calculate $\mathbf{K}_{\rm e}(\hat{\mathbf{r}}, T, \omega)$, let us assume that the particle is placed inside an opaque cavity of dimensions large compared with the particle and any wavelength under consideration (Fig. 2.4a). If the cavity and the particle are maintained at the constant absolute temperature T, then the equilibrium electromagnetic radiation inside the cavity is isotropic, homogeneous, and unpolarized (Mandel and Wolf 1995). This radiation can be represented as a collection of quasi-monochromatic, unpolarized, incoherent beams propagating in all directions and characterized by the Planck blackbody energy distribution $I_{\rm b}(T, \omega)$. Specifically, at any point inside the cavity the amount of radiant energy per unit frequency interval, confined to a small solid angle $\Delta\Omega$ about any direction, which crosses an area ΔS normal to this direction in unit time is given by

$$I_{\rm b}(T, \omega)\Delta S \Delta\Omega = \frac{\hbar\omega^3}{4\pi^3 c^2 \left[\exp\left(\frac{\hbar\omega}{k_{\rm B}T}\right) - 1\right]} \Delta S \Delta\Omega, \tag{2.182}$$

where $\hbar = h/2\pi$, h is Planck's constant, c is the speed of light in a vacuum, and $k_{\rm B}$ is Boltzmann's constant.

Consider an imaginary collimated, polarization-sensitive detector of electromagnetic radiation with surface ΔS and small solid-angle field of view $\Delta\Omega$, placed at a distance r from the particle (Fig. 2.4a). The dimension of the detector surface is much greater than any dimension of the particle and r is large enough to be in the far-field

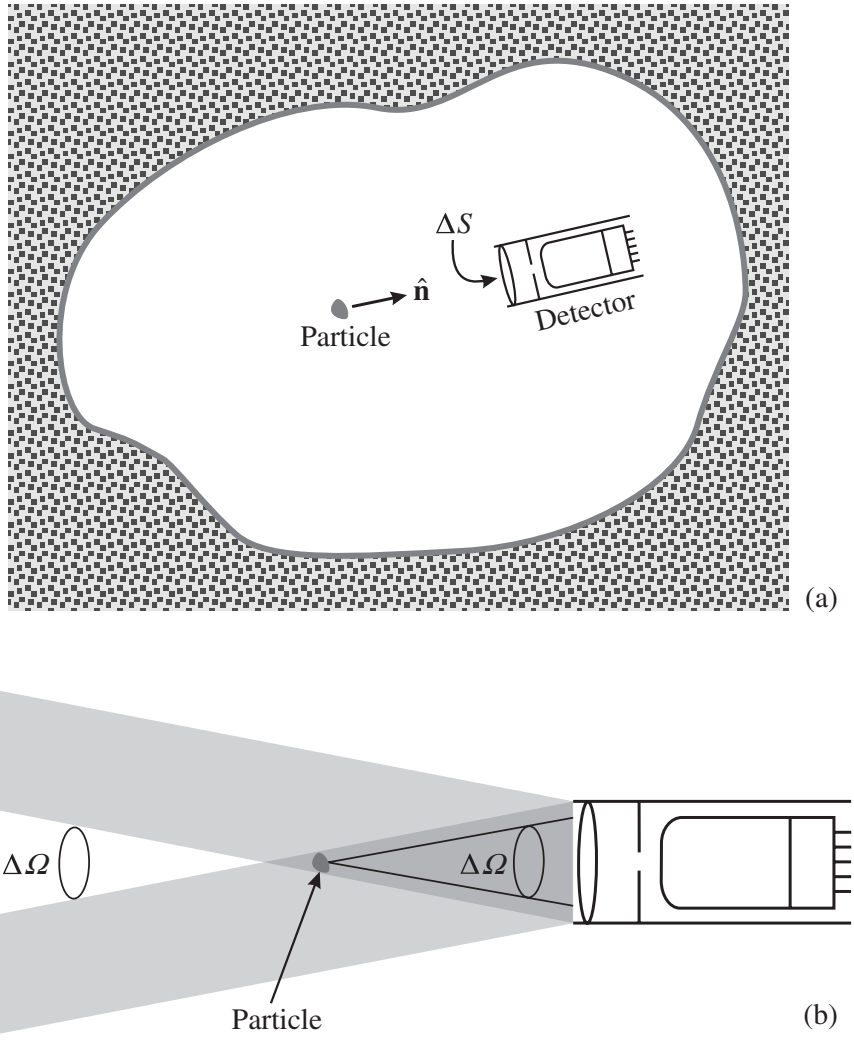

Figure 2.4. (a) Cavity, particle, and electromagnetic radiation field in thermal equilibrium. (b) Illumination geometry.

zone of the particle but smaller than $\sqrt{\Delta S/\Delta\Omega}$. The latter condition ensures that all plane wave fronts incident on the detector in directions falling into its solid-angle field of view $\Delta\Omega$ are equally attenuated by the particle (Fig. 2.4b). The surface ΔS is aligned normal to and centered on $\hat{\mathbf{r}}$, where $\hat{\mathbf{r}}$ is the unit vector originating inside the particle and pointing toward the detector.

In the absence of the particle, the polarized signal per unit frequency interval measured by the detector would be given by

$$\mathbf{I}_{\rm b}(T,\omega)\Delta S\Delta\Omega, \tag{2.183}$$

where

$$\mathbf{I}_{\mathrm{b}}(T, \omega) = \begin{bmatrix} I_{\mathrm{b}}(T, \omega) \\ 0 \\ 0 \\ 0 \end{bmatrix} \tag{2.184}$$

is the blackbody Stokes column vector. The particle attenuates the incident blackbody radiation, emits radiation, and scatters the blackbody radiation coming from all directions in the direction of the detector. Taking into account that only the radiation emitted and scattered by the particle within the solid-angle field of view $\Delta\Omega$ is detected (Fig. 2.4b), we conclude that the polarized signal measured by the detector in the presence of the particle is

$$\mathbf{I}_{\mathrm{b}}(T, \omega)\Delta S\Delta\Omega - \mathbf{K}(\hat{\mathbf{r}}, \omega)\mathbf{I}_{\mathrm{b}}(T, \omega)\Delta\Omega + \mathbf{K}_{\mathrm{e}}(\hat{\mathbf{r}}, T, \omega)\Delta\Omega + \Delta\Omega \int_{4\pi} \mathrm{d}\hat{\mathbf{r}}'\, \mathbf{Z}(\hat{\mathbf{r}}, \hat{\mathbf{r}}', \omega)\mathbf{I}_{\mathrm{b}}(T, \omega) \tag{2.185}$$

(see Eqs. (2.138) and (2.102)). However, in thermal equilibrium the presence of the particle does not change the distribution of radiation. Therefore, we can equate expressions (2.183) and (2.185) and finally derive for the ith component of $\mathbf{K}_{\mathrm{e}}$

$$K_{\mathrm{e}i}(\hat{\mathbf{r}}, T, \omega) = I_{\mathrm{b}}(T, \omega)K_{i1}(\hat{\mathbf{r}}, \omega) - I_{\mathrm{b}}(T, \omega) \int_{4\pi} \mathrm{d}\hat{\mathbf{r}}' Z_{i1}(\hat{\mathbf{r}}, \hat{\mathbf{r}}', \omega), \qquad i = 1, ..., 4. \tag{2.186}$$

This important relation expresses the Stokes emission vector in terms of the leftmost columns of the extinction and phase matrices and the Planck energy distribution. Although our derivation assumed that the particle was in thermal equilibrium with the surrounding radiation field, emissivity is a property of the particle only. Therefore, Eq. (2.186) is valid for any particle, in equilibrium or in nonequilibrium. A more detailed derivation of this formula based on the so-called fluctuation-dissipation theorem is given by Tsang *et al.* (2000).

As we pointed out in Section 2.9, the emitted radiation contributes to the total radiation force exerted on the particle. The emitted radiation is incoherent and does not interact with the incident and scattered radiation, thereby generating an independent component of the radiation force. Furthermore, emission is analogous to scattering in that it generates radiation propagating radially in all directions. Therefore, we can write the emission component of the radiation force by analogy with the scattering component given by the second term on the right-hand side of Eq. (2.176):

$$\mathbf{F}_{\mathrm{e}}(T) = -\frac{1}{c} \int_0^\infty \mathrm{d}\omega \int_{4\pi} \mathrm{d}\hat{\mathbf{r}}\hat{\mathbf{r}} K_{\mathrm{e}1}(\hat{\mathbf{r}}, T, \omega). \tag{2.187}$$

Unlike the extinction and scattering components of the radiation force, the emission component depends on the particle temperature. Another effect of emission is to pro-

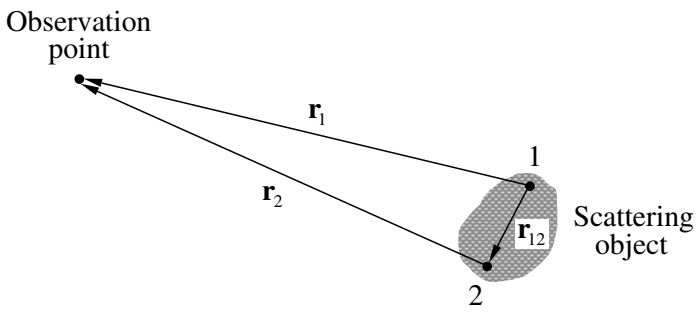

Figure 2.5. The amplitude matrix changes when the origin is shifted. The position vectors $\mathbf{r}_1$ and $\mathbf{r}_2$ originate at points 1 and 2, respectively.

duce a component of the radiation torque independent of that caused by scattering and absorption.

2.11 Translations of the origin

We began Section 2.2 by choosing the origin of the coordinate system close to the geometrical center of the scattering object, and that step was essential in deriving the formulas describing electromagnetic scattering in the far-field zone. Although the origin can be chosen arbitrarily, in general, the amplitude scattering matrix will change if the origin is moved, even if the orientation of the particle with respect to the reference frame remains the same. It is, therefore, important to supplement the rotation transformation law of Eq. (2.72) by a translation law describing the transformation of the amplitude scattering matrix upon a shift in the origin.

Let us consider two reference frames with origins 1 and 2 inside a scattering particle (Fig. 2.5). We assume that both reference frames have the same spatial orientation and denote the respective amplitude scattering matrices as $\mathbf{S}_1$ and $\mathbf{S}_2$. Let the particle be illuminated by a plane electromagnetic wave

$$\mathbf{E}^{\rm inc}(\mathbf{r}_1) = \mathbf{E}_0^{\rm inc} \exp(ik_1 \hat{\mathbf{n}}^{\rm inc} \cdot \mathbf{r}_1), \tag{2.188}$$

where $\mathbf{r}_1$ is the position vector originating at origin 1. Let $\mathbf{r}_2$ be the position vector of the same observation point but originating at origin 2. Since $\mathbf{r}_1 = \mathbf{r}_2 + \mathbf{r}_{12}$, where $\mathbf{r}_{12}$ connects origins 1 and 2, the incident electric field at the same observation point can also be written as

$$\mathbf{E}^{\rm inc}(\mathbf{r}_2) = \mathbf{E}_0^{\rm inc} \exp(ik_1 \hat{\mathbf{n}}^{\rm inc} \cdot \mathbf{r}_2) \exp(ik_1 \hat{\mathbf{n}}^{\rm inc} \cdot \mathbf{r}_{12}). \tag{2.189}$$

The scattered field at an observation point does not depend on how we choose the origin of the coordinate system as long as the incident field remains the same. Therefore, we have in the far-field zone

$$\frac{\mathrm{e}^{\mathrm{i}k_1 r_1}}{r_1}\mathbf{S}_1\left(\frac{\mathbf{r}_1}{r_1},\hat{\mathbf{n}}^{\mathrm{inc}}\right)\begin{bmatrix}E_{0\vartheta}^{\mathrm{inc}}\\E_{0\varphi}^{\mathrm{inc}}\end{bmatrix}=\frac{\mathrm{e}^{\mathrm{i}k_1 r_2}}{r_2}\exp(\mathrm{i}k_1\hat{\mathbf{n}}^{\mathrm{inc}}\cdot\mathbf{r}_{12})\,\mathbf{S}_2\left(\frac{\mathbf{r}_2}{r_2},\hat{\mathbf{n}}^{\mathrm{inc}}\right)\begin{bmatrix}E_{0\vartheta}^{\mathrm{inc}}\\E_{0\varphi}^{\mathrm{inc}}\end{bmatrix}. \tag{2.190}$$

Taking the limits $k_1 r_1 \to \infty$ and $k_1 r_2 \to \infty$ and using the law of cosines,

$$r_2^2 = r_1^2 + r_{12}^2 - 2\mathbf{r}_1\cdot\mathbf{r}_{12},$$

we finally obtain

$$\mathbf{S}_1(\hat{\mathbf{n}}^{\mathrm{sca}},\hat{\mathbf{n}}^{\mathrm{inc}}) = \mathrm{e}^{\mathrm{i}\Delta}\mathbf{S}_2(\hat{\mathbf{n}}^{\mathrm{sca}},\hat{\mathbf{n}}^{\mathrm{inc}}), \tag{2.191}$$

where $\hat{\mathbf{n}}^{\mathrm{sca}} = \mathbf{r}_1/r_1$,

$$\Delta = k_1\,\mathbf{r}_{12}\cdot(\hat{\mathbf{n}}^{\mathrm{inc}} - \hat{\mathbf{n}}^{\mathrm{sca}}), \tag{2.192}$$

and we have assumed that

$$\frac{r_{12}}{r_1} \ll 1 \quad \text{and} \quad \frac{k_1 r_{12}^2}{2r_1} \ll 1. \tag{2.193}$$

Equation (2.191) is the sought translation transformation law for the amplitude scattering matrix. It remains valid even if either origin lies outside the scattering particle, as long as the asymptotic far-field conditions of Eq. (2.193) are satisfied.

Despite the fact that the amplitude scattering matrix changes when the origin is shifted, the extinction and phase matrices remain invariant. Indeed, the factor $\mathrm{e}^{\mathrm{i}\Delta}$ is common to all elements of the amplitude scattering matrix and disappears when multiplied by its complex-conjugate counterpart, whereas the phase Δ vanishes identically in the exact forward-scattering direction (cf. Eqs. (2.106)–(2.121) and (2.140)–(2.146)). It is straightforward to verify that all optical cross sections and efficiency factors, the single-scattering albedo, the phase function, the asymmetry parameter, the emission vector, and the radiation force also remain unchanged.

Further reading

The books by Colton and Kress (1983), Varadan *et al*. (1991) and de Hoop (1995) provide a thorough theoretical introduction to the propagation and scattering of electromagnetic, acoustic, and elastodynamic waves. Appendix 3 of Van Bladel (1964) and chapter 6 of Varadan *et al*. (1991) list important formulas from vector and dyadic algebra and vector and dyadic calculus. The use of dyadics and dyadic Green's functions in electromagnetics is described by Tai (1993).

Chapter 3

Scattering, absorption, and emission by collections of independent particles

The formalism developed in the preceding chapter strictly applies only to the far-field scattering and absorption of monochromatic or quasi-monochromatic light by an isolated particle in the form of a single body or a fixed finite aggregate (Fig. 2.1) and to the thermal emission from such a particle. We will now describe how this formalism can be extended to single and multiple scattering, absorption, and emission by collections of independently scattering particles under certain simplifying assumptions.

3.1 Single scattering, absorption, and emission by a small volume element comprising randomly and sparsely distributed particles

Consider first a small volume element having a linear dimension l, comprising a number N of randomly positioned particles, and illuminated by a plane electromagnetic wave. Although the volume element is assumed to be macroscopically small, its size must still be much larger than the size of the constituent particles and the wavelength of the incident light. We assume that N is sufficiently small that the mean distance between the particles is also much larger than the incident wavelength and the average particle size. We also assume that N is sufficiently small that the main contribution to the total scattered radiation exiting the volume element comes from light scattered only once. In other words, the contribution to the total scattered signal of light scattered two and more times by particles inside the volume element is assumed to be negligibly small. This is equivalent to requiring that the "scattering efficiency"

$N\langle C_{\mathrm{sca}}\rangle l^{-2}$ of the volume element (i.e., the ratio of the total scattering cross section of the particles contained in the volume element to the volume element's geometrical cross section) be much smaller than unity; $\langle C_{\mathrm{sca}}\rangle$ is the average scattering cross section per particle. Finally, we assume that the positions of the particles during the measurement are sufficiently random that there are no systematic phase relations between individual waves scattered by different particles.

Let the incident electric field be given by

$$\mathbf{E}^{\mathrm{inc}}(\mathbf{r}) = \mathbf{E}_0^{\mathrm{inc}} \exp(\mathrm{i}k_1 \hat{\mathbf{n}}^{\mathrm{inc}} \cdot \mathbf{r}), \tag{3.1}$$

where the position vector $\mathbf{r}$ originates at the geometrical center of the volume element O. The total electric field scattered by the volume element at a large distance r from O can be written as the vector sum of the partial fields scattered by the component particles:

$$\mathbf{E}^{\mathrm{sca}}(\mathbf{r}) = \sum_{n=1}^{N} \mathbf{E}_n^{\mathrm{sca}}(\mathbf{r}), \tag{3.2}$$

where the position vector $\mathbf{r}$ of the observation point originates at O, and the index n numbers the particles. Since we ignore multiple scattering, we assume that each particle is excited only by the external incident field but not by the secondary fields scattered by other particles. Furthermore, because the particles are widely separated, each of them scatters the incident wave in exactly the same way as if all other particles did not exist. Therefore, according to Section 2.11, the partial scattered fields are given by

$$\begin{bmatrix} [\mathbf{E}_n^{\mathrm{sca}}(\mathbf{r})]_\vartheta \\ [\mathbf{E}_n^{\mathrm{sca}}(\mathbf{r})]_\varphi \end{bmatrix} = \frac{\mathrm{e}^{\mathrm{i}k_1 r}}{r} \mathrm{e}^{\mathrm{i}\Delta_n} \mathbf{S}_n(\hat{\mathbf{r}}, \hat{\mathbf{n}}^{\mathrm{inc}}) \begin{bmatrix} E_{0\vartheta}^{\mathrm{inc}} \\ E_{0\varphi}^{\mathrm{inc}} \end{bmatrix}, \tag{3.3}$$

where $\hat{\mathbf{r}} = \mathbf{r}/r$, $\mathbf{S}_n(\hat{\mathbf{r}}, \hat{\mathbf{n}}^{\mathrm{inc}})$ is the amplitude scattering matrix of the nth particle, centered inside that particle, the phase Δ_n is given by

$$\Delta_n = k_1 \mathbf{r}_{On} \cdot (\hat{\mathbf{n}}^{\mathrm{inc}} - \hat{\mathbf{r}}), \tag{3.4}$$

and the vector $\mathbf{r}_{On}$ connects the origin of the volume element O with the nth particle's origin. As in Section 2.11, we have assumed that

$$\frac{r_{On}}{r} \ll 1 \quad \text{and} \quad \frac{k_1 r_{On}^2}{2r} \ll 1, \qquad n = 1, \ldots, N, \tag{3.5}$$

or, equivalently,

$$\frac{l}{r} \ll 1 \quad \text{and} \quad \frac{k_1 l^2}{2r} \ll 1. \tag{3.6}$$

These conditions explicitly indicate that the observation point is in the far-field zone of the small volume element as a whole and that the latter is treated as a single scatterer. We thus have

$$\begin{bmatrix} E_{\vartheta}^{\mathrm{sca}}(\mathbf{r}) \\ E_{\varphi}^{\mathrm{sca}}(\mathbf{r}) \end{bmatrix} = \frac{\mathrm{e}^{\mathrm{i}k_1 r}}{r} \mathbf{S}(\hat{\mathbf{r}}, \hat{\mathbf{n}}^{\mathrm{inc}}) \begin{bmatrix} E_{0\vartheta}^{\mathrm{inc}} \\ E_{0\varphi}^{\mathrm{inc}} \end{bmatrix}, \tag{3.7}$$

where the total amplitude scattering matrix of the small volume element centered at O is

$$\mathbf{S}(\hat{\mathbf{r}}, \hat{\mathbf{n}}^{\mathrm{inc}}) = \sum_{n=1}^{N} \mathrm{e}^{\mathrm{i}\Delta_n} \mathbf{S}_n(\hat{\mathbf{r}}, \hat{\mathbf{n}}^{\mathrm{inc}}). \tag{3.8}$$

Since the Δ_n vanish in the exact forward-scattering direction, substituting Eq. (3.8) in Eqs. (2.140)–(2.146) yields the total extinction matrix of the small volume element:

$$\mathbf{K} = \sum_{n=1}^{N} \mathbf{K}_n = N\langle \mathbf{K} \rangle, \tag{3.9}$$

where $\langle \mathbf{K} \rangle$ is the average extinction matrix per particle. Equation (2.159) then gives the total extinction cross section:

$$C_{\mathrm{ext}} = \sum_{n=1}^{N} (C_{\mathrm{ext}})_n = N\langle C_{\mathrm{ext}} \rangle, \tag{3.10}$$

where $\langle C_{\mathrm{ext}} \rangle$ is the average extinction cross section per particle. Analogously, by substituting Eq. (3.8) in Eqs. (2.106)–(2.121) and assuming that particle positions are sufficiently random that

$$\left| \mathrm{Re} \sum_{n} \sum_{n' \neq n} [\mathbf{S}_n(\hat{\mathbf{r}}, \hat{\mathbf{n}}^{\mathrm{inc}})]_{ij} [\mathbf{S}_{n'}(\hat{\mathbf{r}}, \hat{\mathbf{n}}^{\mathrm{inc}})]_{kl}^{*} \exp[\mathrm{i}(\Delta_n - \Delta_{n'})] \right|$$

$$\ll \left| \mathrm{Re} \sum_{n} [\mathbf{S}_n(\hat{\mathbf{r}}, \hat{\mathbf{n}}^{\mathrm{inc}})]_{ij} [\mathbf{S}_n(\hat{\mathbf{r}}, \hat{\mathbf{n}}^{\mathrm{inc}})]_{kl}^{*} \right|, \qquad i, j, k, l = 1, 2 \tag{3.11a}$$

and, if $i \neq k$ or $j \neq l$,

$$\left| \mathrm{Im} \sum_{n} \sum_{n' \neq n} [\mathbf{S}_n(\hat{\mathbf{r}}, \hat{\mathbf{n}}^{\mathrm{inc}})]_{ij} [\mathbf{S}_{n'}(\hat{\mathbf{r}}, \hat{\mathbf{n}}^{\mathrm{inc}})]_{kl}^{*} \exp[\mathrm{i}(\Delta_n - \Delta_{n'})] \right|$$

$$\ll \left| \mathrm{Im} \sum_{n} [\mathbf{S}_n(\hat{\mathbf{r}}, \hat{\mathbf{n}}^{\mathrm{inc}})]_{ij} [\mathbf{S}_n(\hat{\mathbf{r}}, \hat{\mathbf{n}}^{\mathrm{inc}})]_{kl}^{*} \right|, \tag{3.11b}$$

it is straightforward to show that the total phase matrix of the volume element is given by

$$\mathbf{Z} = \sum_{n=1}^{N} \mathbf{Z}_n = N\langle \mathbf{Z} \rangle, \tag{3.12}$$

where $\langle \mathbf{Z} \rangle$ is the average phase matrix per particle. Equations (2.160) and (2.161) then give the total scattering and absorption cross sections of the volume element:

$$C_{\mathrm{sca}} = \sum_{n=1}^{N} (C_{\mathrm{sca}})_n = N\langle C_{\mathrm{sca}} \rangle, \tag{3.13}$$

$$C_{\mathrm{abs}} = \sum_{n=1}^{N} (C_{\mathrm{abs}})_n = N\langle C_{\mathrm{abs}} \rangle, \tag{3.14}$$

where $\langle C_{\mathrm{sca}} \rangle$ is the average scattering cross section and $\langle C_{\mathrm{abs}} \rangle$ the average absorption cross section per particle. Finally, Eqs. (2.166), (2.169), (2.178), and (2.186) yield

$$C_{\mathrm{pr}} = \sum_{n=1}^{N} (C_{\mathrm{pr}})_n = N\langle C_{\mathrm{pr}} \rangle, \tag{3.15}$$

$$\mathbf{K}_{\mathrm{e}} = \sum_{n=1}^{N} (\mathbf{K}_{\mathrm{e}})_n = N\langle \mathbf{K}_{\mathrm{e}} \rangle, \tag{3.16}$$

where $\langle C_{\mathrm{pr}} \rangle$ is the average radiation-pressure cross section and $\langle \mathbf{K}_{\mathrm{e}} \rangle$ the average emission vector per particle. Thus, the optical cross sections, the phase and extinction matrices, and the emission vector of the small volume element comprising randomly positioned, widely separated particles are obtained by adding the respective optical characteristics of the individual particles. Obviously, this property of additivity also holds when the incident light is a parallel quasi-monochromatic beam rather than a plane electromagnetic wave.

It should be recognized that at any given moment, the particles filling the volume element form a certain spatial configuration, and the individual waves scattered by different particles have a specific phase relation and interfere. However, even a minute displacement of the particles or a slight change in the scattering geometry during the measurement may change the phase differences entirely. Therefore, in almost all practical situations the light singly scattered by a collection of randomly positioned particles and measured by a real detector appears to be incoherent, and the optical characteristics of individual particles must be added without regard to phase.

Because the total phase matrix of the volume element is the sum of the phase matrices of the constituent particles, the nine independent quadratic relations between the elements of the single-particle phase matrix as well as some quadratic inequalities (see Section 2.6) generally no longer hold. Still, there are a number of linear and quadratic inequalities that can be used for testing the elements of theoretically or experimentally obtained phase matrices of particle collections (Hovenier and van der Mee 2000). The simplest and most important of them are

$$Z_{11} \geq 0 \tag{3.17}$$

(cf. Eqs. (2.106) and (3.12)) and

$$|Z_{ij}| \leq Z_{11}, \quad i, j = 1, ..., 4. \tag{3.18}$$

Obviously, the reciprocity and symmetry relations (2.124) and (2.147a,b) remain valid for the phase and extinction matrices of the volume element.

3.2 Ensemble averaging

Scattering media encountered in practice are usually mixtures of particles with different sizes, shapes, orientations, and refractive indices. Equations (3.9)–(3.16) imply that theoretical computations of single scattering of light by a small volume element consisting of such particles must include averaging the optical cross sections, the phase and extinction matrices, and the emission vector over a representative particle ensemble. The computation of ensemble averages is, in principle, rather straightforward. For example, for homogeneous ellipsoids with semi-axes $a \in [a_{\min}, a_{\max}]$, $b \in [b_{\min}, b_{\max}]$, and $c \in [c_{\min}, c_{\max}]$ and the same refractive index, the ensemble-averaged phase matrix per particle is

$$\langle \mathbf{Z}(\hat{\mathbf{n}}, \hat{\mathbf{n}}') \rangle = \int_{a_{\min}}^{a_{\max}} \mathrm{d}a \int_{b_{\min}}^{b_{\max}} \mathrm{d}b \int_{c_{\min}}^{c_{\max}} \mathrm{d}c \int_0^{2\pi} \mathrm{d}\alpha \int_0^{\pi} \mathrm{d}\beta \sin\beta \int_0^{2\pi} \mathrm{d}\gamma p(\alpha, \beta, \gamma; a, b, c) \times \mathbf{Z}(\hat{\mathbf{n}}, \hat{\mathbf{n}}'; \alpha, \beta, \gamma; a, b, c), \tag{3.19}$$

where the Euler angles α, β, and γ specify particle orientations with respect to the laboratory reference frame, and $p(\alpha, \beta, \gamma; a, b, c)$ is a probability density function satisfying the normalization condition:

$$\int_{a_{\min}}^{a_{\max}} \mathrm{d}a \int_{b_{\min}}^{b_{\max}} \mathrm{d}b \int_{c_{\min}}^{c_{\max}} \mathrm{d}c \int_0^{2\pi} \mathrm{d}\alpha \int_0^{\pi} \mathrm{d}\beta \sin\beta \int_0^{2\pi} \mathrm{d}\gamma p(\alpha, \beta, \gamma; a, b, c) = 1. \tag{3.20}$$

The integrals in Eq. (3.19) are usually evaluated numerically by using appropriate quadrature formulas. Some theoretical techniques (e.g., the *T*-matrix method) allow analytical averaging over particle orientations, thereby bypassing time-consuming integration over the Euler angles.

It is often assumed that the shape and size distribution and the orientation distribution are statistically independent. The total probability density function can then be simplified by representing it as a product of two functions, one of which, $p_{\mathrm{s}}(a, b, c)$, describes the particle shape and size distribution and the other of which, $p_{\mathrm{o}}(\alpha, \beta, \gamma)$, describes the distribution of particle orientations:

$$p(\alpha, \beta, \gamma; a, b, c) = p_{\mathrm{s}}(a, b, c)\, p_{\mathrm{o}}(\alpha, \beta, \gamma). \tag{3.21}$$

Each is normalized to unity:

$$\int_{a_{\min}}^{a_{\max}} \mathrm{d}a \int_{b_{\min}}^{b_{\max}} \mathrm{d}b \int_{c_{\min}}^{c_{\max}} \mathrm{d}c\, p_{\mathrm{s}}(a, b, c) = 1, \tag{3.22}$$

$$\int_0^{2\pi} \mathrm{d}\alpha \int_0^{\pi} \mathrm{d}\beta \sin\beta \int_0^{2\pi} \mathrm{d}\gamma\, p_{\mathrm{o}}(\alpha, \beta, \gamma) = 1. \tag{3.23}$$

In consequence, the problems of computing the shape and size and the orientation averages are separated. Similarly, it is often convenient to separate averaging over

shapes and sizes by assuming that particle shapes and sizes are statistically independent. For example, the shape of a spheroidal particle can be specified by its aspect ratio ε (the ratio of the largest to the smallest axes) along with the designation of either prolate or oblate, whereas the size of the particle can be specified by an equivalent-sphere radius a. Then the shape and size probability density function $p_s(\varepsilon, a)$ can be represented as a product

$$p_s(\varepsilon, a) = p(\varepsilon)n(a), \tag{3.24}$$

where $p(\varepsilon)$ describes the distribution of spheroid aspect ratios and $n(a)$ is the distribution of equivalent-sphere radii. Again, both $p(\varepsilon)$ and $n(a)$ are normalized to unity:

$$\int_{\varepsilon_{\min}}^{\varepsilon_{\max}} \mathrm{d}\varepsilon p(\varepsilon) = 1, \tag{3.25}$$

$$\int_{a_{\min}}^{a_{\max}} \mathrm{d}a n(a) = 1. \tag{3.26}$$

In the absence of external forces such as magnetic, electrostatic, or aerodynamical forces, all orientations of a nonspherical particle are equiprobable. In this practically important case of randomly oriented particles, the orientation distribution function is uniform with respect to the Euler angles of rotation, and we have

$$p_{\mathrm{o,random}}(\alpha, \beta, \gamma) \equiv \frac{1}{8\pi^2}. \tag{3.27}$$

An external force can make the orientation distribution axially symmetric, the axis of symmetry being given by the direction of the force. For example, interstellar dust grains can be axially oriented by a cosmic magnetic field (Martin 1978), whereas nonspherical hydrometeors can be axially oriented by the aerodynamical force resulting from their non-zero falling velocity (Liou 1992). In this case it is convenient to choose the laboratory reference frame with the z-axis along the external force direction so that the orientation distribution is uniform with respect to the Euler angles α and γ:

$$p_{\mathrm{o,axial}}(\alpha, \beta, \gamma) \equiv \frac{1}{4\pi^2} p_{\mathrm{o}}(\beta). \tag{3.28}$$

Particular details of the particle shape can also simplify the orientation distribution function. For example, for rotationally symmetric bodies it is convenient to direct the z-axis of the particle reference frame along the axis of rotation, in which case the orientation distribution function in the laboratory reference frame becomes independent of the Euler angle γ:

$$p_{\mathrm{o}}(\alpha, \beta, \gamma) \equiv \frac{1}{2\pi} p_{\mathrm{o}}(\alpha, \beta). \tag{3.29}$$

3.3 Condition of independent scattering

The inequalities (3.11a) and (3.11b) require the assumption that scattering is incoherent and that the positions of the particles filling the volume element are uncorrelated during the time necessary to make the measurement. However, it is rather difficult to give general and definitive criteria under which the inequalities (3.11a) and (3.11b) are satisfied. Also, there is no obvious prescription for specifying the minimal interparticle separation that allows the use of the concept of the single-particle amplitude scattering matrix in Eq. (3.3) and makes particles effectively independent scatterers. Exact computations for a few specific cases can perhaps provide qualitative guidance. Figure 3.1 shows the results of exact T-matrix computations (Chapter 5) of the ratios

$$\frac{Z_{22}(\vartheta^{\rm sca}, \varphi^{\rm sca}=0; \vartheta^{\rm inc}=0, \varphi^{\rm inc}=0)}{Z_{11}(\vartheta^{\rm sca}, \varphi^{\rm sca}=0; \vartheta^{\rm inc}=0, \varphi^{\rm inc}=0)},$$
$$-\frac{Z_{21}(\vartheta^{\rm sca}, \varphi^{\rm sca}=0; \vartheta^{\rm inc}=0, \varphi^{\rm inc}=0)}{Z_{11}(\vartheta^{\rm sca}, \varphi^{\rm sca}=0; \vartheta^{\rm inc}=0, \varphi^{\rm inc}=0)} \tag{3.30}$$

versus $\vartheta^{\rm sca}$ for randomly oriented two-sphere clusters with touching or separated components (Mishchenko *et al*. 1995). The relative refractive index is 1.5 + i0.005, the size parameter of the component spheres is $k_1 a = 5$, where k_1 is the wave number in the surrounding medium and a is the sphere radius, and the distance d between the centers of the cluster components varies from $2a$ for touching spheres to $8a$. For comparison, in the lower panel the thin solid curve depicts the results for single scattering by independent spheres with $k_1 a = 5$ (regarding the upper panel, note that in this case $Z_{22}/Z_{11} \equiv 1$; see Section 4.8). Obviously, the results for $d = 8a$ are hardly distinguishable from those for the independently scattering spheres. Even as small a distance between the component sphere centers as four times their radii combined with averaging over cluster orientations is already sufficient to reduce greatly the near-field and interference effects and produce scattering patterns very similar to those for the independent particles. For still larger spheres, with $k_1 a = 15$, the comparisons that can be made from Fig. 3.2 suggest qualitative independence at even smaller separations. While these results with separation measured in terms of particle size may be expected to become inapplicable for particles significantly smaller than a wavelength, they suggest a simple approximate condition of independent scattering by particles comparable to and larger than a wavelength.

3.4 Radiative transfer equation and coherent backscattering

Let us now relax the requirement that the scattering medium be macroscopically small and optically thin and be viewed from a distance much larger than its size. We thus assume that N is so large that the condition $N\langle C_{\rm sca}\rangle l^{-2} \ll 1$ is violated, and the

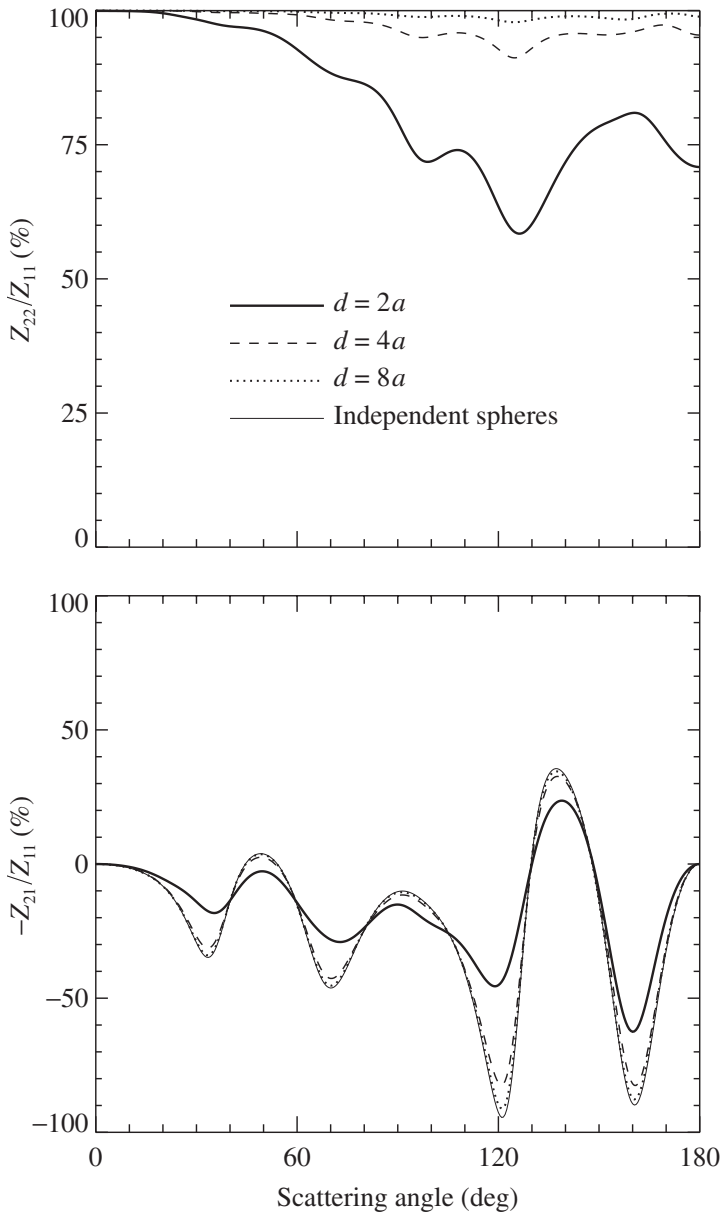

Figure 3.1. The ratios Z_{22}/Z_{11} and $-Z_{21}/Z_{11}$ (%) for randomly oriented two-sphere clusters with touching $(d = 2a)$ and separated components and independently scattering spheres. The component sphere size parameter $k_1 a$ is 5 and the relative refractive index is 1.5 + i0.005.

contribution of multiply scattered light to the total signal scattered by the medium can no longer be ignored. Furthermore, although the observation point is assumed to be in the far-field zone of each constituent particle, it is not necessarily in the far-field zone of the scattering medium as a whole, so that the observer may see scattered light coming from different directions. A traditional approach in such cases is to assume that scattering by different particles is still independent (which implies that the particles are randomly positioned and widely separated) and compute the characteristics of

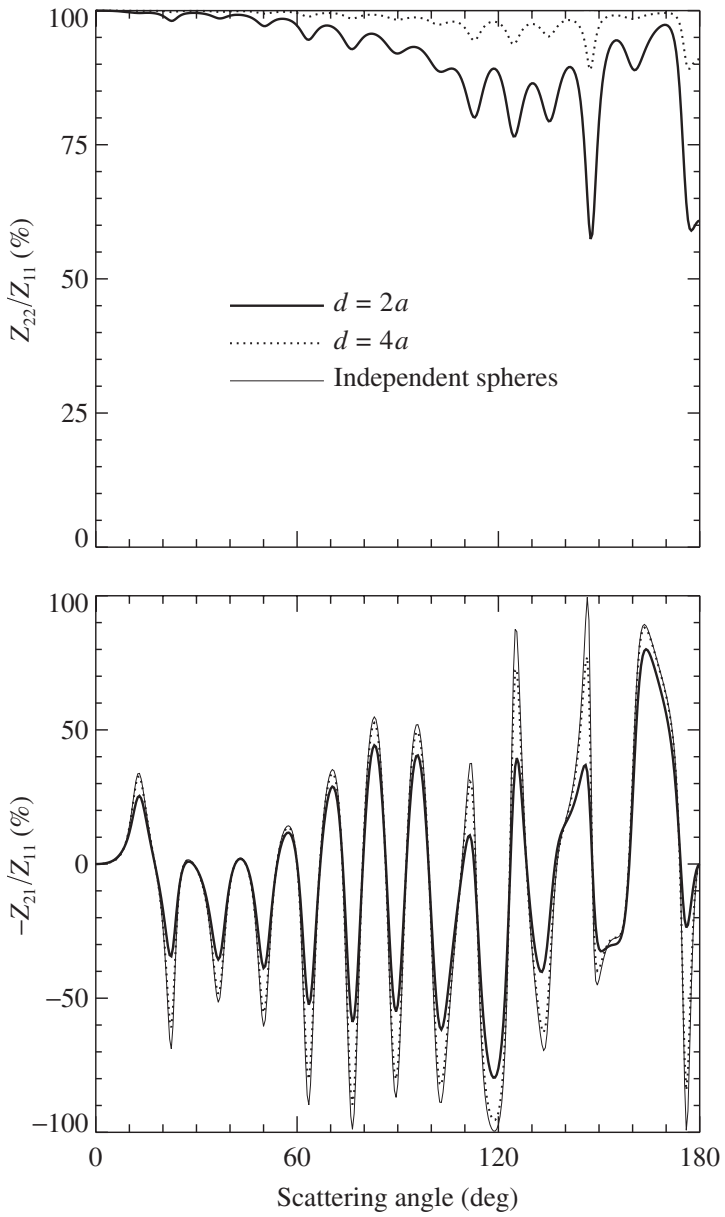

Figure 3.2. As in Fig. 3.1, but for $k_1 a = 15$.

multiply scattered radiation by solving the so-called radiative transfer equation (RTE).

Radiative transfer theory originated as a phenomenological approach based on considering the transport of energy through a medium filled with a large number of particles and ensuring energy conservation (e.g., Chandrasekhar 1960; Sobolev 1974; van de Hulst 1980; Apresyan and Kravtsov 1996; Lagendijk and van Tiggelen 1996; Ishimaru 1997). It has been demonstrated, however, that the RTE can in fact be derived from the electromagnetic theory of multiple wave scattering in discrete random media under certain simplifying assumptions (Mishchenko, 2002, 2003). This deriva-

tion has clarified the physical meaning of the quantities entering the RTE and their relation to single-scattering solutions of the Maxwell equations.

Instead of going into the details of this derivation, we will simply summarize the main concepts of the phenomenological radiative transfer theory, present the conventional form of the RTE, and explain the meaning of the quantities appearing in this equation. The electromagnetic radiation field at each point $\mathbf{r}$ inside the scattering medium is approximated by a collection of quasi-monochromatic beams with a continuous distribution of propagation directions $\hat{\mathbf{n}}$ and angular frequencies ω and is characterized by the local four-component monochromatic specific intensity column vector

$$\mathbf{I}(\mathbf{r}, \hat{\mathbf{n}}, \omega) = \begin{bmatrix} I(\mathbf{r}, \hat{\mathbf{n}}, \omega) \\ Q(\mathbf{r}, \hat{\mathbf{n}}, \omega) \\ U(\mathbf{r}, \hat{\mathbf{n}}, \omega) \\ V(\mathbf{r}, \hat{\mathbf{n}}, \omega) \end{bmatrix}. \tag{3.31}$$

It is assumed that the elementary beams are incoherent and make independent contributions to $\mathbf{I}(\mathbf{r}, \hat{\mathbf{n}}, \omega)$. The elements $Q(\mathbf{r}, \hat{\mathbf{n}}, \omega)$, $U(\mathbf{r}, \hat{\mathbf{n}}, \omega)$, and $V(\mathbf{r}, \hat{\mathbf{n}}, \omega)$ describe the polarization state of light propagating in the direction $\hat{\mathbf{n}}$ at the observation point specified by the position vector $\mathbf{r}$, and the monochromatic specific intensity (or radiance) $I(\mathbf{r}, \hat{\mathbf{n}}, \omega)$ is defined such that

$$I(\mathbf{r}, \hat{\mathbf{n}}, \omega)\, \mathrm{d}\omega\, \mathrm{d}t\, \mathrm{d}S\, \mathrm{d}\Omega \tag{3.32}$$

is the amount of electromagnetic energy in an angular frequency interval $(\omega, \omega + \mathrm{d}\omega)$ which is transported in a time interval $\mathrm{d}t$ through a surface element $\mathrm{d}S$ normal to $\hat{\mathbf{n}}$ and centered at $\mathbf{r}$ in directions confined to a solid angle element $\mathrm{d}\Omega$ centered at the direction of propagation $\hat{\mathbf{n}}$. All elements of the specific intensity vector have the dimension of monochromatic radiance: energy per unit frequency interval per unit time per unit area per unit solid angle.

In the phenomenological radiative transfer theory, a medium filled with a large number of discrete, sparsely and randomly distributed particles is treated as continuous and locally homogeneous. The concept of single scattering and absorption by an individual particle is thus replaced with the concept of single scattering and absorption by a small homogeneous volume element. Furthermore, it is assumed that the result of scattering is not the transformation of a plane incident wave into a spherical scattered wave but, rather, the transformation of the specific intensity vector of the incident light into the specific intensity vector of the scattered light:

$$\mathbf{I}(\mathbf{r}, \hat{\mathbf{n}}^{\mathrm{sca}}, \omega) = \mathbf{Z}(\mathbf{r}, \hat{\mathbf{n}}^{\mathrm{sca}}, \hat{\mathbf{n}}^{\mathrm{inc}}, \omega)\, \mathbf{I}(\mathbf{r}, \hat{\mathbf{n}}^{\mathrm{inc}}, \omega),$$

where $\mathbf{Z}(\mathbf{r}, \hat{\mathbf{n}}^{\mathrm{sca}}, \hat{\mathbf{n}}^{\mathrm{inc}}, \omega)$ is the phase matrix of the small volume element.

An informal way to justify this assumption is to note that the product $\mathbf{Z}(\hat{\mathbf{n}}^{\mathrm{sca}}, \hat{\mathbf{n}}^{\mathrm{inc}})\mathbf{I}^{\mathrm{inc}}$ in Eq. (2.102) may be interpreted as the scattered polarized power per unit solid angle.

Specifically, the polarized energy flow across a surface element ΔS normal to $\hat{\mathbf{n}}^{\rm sca}$ at a distance r from the particle is given by $\Delta S r^{-2}\mathbf{Z}(\hat{\mathbf{n}}^{\rm sca}, \hat{\mathbf{n}}^{\rm inc})\mathbf{I}^{\rm inc}$ and is, at the same time, equal to the polarized power scattered within the solid angle element $\Delta\Omega = \Delta S r^{-2}$ centered at $\hat{\mathbf{n}}^{\rm sca}$.

Another assumption in the phenomenological radiative transfer theory is that the scattering, absorption, and emission characteristics of the small volume element follow from the Maxwell equations and are given by the incoherent sums of the respective characteristics of the constituent particles according to Eqs. (3.9), (3.10), (3.12)–(3.14), and (3.16).

The change in the specific intensity vector along the direction of propagation $\hat{\mathbf{n}}$ in a medium containing sparsely and randomly distributed, arbitrarily oriented particles is described by the following classical RTE (Rozenberg 1977; Tsang *et al*. 1985; Mishchenko 2002):

$$\begin{aligned}\frac{\rm d}{{\rm d}s}\mathbf{I}(\mathbf{r}, \hat{\mathbf{n}}, \omega) = &-n_0(\mathbf{r})\langle\mathbf{K}(\mathbf{r}, \hat{\mathbf{n}}, \omega)\rangle\mathbf{I}(\mathbf{r}, \hat{\mathbf{n}}, \omega)\\ &+n_0(\mathbf{r})\int_{4\pi}{\rm d}\hat{\mathbf{n}}'\langle\mathbf{Z}(\mathbf{r}, \hat{\mathbf{n}}, \hat{\mathbf{n}}', \omega)\rangle\mathbf{I}(\mathbf{r}, \hat{\mathbf{n}}', \omega)\\ &+n_0(\mathbf{r})\langle\mathbf{K}_{\rm e}[\mathbf{r}, \hat{\mathbf{n}}, T(\mathbf{r}), \omega]\rangle,\end{aligned} \tag{3.33}$$

where the path-length element ${\rm d}s$ is measured along the unit vector $\hat{\mathbf{n}}$, $n_0(\mathbf{r})$ is the local particle number density, and $\langle\mathbf{K}(\mathbf{r}, \hat{\mathbf{n}}, \omega)\rangle$, $\langle\mathbf{Z}(\mathbf{r}, \hat{\mathbf{n}}, \hat{\mathbf{n}}', \omega)\rangle$, and $\langle\mathbf{K}_{\rm e}[\mathbf{r}, \hat{\mathbf{n}}, T(\mathbf{r}), \omega]\rangle$ are the local ensemble-averaged extinction and phase matrices and emission vector per particle, respectively. The first term on the right-hand side of Eq. (3.33) describes the change in the specific intensity vector over the distance ${\rm d}s$ caused by extinction and dichroism, the second term describes the contribution of light illuminating a small volume element centered at $\mathbf{r}$ from all directions $\hat{\mathbf{n}}'$ and scattered into the direction $\hat{\mathbf{n}}$, and the third term describes the contribution of the emitted light.

The radiative transfer equation must be supplemented by boundary conditions appropriate for a given physical problem. In particular, the boundary conditions must correspond to the macroscopic geometry of the scattering medium and specify the direction, polarization state, and frequency distribution of the external incident light. For example, in the case of light scattering by the atmosphere, a standard model is a plane-parallel particulate medium illuminated from above by a parallel beam representing solar radiation and bounded from below by a reflecting surface. The solution of the RTE yields the specific intensity vector of the outgoing radiation at each boundary point and, thereby, the angular distribution and polarization state of light multiply scattered (reflected and transmitted) by the medium. It also provides the specific intensity vector of the internal radiation field. General solutions of Eq. (3.33) have been discussed by, e.g., Mishchenko (1990a) and Haferman (2000).

Despite the approximate character of the standard radiative transfer theory, it pro-

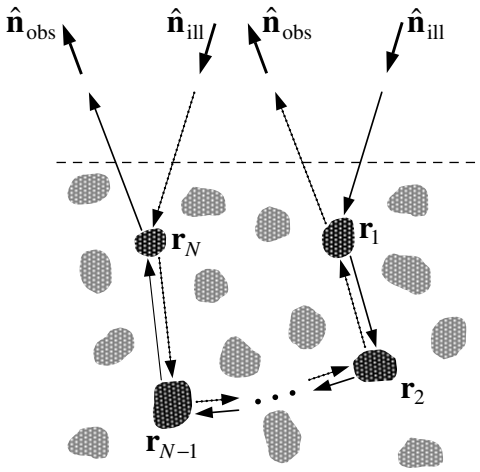

Figure 3.3. Schematic explanation of coherent backscattering.

vides a powerful and reasonably general prescription for the treatment of the interaction of light with particulate media and is accordingly applicable to a broad range of practical situations. However, owing to some of the basic assumptions in the development of the classical RTE, there are circumstances for which it is not sufficient. For example, since the classical RTE does not take full account of interference effects it does not describe directly the so-called coherent backscattering of light (otherwise known as weak photon localization) (Watson 1969). To explain the physical origin of this phenomenon, let us consider a layer composed of discrete, randomly positioned scattering particles and illuminated by a parallel beam of light incident in the direction $\hat{\mathbf{n}}_{\text{ill}}$ (Fig. 3.3). The distant observer measures the intensity of light reflected by the layer in the direction $\hat{\mathbf{n}}_{\text{obs}}$. The reflected signal is composed of the contributions made by waves scattered along various paths inside the layer involving different combinations of particles. Let us consider the two conjugate scattering paths shown in Fig. 3.3 by solid and broken lines. These paths go through the same group of N particles, denoted by their positions $\mathbf{r}_1, \mathbf{r}_2, \ldots, \mathbf{r}_N$, but in opposite directions. The waves scattered along the two conjugate paths interfere, the interference being constructive or destructive depending on the phase difference

$$\Delta = k_1(\mathbf{r}_N - \mathbf{r}_1)\cdot(\hat{\mathbf{n}}_{\text{ill}} + \hat{\mathbf{n}}_{\text{obs}}), \tag{3.34}$$

where k_1 is the wave number in the surrounding medium. If the observation direction is far from the exact backscattering direction given by $-\hat{\mathbf{n}}_{\text{ill}}$, then the waves scattered along conjugate paths involving different groups of particles interfere in different ways, and the average effect of the interference is zero owing to the randomness of particle positions. Consequently, the observer measures some average, incoherent intensity that is well described by the classical radiative transfer theory. However, at exactly the backscattering direction ($\hat{\mathbf{n}}_{\text{obs}} = -\hat{\mathbf{n}}_{\text{ill}}$), the phase difference between conjugate paths involving any group of particles is identically equal to zero, Eq. (3.34), and the interference is always constructive, thereby resulting in a coherent

backscattering intensity peak superposed on the incoherent background (Tsang *et al*. 1985; Barabanenkov *et al.* 1991; Sheng 1995). The scattering paths involving only one particle do not have conjugate counterparts and do not contribute to the coherent intensity peak. Kuga and Ishimaru (1984) were the first to detect coherent backscattering in a controlled laboratory experiment, although it may have been unknowingly observed by Lyot (1929) in the form of the so-called coherent polarization opposition effect (Mishchenko *et al*. 2000e).

An exact computation of the coherent backscattering effect based on solving the Maxwell equations is feasible only for few-component clusters and is complicated by several factors. First, the scattering pattern for a monodisperse cluster in a fixed orientation is always heavily burdened by multiple maxima and minima resulting from the interference of partial waves scattered by the cluster components and by the intricate resonance structure of the single-scattering contribution (Section 9.1). Second, the scattering pattern can be further affected by near-field effects that result from the close proximity of the component particles. Third, simple trigonometry shows that the angular width of the coherent backscattering intensity peak is of the order $1/k_1\langle d\rangle = \lambda_1/2\pi\langle d\rangle$, where $\langle d\rangle$ is the average distance between the cluster components and λ_1 is the wavelength in the surrounding medium. Therefore, the peak may be too broad to be identified reliably unless the cluster components are widely separated. However, increasing the distance between the cluster components diminishes the contribution of multiple scattering and, thus, the amplitude of the coherent backscattering peak, thereby making it difficult to detect.

To smooth out the effect of the first factor and make the backscattering peak detectable, one must compute a scattering pattern that is averaged over particle sizes, cluster orientations, and distances between the components. Furthermore, the average distance between the cluster components must be much larger than the size of the components and the wavelength but yet small enough that the multiple-scattering contribution to the total signal is still significant.

Ismagilov and Kravtsov (1993) studied analytically the simplest case, two widely separated spheres with diameters much smaller than the wavelength, but found that the amplitude of the coherent backscattering intensity peak was extremely small because of the weakness of the multiple-scattering contribution to the total scattered signal. Mishchenko (1996a) used the exact superposition *T*-matrix method (Section 5.9) to compute far-field scattering by polydisperse, randomly oriented clusters composed of two equal wavelength-sized spheres with varying center-to-center distances. He computed the ratio of the intensity scattered by the clusters to the intensity scattered by two independent polydisperse spheres of the same average size, assuming unpolarized incident light. Figure 3.4 shows this ratio versus scattering angle (the angle between the incidence and scattering directions) calculated for $k_1\langle d\rangle = 25$, average component sphere size parameter $k_1\langle a\rangle = 5$, and relative refractive index m = 1.2. The curve clearly exhibits a backscattering enhancement with an angular width comparable to $1/k_1\langle d\rangle$ and an amplitude of about 1.03. Mishchenko (1996a) found

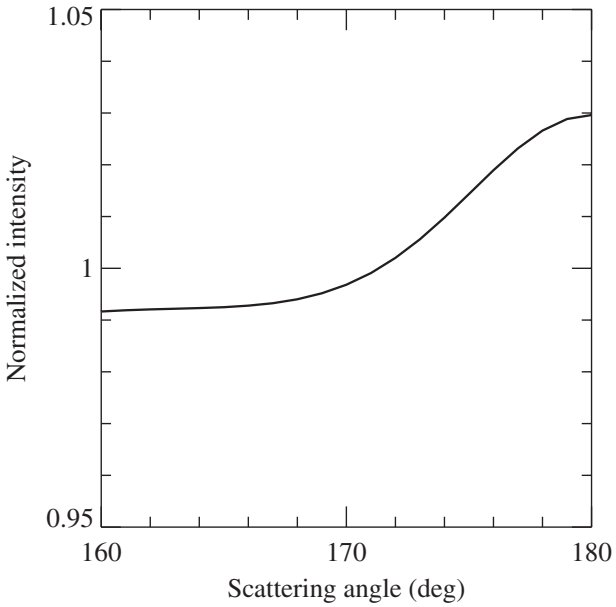

Figure 3.4. Coherent backscattering by polydisperse, randomly oriented two-sphere clusters.

that this feature persisted when $k_1\langle d\rangle$, $k_1\langle a\rangle$, and m were varied, thereby indicating that it was indeed caused by coherent backscattering.

The amplitude of the coherent backscattering peak (the ratio of the intensity in the center of the peak to the background value) can be significantly greater for very large collections of particles because of the much stronger contribution of multiple scattering (van Albada and Lagendijk 1985; Wolf *et al*. 1988; Labeyrie *et al*. 2000). For example, the measurement results depicted in Fig. 3.5 show an amplitude of almost 1.8. Unfortunately, the exact theory of coherent backscattering for large particle collections is extremely complicated and has been developed only for the case of reflection of light by a semi-infinite layer composed of nonabsorbing particles with sizes much smaller than the wavelength (Ozrin 1992; Amic *et al.* 1997). An exact result was obtained by Mishchenko (1992b), who used the reciprocity relation of Eq. (2.124) to show that the photometric and polarization characteristics of coherent backscattering at exactly the backscattering direction as well as outside the backscattering peak can be expressed in terms of the solution of the classical RTE. Other theoretical approaches are based on the so-called diffusion approximation (Stephen and Cwilich 1986) and the Monte Carlo technique (van Albada and Lagendijk 1987; Martinez and Maynard 1994; Iwai *et al*. 1995).

Because the angular width of the intensity peak caused by coherent backscattering from optically thick layers is proportional to the ratio of the wavelength to the photon mean free path, it is negligibly small for sparse particle collections and does not affect the results of remote sensing observations of such tenuous objects as clouds, aerosols, and precipitation. However, measurements of coherent backscattering have proved to

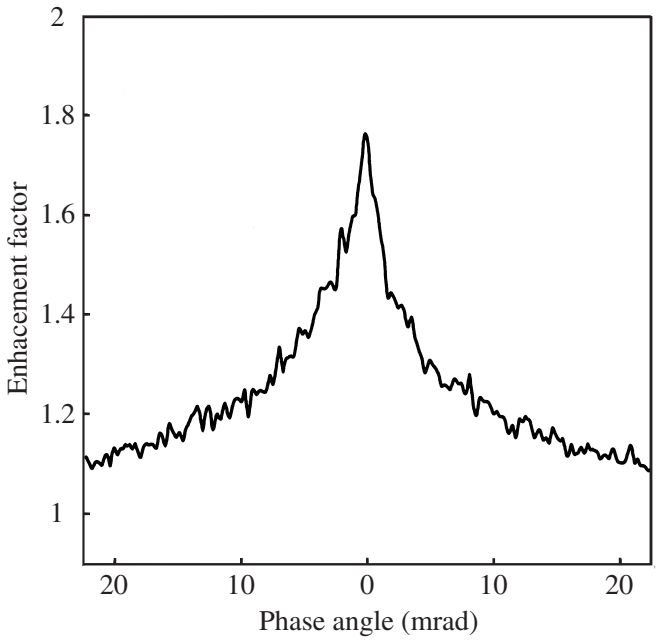

Figure 3.5. Angular profile of the coherent backscattering peak produced by a 1500-μm-thick slab of 9.6 vol% of 0.215-μm-diameter polystyrene spheres suspended in water. The slab was illuminated by a linearly polarized laser beam ($\lambda_1 = 633$ nm) incident normally to the slab surface. The scattering plane (i.e., the plane through the vectors $\hat{\mathbf{n}}_{\rm ill}$ and $\hat{\mathbf{n}}_{\rm obs}$, Fig. 3.3) was fixed in such a way that the electric vector of the incident beam vibrated in this plane. The detector measured the component of the backscattered intensity polarized parallel to the scattering plane. The curve shows the profile of the backscattered intensity normalized by the intensity of the incoherent background as a function of the phase angle. The latter is defined as the angle between the vectors $\hat{\mathbf{n}}_{\rm obs}$ and $-\hat{\mathbf{n}}_{\rm ill}$. (After van Albada *et al.* 1987.)

be a valuable characterization tool in laboratory and remote sensing studies of layers composed of more closely spaced particles, such as particle suspensions and natural and artificial particulate surfaces (e.g., Muinonen 1993; Shkuratov 1994; Mishchenko 1996b; POAN Research Group 1998; Lenke and Maret 2000).

Further reading

A detailed discussion of the concept of single scattering by a small volume element was recently presented by Mishchenko *et al*. (2004a).

Chapter 4

Scattering matrix and macroscopically isotropic and mirror-symmetric scattering media

By definition, the phase matrix relates the Stokes parameters of the incident and scattered beams, defined relative to their respective meridional planes. In contrast to the phase matrix, the scattering matrix $\mathbf{F}$ relates the Stokes parameters of the incident and scattered beams defined with respect to the scattering plane, that is, the plane through the unit vectors $\hat{\mathbf{n}}^{\rm inc}$ and $\hat{\mathbf{n}}^{\rm sca}$ (van de Hulst 1957).

A simple way to introduce the scattering matrix is to direct the z-axis of the reference frame along the incident beam and superpose the meridional plane with $\varphi = 0$ and the scattering plane (Fig. 4.1). Then the scattering matrix $\mathbf{F}$ can be defined as

$$\mathbf{F}(\vartheta^{\rm sca}) = \mathbf{Z}(\vartheta^{\rm sca}, \varphi^{\rm sca} = 0; \vartheta^{\rm inc} = 0, \varphi^{\rm inc} = 0). \tag{4.1}$$

In general, all 16 elements of the scattering matrix are non-zero and depend on the particle orientation with respect to the incident and scattered beams.

The choice of laboratory reference frame, with z-axis along the incidence direction and the xz-plane with $x \geq 0$ coinciding with the scattering plane, can often be inconvenient because any change in the incidence direction and/or orientation of the scattering plane also changes the orientation of the scattering particle with respect to the coordinate system. However, we will show in this chapter that the concept of the scattering matrix can be very useful in application to so-called macroscopically isotropic and mirror-symmetric scattering media, because the scattering matrix of such a particle collection becomes independent of incidence direction and orientation of the scattering plane, depends only on the angle $\Theta = \arccos(\hat{\mathbf{n}}^{\rm inc} \cdot \hat{\mathbf{n}}^{\rm sca})$ between the incidence and scattering directions, and has a simple block-diagonal structure.

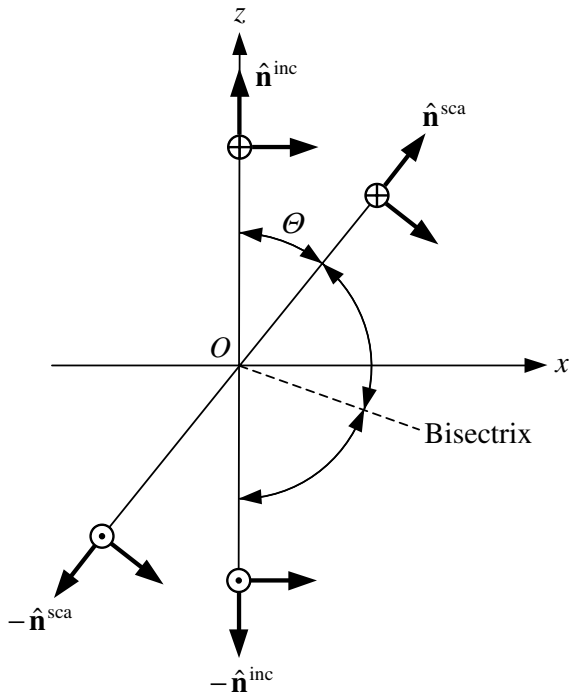

Figure 4.1. The *xz*-plane of the reference frame acts as the scattering plane. The arrows perpendicular to the unit $\hat{\mathbf{n}}$ - vectors show the corresponding unit $\hat{\boldsymbol{\vartheta}}$ - vectors. The symbols $\oplus$ and $\odot$ indicate the corresponding unit $\hat{\boldsymbol{\varphi}}$ - vectors, which are directed into and out of the paper, respectively.

4.1 Symmetries of the Stokes scattering matrix

We begin by considering special symmetry properties of the amplitude scattering matrix that exist when both the incidence and the scattering directions lie in the *xz*-plane (van de Hulst 1957). For the particle shown schematically in Fig. 4.2(a), let

$$\begin{bmatrix} S_{11} & S_{12} \\ S_{21} & S_{22} \end{bmatrix} \tag{4.2a}$$

be the amplitude scattering matrix that corresponds to the directions of incidence and scattering given by $\hat{\mathbf{n}}^{\rm inc}$ and $\hat{\mathbf{n}}^{\rm sca}$, respectively (Fig. 4.1). Rotating this particle by 180º about the bisectrix (i.e., the line in the scattering plane that bisects the angle $\pi - \Theta$ between the unit vectors $-\hat{\mathbf{n}}^{\rm inc}$ and $\hat{\mathbf{n}}^{\rm sca}$ in Fig. 4.1) puts it in the orientation schematically shown in Fig. 4.2(b). It is clear that the amplitude scattering matrix (4.2a) is also the amplitude scattering matrix for this rotated particle when the directions of incidence and scattering are given by $-\hat{\mathbf{n}}^{\rm sca}$ and $-\hat{\mathbf{n}}^{\rm inc}$, respectively. Therefore, the reciprocity relation (2.64) implies that the amplitude scattering matrix of the

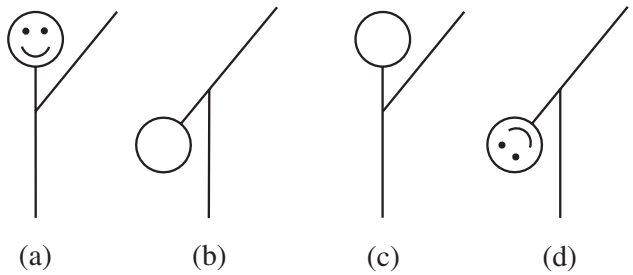

Figure 4.2. Two orientations of an arbitrary particle and two orientations of its mirror-symmetric particle that give rise to certain symmetries in scattering patterns. (After van de Hulst 1957.)

particle shown in Fig. 4.2(b) that corresponds to the original directions of incidence and scattering, $\hat{\mathbf{n}}^{\text{inc}}$ and $\hat{\mathbf{n}}^{\text{sca}}$, is simply

$$\begin{bmatrix} S_{11} & -S_{21} \\ -S_{12} & S_{22} \end{bmatrix}. \tag{4.2b}$$

Mirroring the original particle, Fig. 4.2(a), with respect to the scattering plane gives the particle shown in Fig. 4.2(c). If we also reversed the direction of the unit vectors $\hat{\boldsymbol{\varphi}}^{\text{inc}}$ and $\hat{\boldsymbol{\varphi}}^{\text{sca}}$ in Fig. (4.1), then we would have the same scattering problem as for the particle shown in Fig. 4.2(a). We may thus conclude that the amplitude scattering matrix for the particle shown in Fig. 4.2(c) that corresponds to the directions of incidence and scattering $\hat{\mathbf{n}}^{\text{inc}}$ and $\hat{\mathbf{n}}^{\text{sca}}$ is

$$\begin{bmatrix} S_{11} & -S_{12} \\ -S_{21} & S_{22} \end{bmatrix}. \tag{4.2c}$$

Finally, mirroring the original particle with respect to the bisectrix plane (i.e., the plane through the bisectrix and the y-axis) gives the particle shown in Fig. 4.2(d). Since this particle is simply the mirror-symmetric counterpart of the particle shown in Fig. 4.2(b), its amplitude scattering matrix corresponding to the directions of incidence and scattering $\hat{\mathbf{n}}^{\text{inc}}$ and $\hat{\mathbf{n}}^{\text{sca}}$ is

$$\begin{bmatrix} S_{11} & S_{21} \\ S_{12} & S_{22} \end{bmatrix}. \tag{4.2d}$$

It can be seen that any two of the three transformations shown in Figs. 4.2(b)–4.2(d) give the third.

We will now discuss the implications of Eqs. (4.2a)–(4.2d) for Stokes scattering matrices of collections of independently scattering particles, by considering the following four examples (van de Hulst 1957).

(1) Let us first assume that a small volume element contains only one kind of particle and that each particle in a specific position, say Fig. 4.2(a), is accompanied by a particle in the reciprocal position, Fig. 4.2(b). It then follows from Eqs. (2.106)–

(2.121), (3.12), (4.1), (4.2a), and (4.2b) that the scattering matrix of the small volume element has the following symmetry:

$$\begin{bmatrix} F_{11} & F_{12} & F_{13} & F_{14} \\ F_{12} & F_{22} & F_{23} & F_{24} \\ -F_{13} & -F_{23} & F_{33} & F_{34} \\ F_{14} & F_{24} & -F_{34} & F_{44} \end{bmatrix}. \tag{4.3}$$

The number of independent matrix elements is 10.

(2) As a second example, let us assume that the volume element contains particles and their mirror-symmetric counterparts such that for each particle in orientation (a) a mirror-symmetric particle in orientation (c) is present (Fig. 4.2). This excludes, for example, scattering media composed of only right-handed or only left-handed helices. It is easy to verify that the resulting scattering matrix involves eight independent elements and has the following structure:

$$\begin{bmatrix} F_{11} & F_{12} & 0 & 0 \\ F_{21} & F_{22} & 0 & 0 \\ 0 & 0 & F_{33} & F_{34} \\ 0 & 0 & F_{43} & F_{44} \end{bmatrix}. \tag{4.4}$$

(3) As a third example, consider a volume element containing particles and their mirror-symmetric counterparts and assume that any particle in orientation (a) is accompanied by a mirror-symmetric particle in orientation (d), Fig. 4.2. The scattering matrix becomes

$$\begin{bmatrix} F_{11} & F_{12} & F_{13} & F_{14} \\ F_{12} & F_{22} & F_{23} & F_{24} \\ F_{13} & F_{23} & F_{33} & F_{34} \\ -F_{14} & -F_{24} & -F_{34} & F_{44} \end{bmatrix} \tag{4.5}$$

and has 10 independent elements.

(4) Finally, consider a volume element containing particles and their mirror-symmetric counterparts and make any two of the preceding assumptions. The third assumption follows automatically, so that there are equal numbers of particles in orientations (a), (b), (c), and (d). The resulting scattering matrix is

$$\begin{bmatrix} F_{11} & F_{12} & 0 & 0 \\ F_{12} & F_{22} & 0 & 0 \\ 0 & 0 & F_{33} & F_{34} \\ 0 & 0 & -F_{34} & F_{44} \end{bmatrix} \tag{4.6}$$

and has eight non-zero elements, of which only six are independent.

4.2 Macroscopically isotropic and mirror-symmetric scattering medium

Now we are ready to consider scattering by a small volume element containing *randomly oriented* particles. This means that there are many particles of each type and their orientation distribution is uniform (see Eq. (3.27)). In this case the assumptions of example (1) from the previous section are satisfied, and the total scattering matrix is given by Eq. (4.3). Furthermore, if particles and their mirror-symmetric counterparts are present in equal numbers or each particle has a plane of symmetry, then the assumptions of example 4 are satisfied, and the resulting scattering matrix is given by Eq. (4.6).

As a consequence of random particle orientation, the scattering medium is *macroscopically isotropic* (i.e., there is no preferred propagation direction and no preferred plane through the incidence direction). Therefore, the scattering matrix becomes independent of the incidence direction and the orientation of the scattering plane and depends only on the angle between the incidence and scattering directions, that is, the scattering angle

$$\Theta = \arccos(\hat{\mathbf{n}}^{\mathrm{inc}} \cdot \hat{\mathbf{n}}^{\mathrm{sca}}), \qquad \Theta \in [0, \pi].$$

Furthermore, the assumptions of example (4) ensure that the scattering medium is *macroscopically mirror-symmetric* with respect to any plane and make the structure of the scattering matrix especially simple. Therefore, scattering media composed of equal numbers of randomly oriented particles and their mirror-symmetric counterparts and/or randomly oriented particles having a plane of symmetry can be called *macroscopically isotropic and mirror-symmetric*. Although this type of scattering medium might be thought to be a rather special case, it nonetheless provides a very good numerical description of the scattering properties of many particle collections encountered in practice and is by far the most often used theoretical model. To emphasize that the scattering matrix of a macroscopically isotropic and mirror-symmetric scattering medium depends only on the scattering angle, we rewrite Eq. (4.6) as

$$\mathbf{F}(\Theta) = \begin{bmatrix} F_{11}(\Theta) & F_{12}(\Theta) & 0 & 0 \\ F_{12}(\Theta) & F_{22}(\Theta) & 0 & 0 \\ 0 & 0 & F_{33}(\Theta) & F_{34}(\Theta) \\ 0 & 0 & -F_{34}(\Theta) & F_{44}(\Theta) \end{bmatrix} = N\langle \mathbf{F}(\Theta) \rangle, \tag{4.7}$$

where N is the number of particles in the volume element and $\langle \mathbf{F}(\Theta) \rangle$ is the ensemble-averaged scattering matrix per particle.

As a direct consequence of Eqs. (3.17) and (3.18) we have the inequalities

$$F_{11} \geq 0, \tag{4.8}$$

$$|F_{ij}| \leq F_{11}, \qquad i, j = 1, \ldots, 4. \tag{4.9}$$

Additional general inequalities for the elements of the scattering matrix (4.7) are

$$(F_{33}+F_{44})^2+4F_{34}^2 \le (F_{11}+F_{22})^2-4F_{12}^2, \tag{4.10}$$

$$|F_{33}-F_{44}| \le F_{11}-F_{22}, \tag{4.11}$$

$$|F_{22}-F_{12}| \le F_{11}-F_{12}, \tag{4.12}$$

$$|F_{22}+F_{12}| \le F_{11}+F_{12}. \tag{4.13}$$

The proof of these and other useful inequalities is given in Hovenier *et al.* (1986).

4.3 Phase matrix

Knowledge of the matrix $\mathbf{F}(\Theta)$ can be used to calculate the Stokes phase matrix for a macroscopically isotropic and mirror-symmetric scattering medium. Assume that $0<\varphi^{\rm sca}-\varphi^{\rm inc}<\pi$ and consider phase matrices $\mathbf{Z}(\vartheta^{\rm sca},\varphi^{\rm sca};\vartheta^{\rm inc},\varphi^{\rm inc})$ and $\mathbf{Z}(\vartheta^{\rm sca},\varphi^{\rm inc};\vartheta^{\rm inc},\varphi^{\rm sca})$. The second matrix involves the same zenith angles of the incident and scattered beams as the first, but the azimuth angles are switched, as indicated in their respective scattering geometries; these are shown in Figs. 4.3(a), (b). The phase matrix links the Stokes vectors of the incident and scattered beams, specified relative to their respective meridional planes. Therefore, to compute the Stokes vector of the scattered beam with respect to its meridional plane, we must

- calculate the Stokes vector of the incident beam with respect to the scattering plane;
- multiply it by the scattering matrix, thereby obtaining the Stokes vector of the scattered beam with respect to the scattering plane; and finally
- compute the Stokes vector of the scattered beam with respect to its meridional plane (Chandrasekhar 1960).

This procedure involves two rotations of the reference plane, as shown in Figs. 4.3(a), (b), and yields

$$\mathbf{Z}(\vartheta^{\rm sca},\varphi^{\rm sca};\vartheta^{\rm inc},\varphi^{\rm inc})=\mathbf{L}(-\sigma_2)\mathbf{F}(\Theta)\mathbf{L}(\pi-\sigma_1)$$

$$=\begin{bmatrix} F_{11}(\Theta) & C_1F_{12}(\Theta) & S_1F_{12}(\Theta) & 0 \\ C_2F_{12}(\Theta) & C_1C_2F_{22}(\Theta)-S_1S_2F_{33}(\Theta) & S_1C_2F_{22}(\Theta)+C_1S_2F_{33}(\Theta) & S_2F_{34}(\Theta) \\ -S_2F_{12}(\Theta) & -C_1S_2F_{22}(\Theta)-S_1C_2F_{33}(\Theta) & -S_1S_2F_{22}(\Theta)+C_1C_2F_{33}(\Theta) & C_2F_{34}(\Theta) \\ 0 & S_1F_{34}(\Theta) & -C_1F_{34}(\Theta) & F_{44}(\Theta) \end{bmatrix}, \tag{4.14}$$

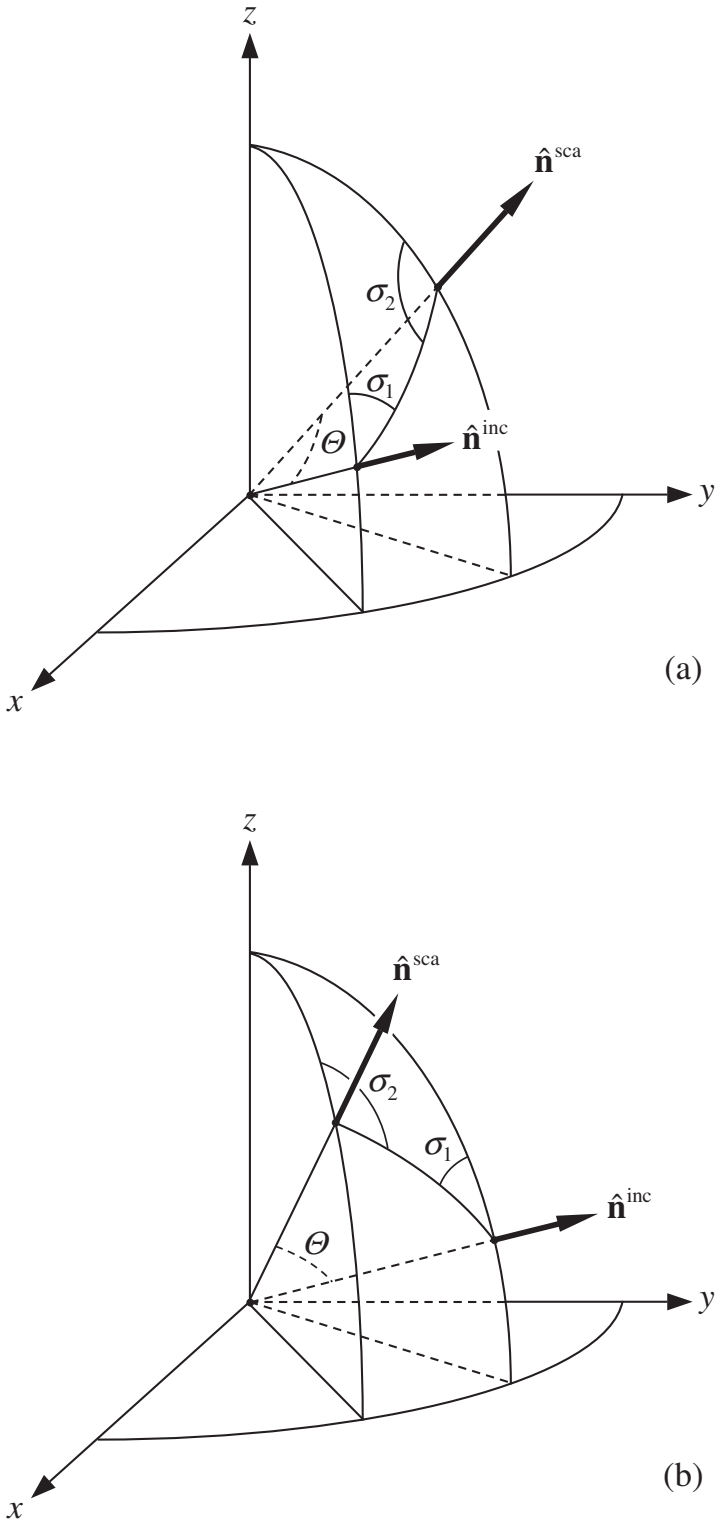

Figure 4.3. Illustration of the relationship between the phase and scattering matrices.

$$\mathbf{Z}(\vartheta^{\rm sca}, \varphi^{\rm inc}; \vartheta^{\rm inc}, \varphi^{\rm sca}) = \mathbf{L}(\sigma_2 - \pi)\mathbf{F}(\Theta)\mathbf{L}(\sigma_1)$$

$$= \begin{bmatrix} F_{11}(\Theta) & C_1 F_{12}(\Theta) & -S_1 F_{12}(\Theta) & 0 \\ C_2 F_{12}(\Theta) & C_1 C_2 F_{22}(\Theta) - S_1 S_2 F_{33}(\Theta) & -S_1 C_2 F_{22}(\Theta) - C_1 S_2 F_{33}(\Theta) & -S_2 F_{34}(\Theta) \\ S_2 F_{12}(\Theta) & C_1 S_2 F_{22}(\Theta) + S_1 C_2 F_{33}(\Theta) & -S_1 S_2 F_{22}(\Theta) + C_1 C_2 F_{33}(\Theta) & C_2 F_{34}(\Theta) \\ 0 & -S_1 F_{34}(\Theta) & -C_1 F_{34}(\Theta) & F_{44}(\Theta) \end{bmatrix}, \tag{4.15}$$

where

$$C_i = \cos 2\sigma_i, \quad S_i = \sin 2\sigma_i, \quad i = 1, 2, \tag{4.16}$$

and the rotation matrix $\mathbf{L}$ is defined by Eq. (1.97). (Recall that a rotation angle is positive if the rotation is performed in the clockwise direction when one is looking in the direction of propagation; see Section 1.5.) The scattering angle Θ and the angles σ_1 and σ_2 can be calculated from $\vartheta^{\rm sca}$, $\vartheta^{\rm inc}$, $\varphi^{\rm sca}$, and $\varphi^{\rm inc}$ using spherical trigonometry:

$$\cos\Theta = \cos\vartheta^{\rm sca}\cos\vartheta^{\rm inc} + \sin\vartheta^{\rm sca}\sin\vartheta^{\rm inc}\cos(\varphi^{\rm sca} - \varphi^{\rm inc}), \tag{4.17}$$

$$\cos\sigma_1 = \frac{\cos\vartheta^{\rm sca} - \cos\vartheta^{\rm inc}\cos\Theta}{\sin\vartheta^{\rm inc}\sin\Theta}, \tag{4.18}$$

$$\cos\sigma_2 = \frac{\cos\vartheta^{\rm inc} - \cos\vartheta^{\rm sca}\cos\Theta}{\sin\vartheta^{\rm sca}\sin\Theta}. \tag{4.19}$$

Equations (4.14)–(4.19) demonstrate the obvious fact that the phase matrix of a macroscopically isotropic and mirror-symmetric medium depends only on the difference between the azimuthal angles of the scattered and incident beams rather than on their specific values. Comparison of Eqs. (4.14) and (4.15) yields the symmetry relation (Hovenier 1969):

$$\mathbf{Z}(\vartheta^{\rm sca}, \varphi^{\rm inc}; \vartheta^{\rm inc}, \varphi^{\rm sca}) = \mathbf{\Delta}_{34}\mathbf{Z}(\vartheta^{\rm sca}, \varphi^{\rm sca}; \vartheta^{\rm inc}, \varphi^{\rm inc})\mathbf{\Delta}_{34}, \tag{4.20}$$

where

$$\mathbf{\Delta}_{34} = \mathbf{\Delta}_{34}^{\rm T} = \mathbf{\Delta}_{34}^{-1} = \begin{bmatrix} 1 & 0 & 0 & 0 \\ 0 & 1 & 0 & 0 \\ 0 & 0 & -1 & 0 \\ 0 & 0 & 0 & -1 \end{bmatrix}. \tag{4.21}$$

It is also easy to see from either Eq. (4.14) or Eq. (4.15) that (Hovenier 1969)

$$\mathbf{Z}(\pi - \vartheta^{\rm sca}, \varphi^{\rm sca}; \pi - \vartheta^{\rm inc}, \varphi^{\rm inc}) = \mathbf{\Delta}_{34}\mathbf{Z}(\vartheta^{\rm sca}, \varphi^{\rm sca}; \vartheta^{\rm inc}, \varphi^{\rm inc})\mathbf{\Delta}_{34}, \tag{4.22}$$

which is a manifestation of symmetry with respect to the *xy*-plane. Finally, we can verify that

$$\mathbf{Z}(\pi - \vartheta^{\rm inc}, \varphi^{\rm inc} + \pi; \pi - \vartheta^{\rm sca}, \varphi^{\rm sca} + \pi) = \mathbf{\Delta}_3[\mathbf{Z}(\vartheta^{\rm sca}, \varphi^{\rm sca}; \vartheta^{\rm inc}, \varphi^{\rm inc})]^{\rm T}\mathbf{\Delta}_3, \tag{4.23}$$

where the matrix $\mathbf{\Delta}_3$ is given by Eq. (2.125). Obviously, this is the reciprocity relation (2.124). Other symmetry relations can be derived by forming combinations of Eqs. (4.20), (4.22), and (4.23). For example, combining Eqs. (4.20) and (4.22) yields

$$\mathbf{Z}(\pi - \vartheta^{\rm sca}, \varphi^{\rm inc}; \pi - \vartheta^{\rm inc}, \varphi^{\rm sca}) = \mathbf{Z}(\vartheta^{\rm sca}, \varphi^{\rm sca}; \vartheta^{\rm inc}, \varphi^{\rm inc}). \tag{4.24}$$

Although Eq. (4.14) is valid only for $0 < \varphi^{\rm sca} - \varphi^{\rm inc} < \pi$, combining it with Eq. (4.20) yields the phase matrix for all possible incidence and scattering directions. The symmetry relations (4.22) and (4.23) further reduce the range of independent scattering geometries and can be very helpful in theoretical calculations or consistency checks on measurements.

4.4 Forward-scattering direction and extinction matrix

By virtue of spatial isotropy, the extinction matrix of a macroscopically isotropic and mirror-symmetric medium is independent of the direction of light propagation and orientation of the reference plane used to define the Stokes parameters. It also follows from Eqs. (2.142)–(2.145), (3.9), and (4.2a)–(4.2d) that $K_{13} = K_{14} = K_{23} = K_{24} = K_{31} = K_{32} = K_{41} = K_{42} = 0$. Furthermore, we are about to show that the remaining off-diagonal elements of the extinction matrix also vanish.

We will assume for simplicity that light is incident along the positive direction of the z-axis of the laboratory reference frame and will use the xz-plane with $x \geq 0$ as the meridional plane of the incident beam. We will also assume that the initial orientation of a particle is such that the particle reference frame coincides with the laboratory reference frame. The forward-scattering amplitude matrix of the particle in the initial orientation computed in the laboratory reference frame is thus equal to the forward-scattering amplitude matrix computed in the particle reference frame. We will denote the latter as $\mathbf{S}_P$. Let us now rotate the particle through an Euler angle α about the z-axis in the clockwise direction as viewed in the positive z-direction (Figs. 2.2 and 4.4) and denote the forward-scattering amplitude matrix of this rotated particle with respect to the laboratory reference frame as $\mathbf{S}_L^{\alpha}$. This matrix relates the column of the electric field vector components of the incident field to that of the field scattered in the exact forward direction:

$$\begin{bmatrix} E_{\vartheta L}^{\rm sca} \\ E_{\varphi L}^{\rm sca} \end{bmatrix} \propto \mathbf{S}_L^{\alpha} \begin{bmatrix} E_{\vartheta L}^{\rm inc} \\ E_{\varphi L}^{\rm inc} \end{bmatrix}, \tag{4.25}$$

where the subscript L indicates that all field components are computed in the laboratory reference frame. Figure 4.4 shows the directions of the respective unit $\hat{\boldsymbol{\vartheta}}$- and $\hat{\boldsymbol{\varphi}}$- vectors for the incident and the forward-scattered beams. Simple trigonometry allows us to express the column of the electric vector components in the particle reference frame in terms of that in the laboratory reference frame by means of a trivial

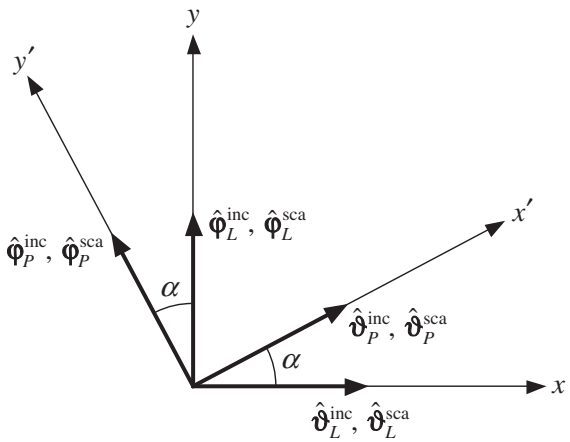

Figure 4.4. Rotation of the particle through an Euler angle α about the z-axis transforms the laboratory reference frame $L\{x, y, z\}$ into the particle reference frame $P\{x', y', z\}$. Since both the incident and the scattered beams propagate in the positive z-direction, their respective unit $\hat{\boldsymbol{\vartheta}}$- and $\hat{\boldsymbol{\varphi}}$- vectors are the same.

matrix multiplication (cf. Fig. 4.4):

$$\begin{bmatrix} E_{\vartheta P}^{\rm inc} \\ E_{\varphi P}^{\rm inc} \end{bmatrix} = \begin{bmatrix} C & S \\ -S & C \end{bmatrix} \begin{bmatrix} E_{\vartheta L}^{\rm inc} \\ E_{\varphi L}^{\rm inc} \end{bmatrix}, \tag{4.26}$$

where $C = \cos\alpha$ and $S = \sin\alpha$. Conversely,

$$\begin{bmatrix} E_{\vartheta L}^{\rm sca} \\ E_{\varphi L}^{\rm sca} \end{bmatrix} = \begin{bmatrix} C & -S \\ S & C \end{bmatrix} \begin{bmatrix} E_{\vartheta P}^{\rm sca} \\ E_{\varphi P}^{\rm sca} \end{bmatrix}. \tag{4.27}$$

Rewriting Eq. (4.25) in the particle reference frame,

$$\begin{bmatrix} E_{\vartheta P}^{\rm sca} \\ E_{\varphi P}^{\rm sca} \end{bmatrix} \propto \mathbf{S}_P \begin{bmatrix} E_{\vartheta P}^{\rm inc} \\ E_{\varphi P}^{\rm inc} \end{bmatrix}, \tag{4.28}$$

and using Eqs. (4.26) and (4.27), we finally derive

$$\begin{aligned} \mathbf{S}_L^{\alpha} &= \begin{bmatrix} C & -S \\ S & C \end{bmatrix} \mathbf{S}_P \begin{bmatrix} C & S \\ -S & C \end{bmatrix} \\ &= \begin{bmatrix} C^2 S_{11P} - SCS_{12P} - SCS_{21P} + S^2 S_{22P} & SCS_{11P} + C^2 S_{12P} - S^2 S_{21P} - SCS_{22P} \\ SCS_{11P} - S^2 S_{12P} + C^2 S_{21P} - SCS_{22P} & S^2 S_{11P} + SCS_{12P} + SCS_{21P} + C^2 S_{22P} \end{bmatrix}. \end{aligned} \tag{4.29}$$

For $\alpha = 0$ and $\alpha = \pi/2$,

$$\mathbf{S}_L^0 = \begin{bmatrix} S_{11P} & S_{12P} \\ S_{21P} & S_{22P} \end{bmatrix}, \tag{4.30}$$

$$\mathbf{S}_L^{\pi/2} = \begin{bmatrix} S_{22P} & -S_{21P} \\ -S_{12P} & S_{11P} \end{bmatrix}. \tag{4.31}$$

Because we are assuming random orientation of the particles in the small volume element, for each particle in the initial orientation, $\alpha = 0$, there is always a particle of the same type but in the orientation corresponding to $\alpha = \pi/2$. It, therefore, follows from Eqs. (2.141), (2.146), (3.9), (4.30), and (4.31) that $K_{12} = K_{21} = K_{34} = K_{43} = 0$. Finally, recalling Eq. (2.159), we conclude that the extinction matrix of a small volume element containing equal numbers of randomly oriented particles and their mirror-symmetric counterparts and/or randomly oriented particles having a plane of symmetry is diagonal:

$$\mathbf{K}(\hat{\mathbf{n}}) \equiv \mathbf{K} = C_{\rm ext}\mathbf{\Delta} = N\langle C_{\rm ext}\rangle\mathbf{\Delta}, \tag{4.32}$$

where

$$\mathbf{\Delta} = \begin{bmatrix} 1 & 0 & 0 & 0 \\ 0 & 1 & 0 & 0 \\ 0 & 0 & 1 & 0 \\ 0 & 0 & 0 & 1 \end{bmatrix}$$

is the 4×4 unit matrix, N is the number of particles in the volume element, and $\langle C_{\rm ext}\rangle$ is the average extinction cross section per particle, which is now independent of the direction of propagation and polarization state of the incident light. This significant simplification is useful in many practical circumstances.

The scattering matrix also becomes simpler when $\Theta = 0$. From Eqs. (2.107), (2.110), (2.117), (2.120), (4.30), and (4.31), we find that $F_{12}(0) = F_{21}(0) = F_{34}(0) = F_{43}(0) = 0$. Equation (4.29) gives for $\alpha = \pi/4$:

$$\mathbf{S}_L^{\pi/4} = \frac{1}{2}\begin{bmatrix} S_{11P} - S_{12P} - S_{21P} + S_{22P} & S_{11P} + S_{12P} - S_{21P} - S_{22P} \\ S_{11P} - S_{12P} + S_{21P} - S_{22P} & S_{11P} + S_{12P} + S_{21P} + S_{22P} \end{bmatrix}. \tag{4.33}$$

Equations (2.111), (2.116), (4.30), and (4.33) and a considerable amount of algebra yield $F_{22}(0) = F_{33}(0)$. Thus, recalling Eq. (4.7), we find that the forward-scattering matrix for a macroscopically isotropic and mirror-symmetric medium is diagonal and has only three independent elements:

$$\mathbf{F}(0) = \begin{bmatrix} F_{11}(0) & 0 & 0 & 0 \\ 0 & F_{22}(0) & 0 & 0 \\ 0 & 0 & F_{22}(0) & 0 \\ 0 & 0 & 0 & F_{44}(0) \end{bmatrix} \tag{4.34}$$

(van de Hulst 1957).

Rotationally-symmetric particles are obviously mirror-symmetric with respect to the plane through the direction of propagation and the axis of symmetry. Choosing this plane as the $x'z'$-plane of the particle reference frame, we see from Eq. (4.2c) that $S_{12P} = S_{21P} = 0$. This simplifies the amplitude scattering matrices (4.30) and (4.33) and ultimately yields

$$F_{44}(0) = 2F_{22}(0) - F_{11}(0), \qquad 0 \le F_{22}(0) \le F_{11}(0) \tag{4.35}$$

(Mishchenko and Travis 1994c; Hovenier and Mackowski 1998).

4.5 Backward scattering

Equation (4.1) provides an unambiguous definition of the scattering matrix in terms of the phase matrix, except for the exact backscattering direction. Indeed, the backscattering direction for an incidence direction $(\vartheta^{\rm inc}, \varphi^{\rm inc})$ is given by $(\pi - \vartheta^{\rm inc}, \varphi^{\rm inc} + \pi)$. Therefore, the complete definition of the scattering matrix should be as follows:

$$\mathbf{F}(\vartheta^{\rm sca}) = \begin{cases} \mathbf{Z}(\vartheta^{\rm sca}, 0; 0, 0) & \text{for } \vartheta^{\rm sca} \in [0, \pi), \\ \mathbf{Z}(\pi, \pi; 0, 0) & \text{for } \vartheta^{\rm sca} = \pi, \end{cases}$$

which seems to be different from Eq. (4.1). It is easy to see, however, that $\mathbf{Z}(\pi, 0; 0, 0) = \mathbf{L}(\pi)\mathbf{Z}(\pi, \pi; 0, 0) \equiv \mathbf{Z}(\pi, \pi; 0, 0)$, cf. Eq. (1.97), which demonstrates the equivalence of the two definitions.

We are ready now to consider the case of scattering in the exact backward direction, using the complete definition of the scattering matrix and the backscattering theorem derived in Section 2.3. Let us assume that light is incident along the positive z-axis of the laboratory coordinate system and is scattered in the opposite direction; we use the xz-plane with $x \ge 0$ as the meridional plane of the incident beam. As in the previous section, we consider two particle orientations relative to the laboratory reference frame: (i) the initial orientation, when the particle reference frame coincides with the laboratory reference frame, and (ii) the orientation obtained by rotating the particle about the z-axis through a positive Euler angle α. Figure 4.5 shows the respective unit $\hat{\boldsymbol{\vartheta}}$- and $\hat{\boldsymbol{\varphi}}$- vectors for the incident and the backscattered beams. Denote the backscattering amplitude matrix in the particle reference frame as $\mathbf{S}_P$ and the backscattering amplitude matrix in the laboratory reference frame for the rotated particle as $\mathbf{S}_L^{\alpha}$. A derivation similar to that in the previous section gives

$$\begin{aligned} \mathbf{S}_L^{\alpha} &= \begin{bmatrix} C & S \\ -S & C \end{bmatrix} \mathbf{S}_P \begin{bmatrix} C & S \\ -S & C \end{bmatrix} \\ &= \begin{bmatrix} C^2 S_{11P} - SCS_{12P} + SCS_{21P} - S^2 S_{22P} & SCS_{11P} + C^2 S_{12P} + S^2 S_{21P} + SCS_{22P} \\ -SCS_{11P} + S^2 S_{12P} + C^2 S_{21P} - SCS_{22P} & -S^2 S_{11P} - SCS_{12P} + SCS_{21P} + C^2 S_{22P} \end{bmatrix}. \end{aligned} \tag{4.36}$$

This formula can be simplified, because the backscattering theorem (2.65) yields $S_{21P} = -S_{12P}$. Assuming that particles are randomly oriented and considering the cases $\alpha = 0$ and $\alpha = \pi/2$, we find that $F_{12}(\pi) = F_{21}(\pi) = F_{34}(\pi) = F_{43}(\pi) = 0$. Similarly, considering the cases $\alpha = 0$ and $\alpha = \pi/4$ yields $F_{33}(\pi) = -F_{22}(\pi)$. Finally, recalling Eqs. (2.131) and (4.7), we conclude that the backscattering matrix for

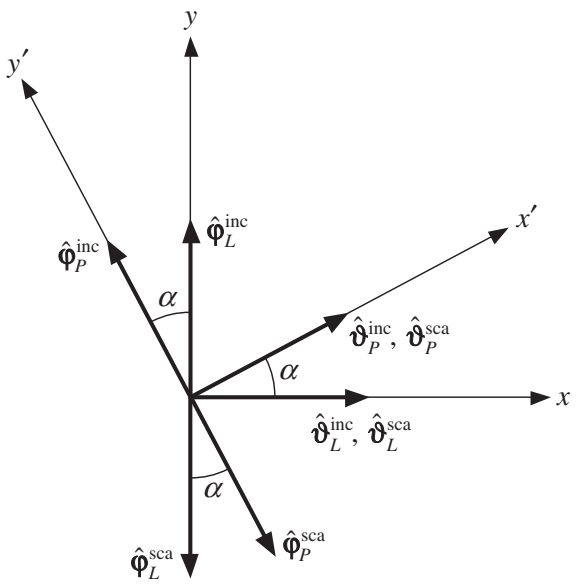

Figure 4.5. As in Fig. 4.4, but for the case of scattering in the exact backward direction.

a macroscopically isotropic and mirror-symmetric medium is diagonal and has only two independent elements:

$$\mathbf{F}(\pi) = \begin{bmatrix} F_{11}(\pi) & 0 & 0 & 0 \\ 0 & F_{22}(\pi) & 0 & 0 \\ 0 & 0 & -F_{22}(\pi) & 0 \\ 0 & 0 & 0 & F_{11}(\pi) - 2F_{22}(\pi) \end{bmatrix}. \tag{4.37}$$

(Mishchenko and Hovenier 1995). According to Eq. (4.9) $F_{44} \leq F_{11}$, so we always have

$$F_{22}(\pi) \geq 0. \tag{4.38}$$

4.6 Scattering cross section, asymmetry parameter, and radiation pressure

Like all other macroscopic scattering characteristics, the average scattering cross section per particle for a macroscopically isotropic and mirror-symmetric medium is independent of the direction of illumination. Therefore, we will evaluate the integral on the right-hand side of Eq. (2.160) assuming that the incident light propagates along the positive z-axis of the laboratory reference frame and that the xz-plane with $x \geq 0$ is the meridional plane of the incident beam. Figure 4.6 shows that in order to compute the Stokes vector of the scattered beam with respect to its own meridional plane, we must rotate the reference frame of the incident beam by the angle φ, thereby modifying the Stokes vector of the incident light according to Eq. (1.97) with $\eta = \varphi$,

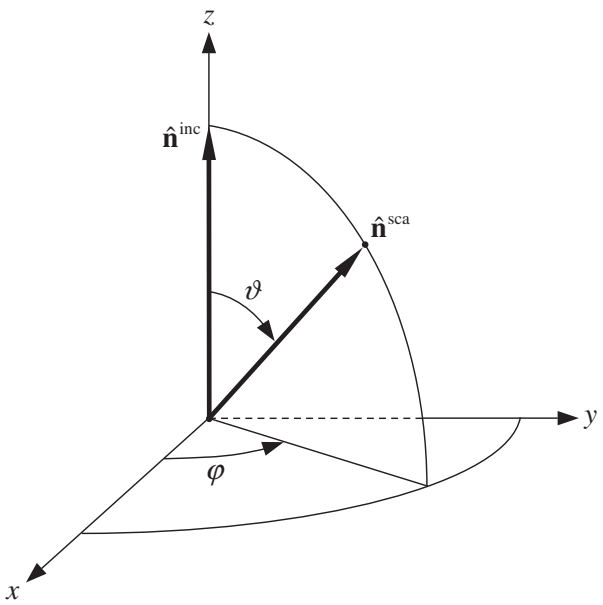

Figure 4.6. Illustration of the relationship between the phase and scattering matrices when the incident light propagates along the positive z-axis.

and then multiply the new Stokes vector of the incident light by the scattering matrix. Therefore, the average phase matrix per particle is simply

$$\langle \mathbf{Z}(\hat{\mathbf{n}}^{\rm sca}, \hat{\mathbf{n}}^{\rm inc})\rangle = \langle \mathbf{F}(\vartheta)\rangle \mathbf{L}(\varphi)$$
$$= \begin{bmatrix} \langle F_{11}(\vartheta)\rangle & \langle F_{12}(\vartheta)\rangle \cos 2\varphi & -\langle F_{12}(\vartheta)\rangle \sin 2\varphi & 0 \\ \langle F_{12}(\vartheta)\rangle & \langle F_{22}(\vartheta)\rangle \cos 2\varphi & -\langle F_{22}(\vartheta)\rangle \sin 2\varphi & 0 \\ 0 & \langle F_{33}(\vartheta)\rangle \sin 2\varphi & \langle F_{33}(\vartheta)\rangle \cos 2\varphi & \langle F_{34}(\vartheta)\rangle \\ 0 & -\langle F_{34}(\vartheta)\rangle \sin 2\varphi & -\langle F_{34}(\vartheta)\rangle \cos 2\varphi & \langle F_{44}(\vartheta)\rangle \end{bmatrix}. \tag{4.39}$$

Substituting this formula in Eq. (2.160), we find that the average scattering cross section per particle is independent of the polarization state of the incident light and is given by

$$\langle C_{\rm sca}\rangle = 2\pi \int_0^\pi {\rm d}\vartheta \sin\vartheta \langle F_{11}(\vartheta)\rangle. \tag{4.40}$$

The ensemble-averaged asymmetry parameter must also be independent of $\hat{\mathbf{n}}^{\rm inc}$, and Eqs. (2.166), (2.169), and (4.39) yield

$$\langle \cos\Theta\rangle = \frac{2\pi}{\langle C_{\rm sca}\rangle} \int_0^\pi {\rm d}\vartheta \sin\vartheta \cos\vartheta \langle F_{11}(\vartheta)\rangle. \tag{4.41}$$

Obviously, $\langle \cos\Theta\rangle$ is polarization-independent. Equations (2.176), (4.39), and (4.41) show that the average radiation force per particle is now directed along $\hat{\mathbf{n}}^{\rm inc}$:

$$\langle \mathbf{F} \rangle = \frac{1}{c} \hat{\mathbf{n}}^{\rm inc} I^{\rm inc} [\langle C_{\rm ext} \rangle - \langle C_{\rm sca} \rangle \langle \cos\Theta \rangle]$$
$$= \frac{1}{c} \hat{\mathbf{n}}^{\rm inc} I^{\rm inc} \langle C_{\rm pr} \rangle, \tag{4.42}$$

where

$$\langle C_{\rm pr} \rangle = \langle C_{\rm ext} \rangle - \langle C_{\rm sca} \rangle \langle \cos\Theta \rangle \tag{4.43}$$

is the polarization- and direction-independent average radiation-pressure cross section per particle. The average absorption cross section per particle,

$$\langle C_{\rm abs} \rangle = \langle C_{\rm ext} \rangle - \langle C_{\rm sca} \rangle, \tag{4.44}$$

and the average single-scattering albedo,

$$\varpi = \frac{\langle C_{\rm sca} \rangle}{\langle C_{\rm ext} \rangle}, \tag{4.45}$$

are also independent of the direction and polarization of the incident beam. The same, of course, is true of the extinction, scattering, absorption, and radiation pressure efficiency factors, defined as

$$Q_{\rm ext} = \frac{\langle C_{\rm ext} \rangle}{\langle G \rangle}, \quad Q_{\rm sca} = \frac{\langle C_{\rm sca} \rangle}{\langle G \rangle}, \quad Q_{\rm abs} = \frac{\langle C_{\rm abs} \rangle}{\langle G \rangle}, \quad Q_{\rm pr} = \frac{\langle C_{\rm pr} \rangle}{\langle G \rangle}, \tag{4.46}$$

respectively, where $\langle G \rangle$ is the average projection area per particle.

4.7 Thermal emission

Because the ensemble-averaged emission vector for a macroscopically isotropic and mirror-symmetric medium must be independent of the emission direction, we will calculate the integral on the right-hand side of Eq. (2.186) for light emitted in the positive direction of the z-axis and will use the meridional plane $\varphi = 0$ as the reference plane for defining the emission Stokes vector. It is then obvious from Fig. 4.7 that the corresponding average phase matrix per particle can be calculated as

$$\langle \mathbf{Z}(\hat{\mathbf{n}}, \hat{\mathbf{n}}') \rangle = \mathbf{L}(-\varphi') \langle \mathbf{F}(\vartheta') \rangle$$
$$= \begin{bmatrix} \langle F_{11}(\vartheta') \rangle & \langle F_{12}(\vartheta') \rangle & 0 & 0 \\ \langle F_{12}(\vartheta') \rangle \cos 2\varphi' & \langle F_{22}(\vartheta') \rangle \cos 2\varphi' & \langle F_{33}(\vartheta') \rangle \sin 2\varphi' & \langle F_{34}(\vartheta') \rangle \sin 2\varphi' \\ -\langle F_{12}(\vartheta') \rangle \sin 2\varphi' & -\langle F_{22}(\vartheta') \rangle \sin 2\varphi' & \langle F_{33}(\vartheta') \rangle \cos 2\varphi' & \langle F_{34}(\vartheta') \rangle \cos 2\varphi' \\ 0 & 0 & -\langle F_{34}(\vartheta') \rangle & \langle F_{44}(\vartheta') \rangle \end{bmatrix}. \tag{4.47}$$

Inserting this formula and Eqs. (4.32) and (4.40) in Eq. (2.186) yields

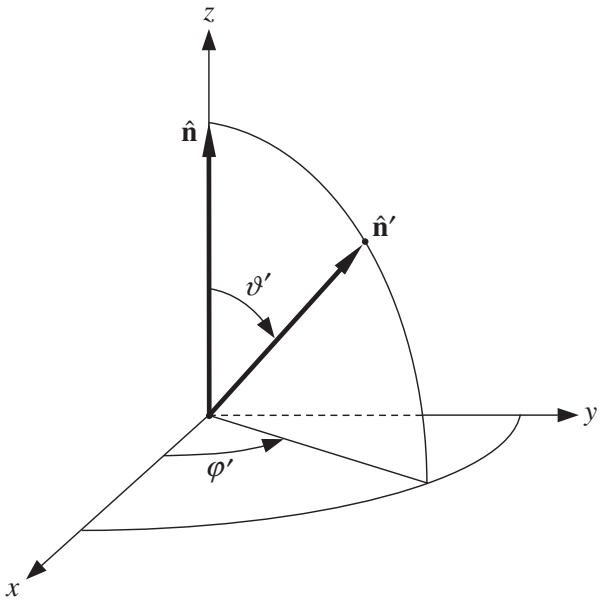

Figure 4.7. Illustration of the relationship between the phase and scattering matrices when the scattered light propagates along the positive z-axis.

$$\langle \mathbf{K}_{\rm e}(\hat{\mathbf{n}}, T, \omega)\rangle \equiv \langle \mathbf{K}_{\rm e}(T, \omega)\rangle = \langle C_{\rm abs}\rangle \mathbf{I}_{\rm b}(T, \omega), \tag{4.48}$$

where $\langle C_{\rm abs}\rangle$ may depend on frequency and $\mathbf{I}_{\rm b}(T, \omega)$ is the blackbody Stokes vector defined by Eq. (2.184). Thus, the radiation emitted by a small volume element comprising equal numbers of randomly oriented particles and their mirror-symmetric counterparts and/or randomly oriented particles having a plane of symmetry is not only isotropic but also unpolarized. The first (and the only non-zero) element of the average emission vector per particle is simply equal to the product of the average absorption cross section and the Planck function. Substituting Eq. (4.48) in Eq. (2.187), we see that the emission component of the average radiation force exerted on particles forming a macroscopically isotropic and mirror-symmetric medium is identically equal to zero:

$$\langle \mathbf{F}_{\rm e}(T)\rangle \equiv 0.$$

4.8 Spherically symmetric particles

The structure of the scattering matrix simplifies further for spherically symmetric particles, that is, for homogeneous or radially inhomogeneous spherical bodies composed of optically isotropic materials. The refractive index inside such particles is a function of only the distance from the particle center. Irrespective of their "orientation" relative to the laboratory reference frame, spherically symmetric particles are obviously mirror-symmetric with respect to the xz-plane. Directing the incident light

along the positive z-axis, restricting the scattering direction to the xz-plane with $x \geq 0$, and using this plane for reference, we find from Eqs. (4.2a) and (4.2c) that the amplitude scattering matrix is always diagonal ($S_{12} = S_{21} = 0$). Therefore, Eqs. (2.106), (2.111), (2.116), (2.121), and (4.7) yield

$$\mathbf{F}(\Theta) = \begin{bmatrix} F_{11}(\Theta) & F_{12}(\Theta) & 0 & 0 \\ F_{12}(\Theta) & F_{11}(\Theta) & 0 & 0 \\ 0 & 0 & F_{33}(\Theta) & F_{34}(\Theta) \\ 0 & 0 & -F_{34}(\Theta) & F_{33}(\Theta) \end{bmatrix}. \tag{4.49}$$

A scattering matrix of this type appears in the standard Lorenz–Mie theory of light scattering by homogeneous isotropic spheres; therefore, the above matrix will be referred to as the Lorenz–Mie scattering matrix. The results of the previous sections on forward and backward scattering imply that

$$F_{33}(0) = F_{11}(0) \quad \text{and} \quad F_{33}(\pi) = -F_{11}(\pi). \tag{4.50}$$

4.9 Effects of nonsphericity and orientation

The previous discussion of symmetries enables us to summarize the most fundamental effects of particle nonsphericity and orientation on single-scattering patterns. If particles are not spherically symmetric and do not form a macroscopically isotropic and mirror-symmetric medium, then, in general,

- the 4×4 extinction matrix does not degenerate to a direction- and polarization-independent scalar extinction cross section;
- the extinction, scattering, absorption, and radiation-pressure cross sections, the single-scattering albedo, and the asymmetry parameter depend on the direction and polarization state of the incident beam;
- all four elements of the emission vector are non-zero and orientation dependent;
- the direction of the radiation force does not coincide with the direction of incidence, and the emission component of the radiation force is non-zero;
- the scattering matrix $\mathbf{F}$ does not have the simple block-diagonal structure of Eq. (4.7): all 16 elements of the scattering matrix can be non-zero and depend on the incidence direction and the orientation of the scattering plane rather than only on the scattering angle;
- the phase matrix depends on the specific values of the azimuthal angles of the incidence and scattering directions rather than on their difference, it cannot be represented in the form of Eqs. (4.14) and (4.15), and it does not obey the symmetry relations (4.20) and (4.22).

Any of these effects can directly indicate the presence of oriented particles lacking spherical symmetry. For example, measurements of interstellar polarization are used in

astrophysics to detect preferentially oriented dust grains causing different values of extinction for different polarization components of the transmitted starlight (Martin 1978). Similarly, the depolarization of radiowave signals propagating through the Earth's atmosphere may indicate the presence of partially aligned nonspherical hydrometeors (Oguchi 1983).

If nonspherical particles are randomly oriented and form a macroscopically isotropic and mirror-symmetric scattering medium, then

- the extinction matrix reduces to the scalar extinction cross section, Eq. (4.32);
- all optical cross sections, the single-scattering albedo, and the asymmetry parameter become orientation and polarization independent;
- the emitted radiation becomes isotropic and unpolarized;
- the radiation force is directed along the incident beam, and the emission component of the radiation force vanishes;
- the phase matrix depends only on the difference between the azimuthal angles of the incidence and scattering directions rather than on their specific values, has the structure specified by Eqs. (4.14) and (4.15), and obeys the symmetry relations (4.20) and (4.22);
- the scattering matrix becomes block-diagonal (Eq. (4.7)), depends only on the scattering angle, and possesses almost the same structure as the Lorenz–Mie scattering matrix (4.49).

However, the remaining key point is that the Lorenz–Mie identities $F_{22}(\Theta) \equiv F_{11}(\Theta)$ and $F_{44}(\Theta) \equiv F_{33}(\Theta)$ do not hold, in general, for nonspherical particles. This difference makes measurements of the linear backscattering depolarization ratio $\delta_{\rm L} = [F_{11}(\pi) - F_{22}(\pi)]/[F_{11}(\pi) + F_{22}(\pi)]$ and the closely related circular backscattering depolarization ratio $\delta_{\rm C}$ the most reliable indicators of particle nonsphericity (Sections 10.2 and 10.11). Besides this qualitative distinction, which unequivocally distinguishes randomly oriented nonspherical particles from spheres, there can be significant quantitative differences in specific scattering patterns. They will be discussed in detail in the following chapters.

4.10 Normalized scattering and phase matrices

It is convenient and customary in many types of applications to use the so-called normalized scattering matrix

$$\widetilde{\mathbf{F}}(\Theta) = \frac{4\pi}{C_{\rm sca}}\mathbf{F}(\Theta) = \frac{4\pi}{\langle C_{\rm sca}\rangle}\langle\mathbf{F}(\Theta)\rangle = \begin{bmatrix} a_1(\Theta) & b_1(\Theta) & 0 & 0 \\ b_1(\Theta) & a_2(\Theta) & 0 & 0 \\ 0 & 0 & a_3(\Theta) & b_2(\Theta) \\ 0 & 0 & -b_2(\Theta) & a_4(\Theta) \end{bmatrix}, \tag{4.51}$$

the elements of which are dimensionless. Similarly, the normalized phase matrix can

be defined as

$$\widetilde{\mathbf{Z}}(\vartheta^{\rm sca}, \varphi^{\rm sca}; \vartheta^{\rm inc}, \varphi^{\rm inc}) = \frac{4\pi}{C_{\rm sca}} \mathbf{Z}(\vartheta^{\rm sca}, \varphi^{\rm sca}; \vartheta^{\rm inc}, \varphi^{\rm inc})$$
$$= \frac{4\pi}{\langle C_{\rm sca} \rangle} \langle \mathbf{Z}(\vartheta^{\rm sca}, \varphi^{\rm sca}; \vartheta^{\rm inc}, \varphi^{\rm inc}) \rangle. \tag{4.52}$$

The (1,1) element of the normalized scattering matrix, $a_1(\Theta)$, is traditionally called the phase function and, as follows from Eqs. (4.40) and (4.51), satisfies the normalization condition:

$$\frac{1}{2} \int_0^\pi {\rm d}\Theta \sin\Theta \, a_1(\Theta) = 1. \tag{4.53}$$

Remember that we have already used the term "phase function" to name the quantity p defined by Eq. (2.167). It can be easily seen from Eqs. (2.166), (2.167), (4.1), and (4.51) that the differential scattering cross section ${\rm d}C_{\rm sca}/{\rm d}\Omega$ reduces to $\langle F_{11} \rangle$, and so p reduces to a_1, when unpolarized incident light propagates along the positive z-axis and is scattered in the xz-plane with $x \geq 0$. Equations (4.41) and (4.51) yield

$$\langle \cos\Theta \rangle = \frac{1}{2} \int_0^\pi {\rm d}\Theta \sin\Theta \, a_1(\Theta) \cos\Theta. \tag{4.54}$$

The normalized scattering matrix possesses many properties of the regular scattering matrix, e.g.,

$$a_1 \geq 0, \tag{4.55}$$

$$|a_i| \leq a_1, \quad i = 2, 3, 4, \qquad |b_i| \leq a_1, \quad i = 1, 2, \tag{4.56}$$

$$(a_3 + a_4)^2 + 4b_2^2 \leq (a_1 + a_2)^2 - 4b_1^2, \tag{4.57}$$

$$|a_3 - a_4| \leq a_1 - a_2, \tag{4.58}$$

$$|a_2 - b_1| \leq a_1 - b_1, \tag{4.59}$$

$$|a_2 + b_1| \leq a_1 + b_1, \tag{4.60}$$

$$\widetilde{\mathbf{F}}(0) = \begin{bmatrix} a_1(0) & 0 & 0 & 0 \\ 0 & a_2(0) & 0 & 0 \\ 0 & 0 & a_2(0) & 0 \\ 0 & 0 & 0 & a_4(0) \end{bmatrix}, \tag{4.61}$$

$$\widetilde{\mathbf{F}}(\pi) = \begin{bmatrix} a_1(\pi) & 0 & 0 & 0 \\ 0 & a_2(\pi) & 0 & 0 \\ 0 & 0 & -a_2(\pi) & 0 \\ 0 & 0 & 0 & a_4(\pi) \end{bmatrix}, \tag{4.62}$$

$$a_4(\pi) = a_1(\pi) - 2a_2(\pi), \qquad a_2(\pi) \geq 0. \tag{4.63}$$

Also,

$$a_4(0) = 2a_2(0) - a_1(0), \qquad 0 \le a_2(0) \le a_1(0) \tag{4.64}$$

for rotationally symmetric particles and

$$\widetilde{\mathbf{F}}(\Theta) = \begin{bmatrix} a_1(\Theta) & b_1(\Theta) & 0 & 0 \\ b_1(\Theta) & a_1(\Theta) & 0 & 0 \\ 0 & 0 & a_3(\Theta) & b_2(\Theta) \\ 0 & 0 & -b_2(\Theta) & a_3(\Theta) \end{bmatrix}, \tag{4.65}$$

$$a_3(0) = a_1(0), \qquad a_3(\pi) = -a_1(\pi) \tag{4.66}$$

for spherically symmetric particles. Similarly, for $0 < \varphi^{\rm sca} - \varphi^{\rm inc} < \pi$ the normalized phase matrix is given by

$$\widetilde{\mathbf{Z}}(\vartheta^{\rm sca}, \varphi^{\rm sca}; \vartheta^{\rm inc}, \varphi^{\rm inc})$$

$$= \begin{bmatrix} a_1(\Theta) & C_1 b_1(\Theta) & S_1 b_1(\Theta) & 0 \\ C_2 b_1(\Theta) & C_1 C_2 a_2(\Theta) - S_1 S_2 a_3(\Theta) & S_1 C_2 a_2(\Theta) + C_1 S_2 a_3(\Theta) & S_2 b_2(\Theta) \\ -S_2 b_1(\Theta) & -C_1 S_2 a_2(\Theta) - S_1 C_2 a_3(\Theta) & -S_1 S_2 a_2(\Theta) + C_1 C_2 a_3(\Theta) & C_2 b_2(\Theta) \\ 0 & S_1 b_2(\Theta) & -C_1 b_2(\Theta) & a_4(\Theta) \end{bmatrix} \tag{4.67}$$

(cf. Eq. (4.14)) and has the same symmetry properties as the regular phase matrix:

$$\widetilde{\mathbf{Z}}(\vartheta^{\rm sca}, \varphi^{\rm inc}; \vartheta^{\rm inc}, \varphi^{\rm sca}) = \mathbf{\Delta}_{34} \widetilde{\mathbf{Z}}(\vartheta^{\rm sca}, \varphi^{\rm sca}; \vartheta^{\rm inc}, \varphi^{\rm inc}) \mathbf{\Delta}_{34}, \tag{4.68}$$

$$\widetilde{\mathbf{Z}}(\pi - \vartheta^{\rm sca}, \varphi^{\rm sca}; \pi - \vartheta^{\rm inc}, \varphi^{\rm inc}) = \mathbf{\Delta}_{34} \widetilde{\mathbf{Z}}(\vartheta^{\rm sca}, \varphi^{\rm sca}; \vartheta^{\rm inc}, \varphi^{\rm inc}) \mathbf{\Delta}_{34}, \tag{4.69}$$

$$\widetilde{\mathbf{Z}}(\pi - \vartheta^{\rm inc}, \varphi^{\rm inc} + \pi; \pi - \vartheta^{\rm sca}, \varphi^{\rm sca} + \pi) = \mathbf{\Delta}_3 [\widetilde{\mathbf{Z}}(\vartheta^{\rm sca}, \varphi^{\rm sca}; \vartheta^{\rm inc}, \varphi^{\rm inc})]^{\rm T} \mathbf{\Delta}_3. \tag{4.70}$$

An important difference between the regular and normalized matrices is that the latter do not possess the property of additivity. Consider, for example, a small volume element containing N_1 particles of type 1 and N_2 particles of type 2. The total phase and scattering matrices of the volume element are obtained by adding the phase and scattering matrices of all particles,

$$\mathbf{Z} = N_1 \langle \mathbf{Z}_1 \rangle + N_2 \langle \mathbf{Z}_2 \rangle, \tag{4.71}$$

$$\mathbf{F} = N_1 \langle \mathbf{F}_1 \rangle + N_2 \langle \mathbf{F}_2 \rangle, \tag{4.72}$$

whereas the respective normalized matrices are given by more complicated relations,

$$\widetilde{\mathbf{Z}} = \frac{N_1 \langle C_{\rm sca1} \rangle \widetilde{\mathbf{Z}}_1 + N_2 \langle C_{\rm sca2} \rangle \widetilde{\mathbf{Z}}_2}{N_1 \langle C_{\rm sca1} \rangle + N_2 \langle C_{\rm sca2} \rangle}, \tag{4.73}$$

$$\widetilde{\mathbf{F}} = \frac{N_1 \langle C_{\rm sca1} \rangle \widetilde{\mathbf{F}}_1 + N_2 \langle C_{\rm sca2} \rangle \widetilde{\mathbf{F}}_2}{N_1 \langle C_{\rm sca1} \rangle + N_2 \langle C_{\rm sca2} \rangle} \tag{4.74}$$

(see Eqs. (4.51) and (4.52)).

4.11 Expansion in generalized spherical functions

A traditional way of specifying the elements of the normalized scattering matrix is to tabulate their numerical values at a representative grid of scattering angles (Deirmendjian 1969). However, a more mathematically appealing and efficient way is to expand the scattering matrix elements in so-called generalized spherical functions $P^s_{mn}(\cos\Theta)$ or, equivalently, in Wigner functions $d^s_{mn}(\Theta) = \mathrm{i}^{n-m} P^s_{mn}(\cos\Theta)$ (Siewert 1981; de Haan *et al.* 1987):

$$a_1(\Theta) = \sum_{s=0}^{s_{\max}} \alpha_1^s P^s_{00}(\cos\Theta) = \sum_{s=0}^{s_{\max}} \alpha_1^s d^s_{00}(\Theta), \tag{4.75}$$

$$a_2(\Theta) + a_3(\Theta) = \sum_{s=2}^{s_{\max}} (\alpha_2^s + \alpha_3^s) P^s_{22}(\cos\Theta) = \sum_{s=2}^{s_{\max}} (\alpha_2^s + \alpha_3^s) d^s_{22}(\Theta), \tag{4.76}$$

$$a_2(\Theta) - a_3(\Theta) = \sum_{s=2}^{s_{\max}} (\alpha_2^s - \alpha_3^s) P^s_{2,-2}(\cos\Theta) = \sum_{s=2}^{s_{\max}} (\alpha_2^s - \alpha_3^s) d^s_{2,-2}(\Theta), \tag{4.77}$$

$$a_4(\Theta) = \sum_{s=0}^{s_{\max}} \alpha_4^s P^s_{00}(\cos\Theta) = \sum_{s=0}^{s_{\max}} \alpha_4^s d^s_{00}(\Theta), \tag{4.78}$$

$$b_1(\Theta) = \sum_{s=2}^{s_{\max}} \beta_1^s P^s_{02}(\cos\Theta) = -\sum_{s=2}^{s_{\max}} \beta_1^s d^s_{02}(\Theta), \tag{4.79}$$

$$b_2(\Theta) = \sum_{s=2}^{s_{\max}} \beta_2^s P^s_{02}(\cos\Theta) = -\sum_{s=2}^{s_{\max}} \beta_2^s d^s_{02}(\Theta). \tag{4.80}$$

The number of non-zero terms in the expansions (4.75)–(4.80) is in principle infinite. In practice, however, the expansions are truncated at $s = s_{\max}$, $s_{\max}$ being chosen such that the corresponding finite sums differ from the respective scattering matrix elements on the entire interval $\Theta \in [0, \pi]$ of scattering angles within the desired numerical accuracy.

The properties of the generalized spherical functions and the Wigner *d*-functions are summarized in Appendix B. For given *m* and *n*, either type of function with $s \geq \max(|m|, |n|)$, when multiplied by $\sqrt{s+\frac{1}{2}}$, forms a complete orthonormal set of functions of $\cos\Theta \in [-1, +1]$ (see Eqs. (B.17) and (B.33)). Therefore, using the orthogonality relation (B.17), we obtain from Eqs. (4.75)–(4.80)

$$\alpha_1^s = (s+\tfrac{1}{2}) \int_0^\pi \mathrm{d}\Theta \sin\Theta\, a_1(\Theta)\, d^s_{00}(\Theta), \tag{4.81}$$

$$\alpha_2^s + \alpha_3^s = (s+\tfrac{1}{2}) \int_0^\pi \mathrm{d}\Theta \sin\Theta\, [a_2(\Theta) + a_3(\Theta)]\, d_{22}^s(\Theta), \tag{4.82}$$

$$\alpha_2^s - \alpha_3^s = (s+\tfrac{1}{2}) \int_0^\pi \mathrm{d}\Theta \sin\Theta\, [a_2(\Theta) - a_3(\Theta)]\, d_{2,-2}^s(\Theta), \tag{4.83}$$

$$\alpha_4^s = (s+\tfrac{1}{2}) \int_0^\pi \mathrm{d}\Theta \sin\Theta\, a_4(\Theta)\, d_{00}^s(\Theta), \tag{4.84}$$

$$\beta_1^s = -(s+\tfrac{1}{2}) \int_0^\pi \mathrm{d}\Theta \sin\Theta\, b_1(\Theta)\, d_{02}^s(\Theta), \tag{4.85}$$

$$\beta_2^s = -(s+\tfrac{1}{2}) \int_0^\pi \mathrm{d}\Theta \sin\Theta\, b_2(\Theta)\, d_{02}^s(\Theta) \tag{4.86}$$

(cf. Eq. (B.21)). These formulas suggest a simple, albeit not always the most elegant and efficient, way to compute the expansion coefficients by evaluating the integrals numerically using a suitable quadrature formula (de Rooij and van der Stap 1984). Of course, this procedure assumes the knowledge of the scattering matrix elements at the quadrature division points. The expansions (4.75)–(4.80) converge (in the sense of Eqs. (B.34)–(B.37) or Eqs. (B.18)–(B.21)) to the respective elements of the normalized scattering matrix if these elements are square integrable on the interval $\Theta \in [0, \pi]$. In view of the general inequality (4.56), it is sufficient to require that the phase function $a_1(\Theta)$ be square integrable to ensure such convergence.

Because the Wigner *d*-functions possess well-known and convenient mathematical properties and can be efficiently computed by using a simple and numerically stable recurrence relation, expansions (4.75)–(4.80) offer several practical advantages. First, we note that according to Eqs. (B.6)–(B.7),

$$d_{2,-2}^s(0) = d_{02}^s(0) = 0 \tag{4.87}$$

and

$$d_{22}^s(\pi) = d_{02}^s(\pi) = 0. \tag{4.88}$$

Therefore, Eqs. (4.76), (4.77), (4.79), and (4.80) reproduce identically the specific structure of the normalized scattering matrix for the exact forward and backward directions, Eqs. (4.61) and (4.62) (cf. Domke 1974). Second, when the expansion coefficients appearing in these expansions are known, then the elements of the normalized scattering matrix can be calculated easily for practically any number of scattering angles and with a minimal expenditure of computer time. Thus, instead of tabulating the elements of the scattering matrix for a large number of scattering angles (cf. Deirmendjian 1969) and resorting to interpolation in order to find the scattering matrix at intermediate points, one can provide a complete and accurate specification of the scattering matrix by tabulating a limited (and usually small) number of numerically significant expansion coefficients. This also explains why the expansion coefficients are especially convenient

in ensemble averaging: instead of computing ensemble-averaged scattering matrix elements, one can average a (much) smaller number of expansion coefficients.

An additional advantage of expanding the scattering matrix elements in generalized spherical functions is that the latter obey an addition theorem and thereby provide an elegant analytical way of calculating the coefficients in a Fourier decomposition of the normalized phase matrix (Kuščer and Ribarič 1959; Domke 1974; de Haan *et al.* 1987). This Fourier decomposition is then used to handle the azimuthal dependence of the solution of the vector radiative transfer equation efficiently. Another important advantage offered by expansions (4.75)–(4.80) is that the expansion coefficients for certain types of nonspherical particle can be calculated analytically without computing the scattering matrix itself (Section 5.5).

The expansion coefficients obey the general inequalities

$$|\alpha_j^s| \le 2s+1, \quad j=1,2,3,4, \tag{4.89}$$

$$|\beta_j^s| < (2s+1)/\sqrt{2}, \quad j=1,2. \tag{4.90}$$

These and other useful inequalities were derived by van der Mee and Hovenier (1990). Since, for each s, $d_{00}^s(\Theta)$ is a Legendre polynomial $P_s(\cos\Theta)$, Eq. (4.75) is also the well-known expansion of the phase function in Legendre polynomials (Chandrasekhar 1960; Sobolev 1974; van de Hulst 1980). Equation (B.12) gives $d_{00}^0(\Theta) \equiv 1$. Therefore, Eq. (4.81) and the normalization condition (4.53) yield the identity

$$\alpha_1^0 \equiv 1. \tag{4.91}$$

Similarly, the average asymmetry parameter, Eq. (4.54), can be expressed as

$$\langle \cos\Theta \rangle = \frac{\alpha_1^1}{3}. \tag{4.92}$$

4.12 Circular-polarization representation

Equations (4.75)–(4.80) become more compact and their origin becomes more transparent if one uses the circular-polarization representation of the Stokes vector (Kuščer and Ribarič 1959; Domke 1974; Hovenier and van der Mee 1983). We begin by defining the circular components of a transverse electromagnetic wave as

$$\begin{bmatrix} E_+ \\ E_- \end{bmatrix} = \mathbf{q} \begin{bmatrix} E_\vartheta \\ E_\varphi \end{bmatrix}, \tag{4.93}$$

where

$$\mathbf{q} = \frac{1}{\sqrt{2}} \begin{bmatrix} 1 & \mathrm{i} \\ 1 & -\mathrm{i} \end{bmatrix}. \tag{4.94}$$

Using Eqs. (2.30) and (4.94), we find that the corresponding circular-polarization amplitude scattering matrix $\mathbf{C}$ is expressed in terms of the regular amplitude scattering matrix as

$$\begin{aligned}\mathbf{C} &= \begin{bmatrix} C_{++} & C_{+-} \\ C_{-+} & C_{--} \end{bmatrix} \\ &= \mathbf{qSq}^{-1} \\ &= \frac{1}{2}\begin{bmatrix} S_{11} - iS_{12} + iS_{21} + S_{22} & S_{11} + iS_{12} + iS_{21} - S_{22} \\ S_{11} - iS_{12} - iS_{21} - S_{22} & S_{11} + iS_{12} - iS_{21} + S_{22} \end{bmatrix}\end{aligned} \tag{4.95}$$

where the arguments $(\hat{\mathbf{n}}^{\rm sca}, \hat{\mathbf{n}}^{\rm inc})$ are omitted for brevity and

$$\mathbf{q}^{-1} = \frac{1}{\sqrt{2}}\begin{bmatrix} 1 & 1 \\ -i & i \end{bmatrix}.$$

The usefulness of the circular electric vector components becomes clear from the simple formulas

$$I_2 = E_- E_+^*, \tag{4.96a}$$

$$I_0 = E_+ E_+^*, \tag{4.96b}$$

$$I_{-0} = E_- E_-^*, \tag{4.96c}$$

$$I_{-2} = E_+ E_-^*, \tag{4.96d}$$

which follow, after some algebra, from

$$\begin{bmatrix} E_\vartheta \\ E_\varphi \end{bmatrix} = \mathbf{q}^{-1}\begin{bmatrix} E_+ \\ E_- \end{bmatrix}$$

and Eqs. (1.54) and (1.60). It is easy to verify using the first equality of Eq. (4.95) and (4.96) that the circular-polarization phase matrix is given by

$$\mathbf{Z}^{\rm CP} = \left\| Z_{pq}^{\rm CP} \right\| = \begin{bmatrix} C_{--}C_{++}^* & C_{-+}C_{++}^* & C_{--}C_{+-}^* & C_{-+}C_{+-}^* \\ C_{+-}C_{++}^* & C_{++}C_{++}^* & C_{+-}C_{+-}^* & C_{++}C_{+-}^* \\ C_{--}C_{-+}^* & C_{-+}C_{-+}^* & C_{--}C_{--}^* & C_{-+}C_{--}^* \\ C_{+-}C_{-+}^* & C_{++}C_{-+}^* & C_{+-}C_{--}^* & C_{++}C_{--}^* \end{bmatrix}, \quad p, q = 2, 0, -0, -2. \tag{4.97}$$

Alternatively, it can be found from Eq. (2.123).

Consider now scattering by a macroscopically isotropic and mirror-symmetric medium. The normalized scattering and phase matrices in the circular-polarization representation are defined by analogy with the matrices $\widetilde{\mathbf{F}}$ and $\widetilde{\mathbf{Z}}$:

$$\widetilde{\mathbf{F}}^{\rm CP}(\Theta) = \frac{4\pi}{\langle C_{\rm sca}\rangle}\langle \mathbf{Z}^{\rm CP}(\vartheta^{\rm sca} = \Theta, \varphi^{\rm sca} = 0; \vartheta^{\rm inc} = 0, \varphi^{\rm inc} = 0)\rangle, \tag{4.98}$$

$$\widetilde{\mathbf{Z}}^{\mathrm{CP}}(\vartheta^{\mathrm{sca}}, \varphi^{\mathrm{sca}}; \vartheta^{\mathrm{inc}}, \varphi^{\mathrm{inc}}) = \frac{4\pi}{\langle C_{\mathrm{sca}} \rangle} \langle \mathbf{Z}^{\mathrm{CP}}(\vartheta^{\mathrm{sca}}, \varphi^{\mathrm{sca}}; \vartheta^{\mathrm{inc}}, \varphi^{\mathrm{inc}}) \rangle, \tag{4.99}$$

where $\langle \mathbf{Z}^{\mathrm{CP}}(\vartheta^{\mathrm{sca}}, \varphi^{\mathrm{sca}}; \vartheta^{\mathrm{inc}}, \varphi^{\mathrm{inc}}) \rangle$ is the average circular-polarization phase matrix per particle. From Eqs. (2.123), (4.51), (1.62), and (1.66) we have

$$\widetilde{\mathbf{F}}^{\mathrm{CP}} = \left\| \widetilde{F}_{pq}^{\mathrm{CP}} \right\| = \frac{1}{2} \begin{bmatrix} a_2 + a_3 & b_1 + \mathrm{i}b_2 & b_1 - \mathrm{i}b_2 & a_2 - a_3 \\ b_1 + \mathrm{i}b_2 & a_1 + a_4 & a_1 - a_4 & b_1 - \mathrm{i}b_2 \\ b_1 - \mathrm{i}b_2 & a_1 - a_4 & a_1 + a_4 & b_1 + \mathrm{i}b_2 \\ a_2 - a_3 & b_1 - \mathrm{i}b_2 & b_1 + \mathrm{i}b_2 & a_2 + a_3 \end{bmatrix},$$
$$p, q = 2, 0, -0, -2. \tag{4.100}$$

Obviously, this matrix has several symmetry properties:

$$\widetilde{F}_{pq}^{\mathrm{CP}}(\Theta) = \widetilde{F}_{qp}^{\mathrm{CP}}(\Theta) = \widetilde{F}_{-p,-q}^{\mathrm{CP}}(\Theta), \tag{4.101}$$

$$\widetilde{F}_{pp}^{\mathrm{CP}}(\Theta),\ \widetilde{F}_{p,-p}^{\mathrm{CP}}(\Theta) \text{ are real}, \tag{4.102}$$

$$\widetilde{F}_{20}^{\mathrm{CP}}(\Theta) = [\widetilde{F}_{2,-0}^{\mathrm{CP}}(\Theta)]^*. \tag{4.103}$$

An elegant and compact way to expand the elements $\widetilde{F}_{pq}^{\mathrm{CP}}$ is to use generalized spherical functions P_{pq}^{s}:

$$\widetilde{F}_{pq}^{\mathrm{CP}}(\Theta) = \sum_{s=\max(|p|,|q|)}^{s_{\max}} g_{pq}^{s} P_{pq}^{s}(\cos\Theta), \qquad p, q = 2, 0, -0, -2, \tag{4.104}$$

which indicates the rationale for the specific choice of values for the p, q indices for the circular-polarization phase matrix and the corresponding Stokes vector component subscripts (Eq. (4.96)). Another justification for this choice of expansion functions comes from the consideration of certain properties of the rotation group (Domke 1974). The expression for the expansion coefficients g_{pq}^{s} follows from Eqs. (4.104) and (B.37):

$$g_{pq}^{s} = \frac{2s+1}{2} \int_{-1}^{+1} \mathrm{d}(\cos\Theta)\, \widetilde{F}_{pq}^{\mathrm{CP}}(\Theta)\, P_{pq}^{s}(\cos\Theta), \qquad p, q = 2, 0, -0, -2. \tag{4.105}$$

Note that for $P_{pq}^{s}(\cos\Theta)$ no distinction is made between $p, q = 0$ and $p, q = -0$. For the values of p and q used here, all functions $P_{pq}^{s}(\cos\Theta)$ are real-valued (see Eq. (B.30)). Using Eqs. (4.101)–(4.103), (4.105), and (B.31), we derive the following symmetry relations:

$$g_{pq}^{s} = g_{qp}^{s} = g_{-p,-q}^{s}, \tag{4.106}$$

$$g_{pp}^{s},\ g_{p,-p}^{s} \text{ are real}, \tag{4.107}$$

$$g_{20}^{s} = (g_{2,-0}^{s})^*. \tag{4.108}$$

Finally, inserting Eq. (4.104) into Eq. (4.100) yields expansions (4.75)–(4.80) with expansion coefficients

$$\alpha_1^s = g_{00}^s + g_{0,-0}^s, \tag{4.109}$$

$$\alpha_2^s = g_{22}^s + g_{2,-2}^s, \tag{4.110}$$

$$\alpha_3^s = g_{22}^s - g_{2,-2}^s, \tag{4.111}$$

$$\alpha_4^s = g_{00}^s - g_{0,-0}^s, \tag{4.112}$$

$$\beta_1^s = 2\,\mathrm{Re}\, g_{02}^s, \tag{4.113}$$

$$\beta_2^s = 2\,\mathrm{Im}\, g_{02}^s. \tag{4.114}$$

By analogy with Eq. (4.14) and using Eqs. (1.101) and (4.100), we find for $0 < \varphi^{\mathrm{sca}} - \varphi^{\mathrm{inc}} < \pi$:

$$\begin{aligned}\widetilde{\mathbf{Z}}^{\mathrm{CP}}(\vartheta^{\mathrm{sca}}, \varphi^{\mathrm{sca}}; \vartheta^{\mathrm{inc}}, \varphi^{\mathrm{inc}}) &= \mathbf{L}^{\mathrm{CP}}(-\sigma_2)\widetilde{\mathbf{F}}^{\mathrm{CP}}(\Theta)\mathbf{L}^{\mathrm{CP}}(\pi - \sigma_1) \\ &= \frac{1}{2}\begin{bmatrix} (a_2 + a_3)\mathrm{e}^{-\mathrm{i}2(\sigma_1+\sigma_2)} & (b_1 + \mathrm{i}b_2)\mathrm{e}^{-\mathrm{i}2\sigma_2} & (b_1 - \mathrm{i}b_2)\mathrm{e}^{-\mathrm{i}2\sigma_2} & (a_2 - a_3)\mathrm{e}^{\mathrm{i}2(\sigma_1-\sigma_2)} \\ (b_1 + \mathrm{i}b_2)\mathrm{e}^{-\mathrm{i}2\sigma_1} & a_1 + a_4 & a_1 - a_4 & (b_1 - \mathrm{i}b_2)\mathrm{e}^{\mathrm{i}2\sigma_1} \\ (b_1 - \mathrm{i}b_2)\mathrm{e}^{-\mathrm{i}2\sigma_1} & a_1 - a_4 & a_1 + a_4 & (b_1 + \mathrm{i}b_2)\mathrm{e}^{\mathrm{i}2\sigma_1} \\ (a_2 - a_3)\mathrm{e}^{\mathrm{i}2(\sigma_2-\sigma_1)} & (b_1 - \mathrm{i}b_2)\mathrm{e}^{\mathrm{i}2\sigma_2} & (b_1 + \mathrm{i}b_2)\mathrm{e}^{\mathrm{i}2\sigma_2} & (a_2 + a_3)\mathrm{e}^{\mathrm{i}2(\sigma_1+\sigma_2)} \end{bmatrix},\end{aligned} \tag{4.115}$$

where we have omitted the argument Θ in the a's and b's. Applying Eq. (2.123) to Eqs. (4.68)–(4.70) we derive, after some algebra, the supplementary symmetry relations

$$\begin{aligned}\widetilde{\mathbf{Z}}^{\mathrm{CP}}(\vartheta^{\mathrm{sca}}, \varphi^{\mathrm{inc}}; \vartheta^{\mathrm{inc}}, \varphi^{\mathrm{sca}}) &= \mathbf{A}\boldsymbol{\Delta}_{34}\mathbf{A}^{-1}\widetilde{\mathbf{Z}}^{\mathrm{CP}}(\vartheta^{\mathrm{sca}}, \varphi^{\mathrm{sca}}; \vartheta^{\mathrm{inc}}, \varphi^{\mathrm{inc}})\mathbf{A}\boldsymbol{\Delta}_{34}\mathbf{A}^{-1} \\ &= \boldsymbol{\Delta}^{\mathrm{CP}}\widetilde{\mathbf{Z}}^{\mathrm{CP}}(\vartheta^{\mathrm{sca}}, \varphi^{\mathrm{sca}}; \vartheta^{\mathrm{inc}}, \varphi^{\mathrm{inc}})\boldsymbol{\Delta}^{\mathrm{CP}},\end{aligned} \tag{4.116}$$

$$\widetilde{\mathbf{Z}}^{\mathrm{CP}}(\pi - \vartheta^{\mathrm{sca}}, \varphi^{\mathrm{sca}}; \pi - \vartheta^{\mathrm{inc}}, \varphi^{\mathrm{inc}}) = \boldsymbol{\Delta}^{\mathrm{CP}}\widetilde{\mathbf{Z}}^{\mathrm{CP}}(\vartheta^{\mathrm{sca}}, \varphi^{\mathrm{sca}}; \vartheta^{\mathrm{inc}}, \varphi^{\mathrm{inc}})\boldsymbol{\Delta}^{\mathrm{CP}}, \tag{4.117}$$

$$\widetilde{\mathbf{Z}}^{\mathrm{CP}}(\pi - \vartheta^{\mathrm{inc}}, \varphi^{\mathrm{inc}} + \pi; \pi - \vartheta^{\mathrm{sca}}, \varphi^{\mathrm{sca}} + \pi) = [\widetilde{\mathbf{Z}}^{\mathrm{CP}}(\vartheta^{\mathrm{sca}}, \varphi^{\mathrm{sca}}; \vartheta^{\mathrm{inc}}, \varphi^{\mathrm{inc}})]^{\mathrm{T}}, \tag{4.118}$$

where

$$\boldsymbol{\Delta}^{\mathrm{CP}} = \begin{bmatrix} 0 & 0 & 0 & 1 \\ 0 & 0 & 1 & 0 \\ 0 & 1 & 0 & 0 \\ 1 & 0 & 0 & 0 \end{bmatrix}. \tag{4.119}$$

4.13 Radiative transfer equation

For macroscopically isotropic and mirror-symmetric media, the radiative transfer equation can be significantly simplified:

$$\frac{\mathrm{d}\mathbf{I}(\mathbf{r};\vartheta,\varphi;\omega)}{\mathrm{d}\tau(\mathbf{r},\omega)} = -\mathbf{I}(\mathbf{r};\vartheta,\varphi;\omega) + \frac{\varpi(\mathbf{r},\omega)}{4\pi}\int_{-1}^{+1}\mathrm{d}(\cos\vartheta')\int_{0}^{2\pi}\mathrm{d}\varphi'\,\widetilde{\mathbf{Z}}(\mathbf{r};\vartheta,\vartheta',\varphi-\varphi';\omega)\mathbf{I}(\mathbf{r};\vartheta',\varphi';\omega) + [1-\varpi(\mathbf{r},\omega)]\mathbf{I}_{\mathrm{b}}[T(\mathbf{r}),\omega], \tag{4.120}$$

where

$$\mathrm{d}\tau(\mathbf{r},\omega) = n_0(\mathbf{r})\langle C_{\mathrm{ext}}(\mathbf{r},\omega)\rangle\mathrm{d}s \tag{4.121}$$

is the optical pathlength element (cf. Eqs. (3.33), (4.32), (4.44), (4.45), (4.48), and (4.52)). By writing the normalized phase matrix in the form $\widetilde{\mathbf{Z}}(\mathbf{r};\vartheta,\vartheta',\varphi-\varphi';\omega)$, we explicitly indicate that it depends on the difference of the azimuthal angles of the scattering and incident directions rather than on their specific values (Section 4.3). This important property enables an efficient analytical treatment of the azimuthal dependence of the multiply scattered light, using a Fourier decomposition of the radiative transfer equation (Kuščer and Ribarič 1959; Domke 1974; de Haan *et al.* 1987). Numerical methods for solving Eq. (4.120) for the plane-parallel geometry are reviewed by Hansen and Travis (1974).

Equation (4.120) can be further simplified by neglecting polarization and so replacing the specific intensity vector by its first element (i.e., the radiance) and the normalized phase matrix by its (1, 1) element (i.e., the phase function):

$$\frac{\mathrm{d}I(\mathbf{r};\vartheta,\varphi;\omega)}{\mathrm{d}\tau(\mathbf{r},\omega)} = -I(\mathbf{r};\vartheta,\varphi;\omega) + \frac{\varpi(\mathbf{r},\omega)}{4\pi}\int_{-1}^{+1}\mathrm{d}(\cos\vartheta')\int_{0}^{2\pi}\mathrm{d}\varphi' a_1(\mathbf{r},\Theta,\omega)I(\mathbf{r};\vartheta',\varphi';\omega) + [1-\varpi(\mathbf{r},\omega)]\,I_{\mathrm{b}}[T(\mathbf{r}),\omega], \tag{4.122}$$

where

$$\cos\Theta = \cos\vartheta\cos\vartheta' + \sin\vartheta\sin\vartheta'\cos(\varphi-\varphi') \tag{4.123}$$

(see Eqs. (2.184), (4.17), and (4.67)). Although ignoring the vector nature of light and replacing the exact vector radiative transfer equation by its approximate scalar counterpart has no rigorous physical justification, this simplification is widely used when the medium is illuminated by unpolarized light and only the intensity of multiply scattered light needs to be computed. The scalar approximation gives poor accuracy when the size of the scattering particles is much smaller than the wavelength (Chandrasekhar 1960; Mishchenko *et al.* 1994), but provides acceptable results for particles comparable to and larger than the wavelength (Hansen 1971). Analytical and numerical solutions of the

scalar radiative transfer equation are discussed by Sobolev (1974), van de Hulst (1980), Lenoble (1985), Yanovitskij (1997), and Thomas and Stamnes (1999).